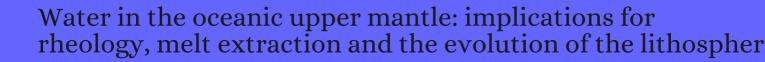
CITATION REPORT List of articles citing



DOI: 10.1016/0012-821x(96)00154-9 Earth and Planetary Science Letters, 1996, 144, 93-108.

Source: https://exaly.com/paper-pdf/26791809/citation-report.pdf

Version: 2024-04-28

This report has been generated based on the citations recorded by exaly.com for the above article. For the latest version of this publication list, visit the link given above.

The third column is the impact factor (IF) of the journal, and the fourth column is the number of citations of the article.

#	Paper	IF	Citations
1353	Seismic structure of the upper mantle in a central Pacific corridor. 1996 , 101, 22291-22309		143
1352	Reading garnet's signature. <i>Nature</i> , 1996 , 384, 215-217	50.4	1
1351	Sensitivity of teleseismic body waves to mineral texture and melt in the mantle beneath a midBcean ridge. 1997 , 355, 217-231		80
1350	A review of melt migration processes in the adiabatically upwelling mantle beneath oceanic spreading ridges. 1997 , 355, 283-318		499
1349	Three-dimensional mantle upwelling, melt generation, and melt migration beneath segment slow spreading ridges. 1997 , 102, 20571-20583		85
1348	Origin of gabbro sills in the Moho transition zone of the Oman ophiolite: Implications for magma transport in the oceanic lower crust. 1997 , 102, 27729-27749		149
1347	Use of the elastic recoil detection analysis (ERDA) microbeam technique for the quantitative determination of hydrogen in materials and hydrogen partitioning between olivine and melt at high pressures. 1997 , 61, 101-113		27
1346	Volatiles in the Earth's mantle: I. Synthesis of CHO fluids at 1273 K and 2.4 GPa. 1997 , 61, 3081-3088		51
1345	The generation of a compositional lithosphere by mid-ocean ridge melting and its effect on subsequent off-axis hotspot upwelling and melting. <i>Earth and Planetary Science Letters</i> , 1997 , 146, 213	-2532	97
1344	The relationship between buoyant mantle flow, melt migration, and gravity bull's eyes at the Mid-Atlantic Ridge between 33°N and 35°N. <i>Earth and Planetary Science Letters</i> , 1997 , 148, 59-67	5.3	56
1343	Gravitational (Rayleigh-Taylor) instability of a layer with non-linear viscosity and convective thinning of continental lithosphere. <i>Geophysical Journal International</i> , 1997 , 128, 125-150	2.6	309
1342	Deformation of subducted oceanic lithosphere. <i>Geophysical Journal International</i> , 1997 , 131, 535-551	2.6	80
1341	VOLCANISM AND TECTONICS ON VENUS. 1998 , 26, 23-51		153
1340	Mechanisms of shear localization in the continental lithosphere: inference from the deformation microstructures of peridotites from the Ivrea zone, northwestern Italy. 1998 , 20, 195-209		132
1339	Phase equilibrium constraints on the origin of basalts, picrites, and komatiites. 1998 , 44, 39-79		130
1338	Effects of eruption and lava drainback on the H2O contents of basaltic magmas at Kilauea Volcano. 1998 , 59, 327-344		107
1337	Thermal and rare gas evolution of the mantle. 1998 , 145, 431-445		31

1336	Water, partial melting and the origin of the seismic low velocity and high attenuation zone in the upper mantle. <i>Earth and Planetary Science Letters</i> , 1998 , 157, 193-207	5.3	423
1335	Asthenosphere flow model of hotspotfidge interactions: a comparison of Iceland and Kerguelen. <i>Earth and Planetary Science Letters</i> , 1998 , 161, 45-56	5.3	47
1334	The depth of the spinel to garnet transition at the peridotite solidus. <i>Earth and Planetary Science Letters</i> , 1998 , 164, 277-284	5.3	328
1333	Silica enrichment in the continental upper mantle via melt/rock reaction. <i>Earth and Planetary Science Letters</i> , 1998 , 164, 387-406	5.3	432
1332	Geodynamics of Lithosphere & Earth⊠ Mantle. 1998 ,		1
1331	Numerical models of convection in a rheologically stratified oceanic upper mantle: Early results. 1998 , 50, 1047-1054		
1330	Major element chemistry of volcanic glasses from the Easter Seamount Chain: Constraints on melting conditions in the plume channel. 1998 , 103, 5287-5304		29
1329	Strength and water weakening of mantle minerals, olivine, wadsleyite and ringwoodite. <i>Geophysical Research Letters</i> , 1998 , 25, 575-578	4.9	68
1328	Water and partial melting in mantle plumes: Inferences from the dissolved H2O concentrations of Hawaiian basaltic magmas. <i>Geophysical Research Letters</i> , 1998 , 25, 3639-3642	4.9	69
1327	Constraints on a buoyant model for the formation of the axial topographic high on the East Pacific Rise. 1998 , 103, 12291-12307		14
1326	Dike ascent in partially molten rock. 1998 , 103, 20901-20919		80
1325	Heat flow and thickness of the lithosphere in the Canadian Shield. 1998 , 103, 15269-15286		150
1324	Joint estimation of afterslip rate and postseismic relaxation following the 1989 Loma Prieta earthquake. 1998 , 103, 26975-26992		102
1323	Magnetotelluric imaging of the Society Islands hotspot. 1998 , 103, 30287-30309		74
1322	Mantle Rheology: Insights from Laboratory Studies of Deformation and Phase Transition. 503-560		1
1321	Sensitivity of teleseismic body waves to mineral texture and melt in the mantle beneath a mid-ocean ridge. 1999 , 1-16		
1320	A review of melt migration processes in the adiabatically upwelling mantle beneath oceanic spreading ridges. 1999 , 67-102		1
1319	The evolution of continental roots in numerical thermo-chemical mantle convection models including differentiation by partial melting. 1999 , 153-170		3

1318	Convective instability of a boundary layer with temperature-and strain-rate-dependent viscosity in terms of 'available buoyancy'. <i>Geophysical Journal International</i> , 1999 , 139, 51-68	.6	54
1317	Simple models for late Holocene and present-day Patagonian glacier fluctuations and predictions of a geodetically detectable isostatic response. <i>Geophysical Journal International</i> , 1999 , 138, 601-624	.6	61
1316	Electromagnetic Studies Of The Lithosphere And Asthenosphere. 1999 , 20, 229-255		45
1315	Single-crystal elastic properties of chondrodite: implications for water in the upper mantle. 1999 , 26, 297-303		27
1314	The evolution of continental roots in numerical thermo-chemical mantle convection models including differentiation by partial melting. 1999 , 48, 153-170		33
1313	Calculation of Peridotite Partial Melting from Thermodynamic Models of Minerals and Melts. III. Controls on Isobaric Melt Production and the Effect of Water on Melt Production. 1999 , 40, 831-851		147
1312	Asymmetric Electrical Structure in the Mantle Beneath the East Pacific Rise at 17 degrees S. 1999 , 286, 752-756		103
1311	Mantle flow, melting, and dehydration of the Iceland mantle plume. <i>Earth and Planetary Science Letters</i> , 1999 , 165, 81-96	-3	164
1310	Two-stage melting and the geochemical evolution of the mantle: a recipe for mantle plum-pudding. Earth and Planetary Science Letters, 1999 , 170, 215-239	.3	165
1309	Seismological structure of the upper mantle: a regional comparison of seismic layering. 1999 , 110, 21-41		127
1308	Seismic structure of the upper mantle beneath the western Philippine Sea. 1999 , 110, 263-283		27
1307	Dynamics of the Galapagos hotspot from helium isotope geochemistry. 1999 , 63, 4139-4156		137
1306	Small-scale convection and divergent plate boundaries. 1999 , 104, 7389-7403		86
1305	Some thoughts on the stability of cratonic lithosphere: Effects of buoyancy and viscosity. 1999 , 104, 12747-12758		129
1304	Flow behavior of fine-grained synthetic dunite in the presence of 0.5 wt% H2O. 1999 , 104, 17823-17845		21
1303	Heat transport in stagnant lid convection with temperature- and pressure-dependent Newtonian or non-Newtonian rheology. 1999 , 104, 12759-12777		111
1302	Dispersion of the Jan Mayen and Iceland mantle plumes in the Arctic: A He-Pb-Nd-Sr isotope tracer study of basalts from the Kolbeinsey, Mohns, and Knipovich Ridges. 1999 , 104, 10543-10569		80
1301	The Relation Between Mantle Dynamics and Plate Tectonics: A Primer. 2000 , 5-46		72

(2000-2000)

1300 The Que	est for Self-Consistent Generation of Plate Tectonics in Mantle Convection Models. 2000 , 47-72		28
1299 Melt mig	gration beneath mid-ocean ridges. <i>Geophysical Journal International</i> , 2000 , 140, 687-697	2.6	54
	tions of flexure and the rheology of oceanic lithosphere. <i>Geophysical Journal International</i> , 12, 855-875	2.6	152
Convect ¹²⁹⁷ 143, 52-	ive instability of thickening mantle lithosphere. <i>Geophysical Journal International</i> , 2000 , 70	2.6	35
1296 Mapping	the Hawaiian plume conduit with converted seismic waves. <i>Nature</i> , 2000 , 405, 938-41	50.4	157
	termination of trace element partition coefficients between garnet, clinopyroxene and basaltic liquids at 20.5 GPa and 10800200°C. 2000 , 53, 165-187		445
1294 Volatile	Components, Magmas, and Critical Fluids in Upwelling Mantle. 2000 , 41, 1195-1206		120
1293 The Stat	istics and Distribution of Helium in the Mantle. 2000 , 42, 289-311		30
1292 In-situ h	igh pressure X-ray diffraction of phase E to 15 GPa. 2000 , 85, 765-769		19
	undance in Depleted to Moderately Enriched Mid-ocean Ridge Magmas; Part I: Incompatible ur, Implications for Mantle Storage, and Origin of Regional Variations. 2000 , 41, 1329-1364		149
1290 Physics	and Chemistry of Partially Molten Rocks. 2000 ,		5
1289 Hydrous	Phases and Hydrogen Bonding at High Pressure. 2000 , 41, 309-333		9
	diabatic instabilities associated with necking processes of an elasto-viscoplastic lithosphere. 8, 89-102		18
1287 Large 23	30Th-excesses in basalts produced by partial melting of spinel lherzolite. 2000 , 162, 127-136		20
	ects of deep damp melting on mantle flow and melt generation beneath mid-ocean ridges. and Planetary Science Letters, 2000 , 176, 339-356	5.3	103
	g out the conduit of the Iceland mantle plume with helium isotopes. <i>Earth and Planetary</i> Letters, 2000 , 176, 45-55	5.3	87
	e of water on plastic deformation of olivine aggregates: 1. Diffusion creep regime. 2000 , 157-21469		388
	e of water on plastic deformation of olivine aggregates: 2. Dislocation creep regime. 2000 , 171-21481		373

1282	Interaction of rifting and hot horizontal plume sheets at volcanic margins. 2000 , 105, 13375-13387		25
1281	Scaling of time-dependent stagnant lid convection: Application to small-scale convection on Earth and other terrestrial planets. 2000 , 105, 21795-21817		269
1280	Crustal structure of the Southwest Indian Ridge at the Atlantis II Fracture Zone. 2000 , 105, 25809-2582	8	65
1279	The influence of plate motions on three-dimensional back arc mantle flow and shear wave splitting. 2000 , 105, 28009-28033		130
1278	Planetary ScienceA Space Odyssey. 2000 , 287, 997-1005		7
1277	Upper mantle velocity structure in the western Pacific rim estimated from short-period recordings at Matsushiro Seismic Array System. 2000 , 52, 459-466		4
1276	Spontaneous melt localization in a deforming solid with viscosity variations due to water weakening. <i>Geophysical Research Letters</i> , 2000 , 27, 9-12	4.9	22
1275	Shallow mantle temperatures under Europe from P and S wave tomography. 2000 , 105, 11153-11169		408
1274	Mobility of continental mantle: Evidence from postseismic geodetic observations following the 1992 Landers earthquake. 2000 , 105, 8035-8054		173
1273	Modeling anisotropy and plate-driven flow in the Tonga subduction zone back arc. 2000 , 105, 16181-16	191	82
1272	Self-consistent generation of tectonic plates in time-dependent, three-dimensional mantle convection simulations 2. Strain weakening and asthenosphere. <i>Geochemistry, Geophysics, Geosystems</i> , 2000 , 1, n/a-n/a	3.6	52
1271	Comparison of continental and oceanic mantle electrical conductivity: Is the Archean lithosphere dry?. <i>Geochemistry, Geophysics, Geosystems</i> , 2000 , 1, n/a-n/a	3.6	103
1270	Mantle solidus: Experimental constraints and the effects of peridotite composition. <i>Geochemistry, Geophysics, Geosystems</i> , 2000 , 1, n/a-n/a	3.6	506
1269	Melt intrusion as a trigger for lithospheric foundering and the eruption of the Siberian flood basalts. <i>Geophysical Research Letters</i> , 2000 , 27, 3937-3940	4.9	101
1268	Rheology of Partially Molten Rocks. 2000 , 3-28		15
1267	Partial Melting and Melt Segregation in a Convecting Mantle. 2000 , 141-178		68
1266	Role of a low-viscosity zone in stabilizing plate tectonics: Implications for comparative terrestrial planetology. <i>Geochemistry, Geophysics, Geosystems</i> , 2001 , 2, n/a-n/a	3.6	163
1265	Causes and consequences of flow organization during melt transport: The reaction infiltration instability in compactible media. 2001 , 106, 2061-2077		193

1264	On the conditions for lower crustal convective instability. 2001 , 106, 6423-6446		364
1263	Evolution of subducting mantle lithosphere at a continental plate boundary. <i>Geophysical Research Letters</i> , 2001 , 28, 4399-4402	4.9	24
1262	Preferential mantle lithospheric extension under the South China margin. 2001 , 18, 929-945		150
1261	Prediction of the Gibbs energies and an improved equation of state for water at extreme conditions from ab initio energies with classical simulations. 2001 , 65, 4067-4075		19
1260	Mantle upwelling and melting beneath slow spreading centers: effects of variable rheology and melt productivity. <i>Earth and Planetary Science Letters</i> , 2001 , 184, 589-604	5.3	62
1259	The water content of olivines from the North Atlantic Volcanic Province. <i>Earth and Planetary Science Letters</i> , 2001 , 186, 401-415	5.3	77
1258	238UØ30Th constraints on mantle upwelling and plume@dge interaction along the Reykjanes Ridge. <i>Earth and Planetary Science Letters</i> , 2001 , 187, 259-272	5.3	50
1257	Low degree melting under the Southwest Indian Ridge: the roles of mantle temperature, conductive cooling and wet melting. <i>Earth and Planetary Science Letters</i> , 2001 , 188, 383-398	5.3	43
1256	A low viscosity wedge in subduction zones. Earth and Planetary Science Letters, 2001, 193, 227-236	5.3	201
1255	Plume-driven upwelling under central Iceland. <i>Earth and Planetary Science Letters</i> , 2001 , 194, 67-82	5.3	101
1254	Subduction zones: observations and geodynamic models. 2001 , 127, 9-24		61
1253	Subduction zone rheology. 2001 , 127, 67-81		29
1252	Rheological structure and deformation of subducted slabs in the mantle transition zone: implications for mantle circulation and deep earthquakes. 2001 , 127, 83-108		249
1251	Water-induced fabric transitions in olivine. 2001 , 293, 1460-3		665
1250	Mantle convection with strong subduction zones. <i>Geophysical Journal International</i> , 2001 , 144, 271-288	2.6	70
1249	Oceanic upper mantle structure from experimental scaling of VS and density at different depths. <i>Geophysical Journal International</i> , 2001 , 147, 199-214	2.6	27
1248	Hydrogen in the Deep Earth. 2001 , 29, 365-418		192
1247	Melt retention and segregation beneath mid-ocean ridges. <i>Nature</i> , 2001 , 410, 920-3	50.4	106

1246	Towards a general theory of biodiversity. <i>Nature</i> , 2001 , 410, 923-6	50.4	68
1245	Reykjanes "V"-shaped ridges originating from a pulsing and dehydrating mantle plume. <i>Nature</i> , 2001 , 411, 681-4	50.4	114
1244	Effects of water on dynamically recrystallized grain-size of olivine. 2001 , 23, 1337-1344		120
1243	Evidence for a plate tectonics debate. 2001 , 55, 235-336		4
1242	Diapiric flow at subduction zones: a recipe for rapid transport. 2001 , 292, 2472-5		139
1241	Steady-state creation of crust-free lithosphere at cold spots in mid-ocean ridges. <i>Geology</i> , 2001 , 29, 979	9 5	26
1240	Mantle flow beneath a continental strike-slip fault: postseismic deformation after the 1999 Hector Mine earthquake. 2001 , 293, 1814-8		224
1239	Anomalous melt production after continental break-up in the southern Iberia Abyssal Plain. 2001 , 187, 537-550		24
1238	Seismic evidence for hotspot-induced buoyant flow beneath the Reykjanes Ridge. 2001 , 293, 1645-7		57
1237	Melt Generation at Very Slow-Spreading Oceanic Ridges: Constraints from Geochemical and Geophysical Data. 2001 , 42, 1171-1196		130
1236	Thermal-rheological controls on deformation within oceanic transforms. 2001 , 186, 65-83		10
1235	The initiation of subduction: criticality by addition of water?. 2001 , 294, 578-80		299
1234	Archaean tectonics: a review, with illustrations from the Slave craton. 2002 , 199, 151-181		61
1233	Theoretical Analysis of Shear Localization in the Lithosphere. 2002 , 51, 387-420		13
1232	High-pressure single-crystal X-ray and powder neutron study of F,OH/OD-chondrodite: Compressibility, structure, and hydrogen bonding. 2002 , 87, 931-939		21
1231	Hydroxyl in MgSiO3 akimotoite: A polarized and high-pressure IR study. 2002 , 87, 603-608		8
1230	The break-up of continents and the formation of new ocean basins. 2002 , 360, 2839-52		7
1229	Focusing of magma in the upper mantle through dike interaction. 2002 , 107, ECV 6-1-ECV 6-17		52

1228	Lithospheric deformation during the early stages of continental collision: Numerical experiments and comparison with South Island, New Zealand. 2002 , 107, ETG 3-1-ETG 3-19		74
1227	Buoyant decompression melting: A possible mechanism for intraplate volcanism. 2002 , 107, ECV 7-1-ECV 7-14		61
1226	Asthenospheric flow and asymmetry of the East Pacific Rise, MELT area. 2002 , 107, ETG 8-1-ETG 8-13		65
1225	Thermal and crustal evolution of Mars. 2002 , 107, 6-1		235
1224	The influence of water on the development of lattice preferred orientation in olivine aggregates. <i>Geophysical Research Letters</i> , 2002 , 29, 17-1	4.9	33
1223	Onset of convection with temperature- and depth-dependent viscosity. <i>Geophysical Research Letters</i> , 2002 , 29, 29-1-29-4	4.9	18
1222	Formation of volcanic rifted margins: Are temperature anomalies required?. <i>Geophysical Research Letters</i> , 2002 , 29, 18-1	4.9	27
1221	On Elteady-state Theat flow and the rheology of oceanic mantle. <i>Geophysical Research Letters</i> , 2002 , 29, 13-1-13-4	4.9	21
1220	Seismic Wave Attenuation: Energy Dissipation in Viscoelastic Crystalline Solids. 2002 , 51, 253-290		58
1219	Strange partners: formation and survival of continental crust and lithospheric mantle. 2002 , 199, 91-10	3	15
1218	Possible implications of modal mineralogy for melting in mantle lherzolites. 2002 , 66, 2091-2098		3
1217	Phase relations in the CH4-H2O-NaCl system at 2 kbar, 300 to 600°C as determined using synthetic fluid inclusions. 2002 , 66, 3971-3986		17
1216	Consequences of diffuse and channelled porous melt migration on uranium series disequilibria. 2002 , 66, 4133-4148		80
1215	SIMS analysis of volatiles in silicate glasses, 2: isotopes and abundances in Hawaiian melt inclusions. 2002 , 183, 115-141		291
1214	Contrasting rifted margin styles south of Greenland: implications for mantle plume dynamics. <i>Earth and Planetary Science Letters</i> , 2002 , 200, 271-286	5.3	49
1213	Asymmetric mantle dynamics in the MELT region of the East Pacific Rise. <i>Earth and Planetary Science Letters</i> , 2002 , 200, 287-295	5.3	63
1212	Influence of melt on the creep behavior of olivineBasalt aggregates under hydrous conditions. <i>Earth and Planetary Science Letters</i> , 2002 , 201, 491-507	5.3	187
1211	Is the Iceland hot spot also wet? Evidence from the water contents of undegassed submarine and subglacial pillow basalts. <i>Earth and Planetary Science Letters</i> , 2002 , 202, 77-87	5.3	130

121 0	Dynamic interaction of cold anomalies with the mid-ocean ridge flow field and its implications for the Australian Antarctic Discordance. <i>Earth and Planetary Science Letters</i> , 2002 , 203, 925-935	5.3	11
1209	The upper mantle transition zone discontinuities in the Pacific as determined by short-period array data. <i>Earth and Planetary Science Letters</i> , 2002 , 204, 347-361	5.3	32
1208	Is the transition zone an empty water reservoir? Inferences from numerical model of mantle dynamics. <i>Earth and Planetary Science Letters</i> , 2002 , 205, 37-51	5.3	51
1207	Crust and upper mantle of Kamchatka from teleseismic receiver functions. 2002 , 358, 233-265		76
1206	Thermal structure of the North American uppermost mantle inferred from seismic tomography. 2002 , 107, ETG 2-1		212
1205	Effects of melt migration on the dynamics and melt generation of diapirs ascending through asthenosphere. 2002 , 107, ETG 4-1-ETG 4-13		6
1204	Volatiles in basaltic glasses from the Easter-Salas y Gomez Seamount Chain and Easter Microplate: Implications for geochemical cycling of volatile elements. <i>Geochemistry, Geophysics, Geosystems</i> , 2002 , 3, 1-29	3.6	107
1203	D/H ratios in basalt glasses from the Salas y Gomez mantle plume interacting with the East Pacific Rise: Water from old D-rich recycled crust or primordial water from the lower mantle?. <i>Geochemistry, Geophysics, Geosystems,</i> 2002 , 3, 1-26	3.6	37
1202	On the importance of offshore data for magnetotelluric studies of ocean-continent subduction systems. <i>Geophysical Research Letters</i> , 2002 , 29, 16-1-16-4	4.9	12
1201	Is small scale convection responsible for the formation of thick igneous crust along volcanic passive margins?. <i>Geophysical Research Letters</i> , 2002 , 29, 3-1-3-4	4.9	6
1200	Pressure dependence of H solubility in magnesiowBitte up to 25 GPa: Implications for the storage of water in the Earth's lower mantle. <i>Geophysical Research Letters</i> , 2002 , 29, 89-1-89-4	4.9	61
1199	Evidence of low flexural rigidity and low viscosity lower continental crust during continental break-up in the South China Sea. 2002 , 19, 951-970		173
1198	9. Seismic Wave Attenuation: Energy Dissipation in Viscoelastic Crystalline Solids. 2002 , 253-290		7
1197	13. Theoretical Analysis of Shear Localization in the Lithosphere. 2002 , 387-420		5
1196	Microstructural and experimental constraints on the rheology of partially molten gabbro beneath oceanic spreading centers. 2002 , 24, 1101-1107		27
1195	The role of an H2O-rich fluid component in the generation of primitive basaltic andesites and andesites from the Mt. Shasta region, N California. 2002 , 142, 375-396		372
1194	On the state of sublithospheric upper mantle beneath a supercontinent. <i>Geophysical Journal International</i> , 2002 , 149, 179-189	2.6	29
1193	Vapour undersaturation in primitive mid-ocean-ridge basalt and the volatile content of Earth's upper mantle. <i>Nature</i> , 2002 , 419, 451-5	50.4	590

1192	Recycled dehydrated lithosphere observed in plume-influenced mid-ocean-ridge basalt. <i>Nature</i> , 2002 , 420, 385-9	50.4	385
1191	Mantle wedge control on back-arc crustal accretion. <i>Nature</i> , 2002 , 416, 417-20	50.4	124
1190	Determinants of extinction in the fossil record. <i>Nature</i> , 2002 , 416, 420-4	50.4	167
1189	Lava without the fizz. <i>Nature</i> , 2002 , 419, 445-6	50.4	8
1188	Art: Imagine space. <i>Nature</i> , 2002 , 419, 446	50.4	1
1187	Volcanoes, Fluids, and Life at Mid-Ocean Ridge Spreading Centers. 2002 , 30, 385-491		319
1186	Hidden melting signatures recorded in the Troodos ophiolite plutonic suite: evidence for widespread generation of depleted melts and intra-crustal melt aggregation. 2003 , 144, 484-506		16
1185	Mineral/melt partitioning of trace elements during hydrous peridotite partial melting. 2003, 145, 391-4	05	87
1184	Flow and fracture maps for basaltic rock deformation at high temperatures. 2003, 120, 25-42		23
1183	Multiscale dynamics of the Tonga-Kermadec subduction zone. <i>Geophysical Journal International</i> , 2003 , 153, 359-388	2.6	130
1182	The interplay between global tectonic processes and the seismic cycle in the Umbria-Marche seismogenic region. <i>Geophysical Journal International</i> , 2003 , 155, 1093-1104	2.6	5
1181	The importance of water to oceanic mantle melting regimes. <i>Nature</i> , 2003 , 421, 815-20	50.4	287
1180	Mantle thermal pulses below the Mid-Atlantic Ridge and temporal variations in the formation of oceanic lithosphere. <i>Nature</i> , 2003 , 423, 499-505	50.4	93
1179	Influence of grain size evolution on convective instability. <i>Geochemistry, Geophysics, Geosystems</i> , 2003 , 4,	3.6	78
1178	Interaction between small-scale mantle diapirs and a continental root. <i>Geochemistry, Geophysics, Geosystems</i> , 2003 , 4,	3.6	10
1177	Hydrogen concentration analyses using SIMS and FTIR: Comparison and calibration for nominally anhydrous minerals. <i>Geochemistry, Geophysics, Geosystems</i> , 2003 , 4,	3.6	166
1176	A new parameterization of hydrous mantle melting. <i>Geochemistry, Geophysics, Geosystems</i> , 2003 , 4, n/a-	-ng/. á s	550
1175	Super-deep low-velocity layer beneath the Arabian plate. <i>Geophysical Research Letters</i> , 2003 , 30,	4.9	35

1174	Longevity and stability of cratonic lithosphere: Insights from numerical simulations of coupled mantle convection and continental tectonics. 2003 , 108,		131
1173	Spacing of faults at the scale of the lithosphere and localization instability: 2. Application to the Central Indian Basin. 2003 , 108,		11
1172	Arc-parallel flow within the mantle wedge: Evidence from the accreted Talkeetna arc, south central Alaska. 2003 , 108,		117
1171	Constraints on the viscosity of the continental crust and mantle from GPS measurements and postseismic deformation models in western Mongolia. 2003 , 108,		62
1170	Timing of formation of Beta Regio and its geodynamical implications. 2003, 108,		13
1169	Clues to the lithospheric structure of Mars from wrinkle ridge sets and localization instability. 2003 , 108,		77
1168	Observational and theoretical studies of the dynamics of mantle plumelhid-ocean ridge interaction. 2003 , 41,		112
1167	Plume-transform interactions at ultra-slow spreading ridges: Implications for the Southwest Indian Ridge. <i>Geochemistry, Geophysics, Geosystems</i> , 2003 , 4, n/a-n/a	3.6	29
1166	Melting, dehydration, and the dynamics of off-axis plume-ridge interaction. <i>Geochemistry, Geophysics, Geosystems</i> , 2003 , 4, n/a-n/a	3.6	32
1165	Energetics of mantle convection and the fate of fossil heat. <i>Geophysical Research Letters</i> , 2003 , 30,	4.9	112
1164	Seismic structure of Cocos and Malpelo Volcanic Ridges and implications for hot spot-ridge interaction. 2003 , 108,		83
1163	Controls on sublithospheric small-scale convection. 2003 , 108,		93
1162	Nature of heterogeneity of the upper mantle beneath the northern Philippine Sea as inferred from attenuation and velocity tomography. 2003 , 140, 331-341		24
1161	Upper mantle beneath Southeast Asia from S velocity tomography. 2003, 108,		220
1160	Partial melting experiments on a MORB-like pyroxenite between 2 and 3 GPa: Constraints on the presence of pyroxenite in basalt source regions from solidus location and melting rate. 2003 , 108,		222
1159	Comparison of dynamic flow models for the Central Aleutian and Tonga-Kermadec subduction zones. <i>Geochemistry, Geophysics, Geosystems</i> , 2003 , 4,	3.6	36
1158	Seismic detection of sublithospheric plume head residue beneath the Pitcairn hot-spot chain. <i>Earth and Planetary Science Letters</i> , 2003 , 209, 71-83	5.3	5
1157	Partitioning of trace elements between crystals and melts. <i>Earth and Planetary Science Letters</i> , 2003 , 210, 383-397	5.3	300

1156	Upwelling and melting of the Iceland plume from radial variation of 238U\(\mathbb{2}\)30Th disequilibria in postglacial volcanic rocks. Earth and Planetary Science Letters, 2003, 214, 167-186	5.3	56
1155	Elasticity and strength of hydrous ringwoodite at high pressure. <i>Earth and Planetary Science Letters</i> , 2003 , 214, 645-654	5.3	64
1154	Transient rheology of the uppermost mantle beneath the Mojave Desert, California. <i>Earth and Planetary Science Letters</i> , 2003 , 215, 89-104	5.3	154
1153	Shape and size of the starting Iceland plume swell. Earth and Planetary Science Letters, 2003, 216, 271-2.	85 3	32
1152	Small-scale convection under the back-arc occurring in the low viscosity wedge. <i>Earth and Planetary Science Letters</i> , 2003 , 216, 703-715	5.3	90
1151	Main-group pallasites: chemical composition, relationship to IIIAB irons, and origin. 2003 , 67, 3079-3096		88
1150	Origin of the AustralianAntarctic Discordance from an ancient slab and mantle wedge. 2003,		15
1149	Styles of mantle convection and their influence on planetary evolution. 2003 , 335, 99-111		49
1148	U-series Constraints on Intraplate Basaltic Magmatism. 2003 , 52, 215-254		42
1147	Rheology of the Upper Mantle and the Mantle Wedge: A View from the Experimentalists. 2003, 83-105		592
1146	Seismic imaging of the downwelling Indian lithosphere beneath central Tibet. 2003 , 300, 1424-7		258
1145	Mantle VolatilesDistribution and Consequences. 2003, 319-361		22
1144	Plate-kinematic explanation for mid-oceanic-ridge depth discontinuities. <i>Geology</i> , 2003 , 31, 399	5	28
1143	Melt segregation and strain partitioning: implications for seismic anisotropy and mantle flow. 2003 , 301, 1227-30		409
1142	A general model of arc-continent collision and subduction polarity reversal from Taiwan and the Irish Caledonides. 2003 , 219, 81-98		46
1141	Water solubility and diffusivity in olivine: its role in planetary tectonics. 2003 , 67, 697-715		30
1140	Synchrotron infrared spectroscopy of OH-chondrodite and OH-clinohumite at high pressure. 2003 , 88, 1412-1415		16
1139	Mapping Water Content in the Upper Mantle. 2003 , 135-152		108

1138	Seismological Constraints on Structure and Flow Patterns within the Mantle Wedge. 2003, 59-81		26
1137	Thermal Structure due to Solid-State Flow in the Mantle Wedge Beneath Arcs. 2003 , 293-311		131
1136	Experimental Constraints on Melt Generation in the Mantle Wedge. 2003, 107-134		33
1135	6. U-series Constraints on Intraplate Basaltic Magmatism. 2003 , 215-254		9
1134	Nucleation and growth kinetics of the <code>ltransformation</code> in Mg2SiO4determined by in situ synchrotron powder X-ray diffraction. 2004 , 89, 285-293		50
1133	Effect of H+ on FeMg interdiffusion in olivine, (Fe,Mg)2SiO4. 2004 , 85, 209-211		48
1132	Chapter 15 Transport properties in deep depths and related condensed-matter phenomena. 2004 , 9, 1041-1203		
1131	Strain modelling, seismic anisotropy and coupling at strike-slip boundaries: applications in New Zealand and the San Andreas fault. 2004 , 227, 9-39		11
1130	Abundance and Partitioning of OH in a High-pressure Magmatic System: Megacrysts from the Monastery Kimberlite, South Africa. 2004 , 45, 1539-1564		143
1129	Mafic Pegmatites Intruding Oceanic Plateau Gabbros and Ultramafic Cumulates from Bolivar, Colombia: Evidence for a 'Wet' Mantle Plume?. 2004 , 45, 1877-1906		27
1128	Rheological Properties of Partially Molten Lherzolite. 2004 , 45, 275-298		82
1127	FTIR Spectrum of Phenocryst Olivine as an Indicator of Silica Saturation in Magmas. 2004 , 46, 603-614		39
1126	Thermal consequences of the formation of a slab window beneath the Mid-Cretaceous southwest Japan arc: A 2-D numerical analysis. 2004 , 13, 520-532		13
1125	A test of laboratory based rheological parameters of olivine from an analysis of late Cenozoic convective removal of mantle lithosphere beneath the Sierra Nevada, California, USA. <i>Geophysical Journal International</i> , 2004 , 156, 555-564	2.6	31
1124	The anisotropic and rheological structure of the oceanic upper mantle from a simple model of plate shear. <i>Geophysical Journal International</i> , 2004 , 158, 287-296	2.6	42
1123	Temperature and melting of a ridge-centred plume with application to Iceland. Part I: Dynamics and crust production. <i>Geophysical Journal International</i> , 2004 , 158, 729-743	2.6	34
1122	The effects of buoyant crust on the gravitational instability of thickened mantle lithosphere at zones of intracontinental convergence. <i>Geophysical Journal International</i> , 2004 , 158, 1134-1150	2.6	55
1121	Earthquakes in the deep continental crust - insights from studies on exhumed high-pressure rocks. <i>Geophysical Journal International</i> , 2004 , 158, 569-576	2.6	30

1120	Temperature and melting of a ridge-centred plume with application to Iceland. Part II: Predictions for electromagnetic and seismic observables. <i>Geophysical Journal International</i> , 2004 , 159, 1097-1111	2.6	37
1119	Wavelet and multitaper coherence methods for assessing the elastic thickness of the Irish Atlantic margin. <i>Geophysical Journal International</i> , 2004 , 159, 445-459	2.6	21
1118	Faulting induced by precipitation of water at grain boundaries in hot subducting oceanic crust. <i>Nature</i> , 2004 , 428, 633-6	50.4	61
1117	Earth science: just add more water. <i>Nature</i> , 2004 , 429, 356-7	50.4	1
1116	Heat-producing Elements-enriched Continental Mantle Lithosphere and Proterozoic Intracontinental Orogens: Insights from Brasiliano/Pan-African Belts. <i>Gondwana Research</i> , 2004 , 7, 427	-436	12
1115	The effect of silica activity on the incorporation mechanisms of water in synthetic forsterite: a polarised infrared spectroscopic study. 2004 , 147, 48-57		127
1114	A hydrous melting and fractionation model for mid-ocean ridge basalts: Application to the Mid-Atlantic Ridge near the Azores. <i>Geochemistry, Geophysics, Geosystems</i> , 2004 , 5, n/a-n/a	3.6	233
1113	Recycled metasomatized lithosphere as the origin of the Enriched Mantle II (EM2) end-member: Evidence from the Samoan Volcanic Chain. <i>Geochemistry, Geophysics, Geosystems</i> , 2004 , 5, n/a-n/a	3.6	293
1112	From rift to drift: Mantle melting during continental breakup. <i>Geochemistry, Geophysics, Geosystems</i> , 2004 , 5,	3.6	67
1111	Melting, dehydration, and the geochemistry of off-axis plume-ridge interaction. <i>Geochemistry, Geophysics, Geosystems</i> , 2004 , 5, n/a-n/a	3.6	10
1110	Evolving force balance during incipient subduction. <i>Geochemistry, Geophysics, Geosystems</i> , 2004 , 5,	3.6	276
1109	Convective cooling of an initially stably stratified fluid with temperature-dependent viscosity: Implications for the role of solid-state convection in planetary evolution. 2004 , 109,		33
1108	Initiation of subduction by small-scale convection. 2004 , 109,		36
1107	Geodetic and seismic constraints on some seismogenic zone processes in Costa Rica. 2004 , 109,		91
1106	The Sumatra subduction zone: A case for a locked fault zone extending into the mantle. 2004 , 109,		73
1105	Glass compositions, plume-ridge interaction, and hydrous melting along the Galpagos Spreading Center, 90.5°W to 98°W. <i>Geochemistry, Geophysics, Geosystems</i> , 2004 , 5,	3.6	65
1104	Deep structure of the Afro-Arabian hotspot by S receiver functions. <i>Geophysical Research Letters</i> , 2004 , 31, n/a-n/a	4.9	39
1103	Hydrogen partition coefficients between nominally anhydrous minerals and basaltic melts. <i>Geophysical Research Letters</i> , 2004 , 31,	4.9	224

1102	Stratification of anisotropy in the Pacific upper mantle. 2004 , 109,		58
1101	Changes in the structure of water deduced from the pressure dependence of the Raman OH frequency. 2004 , 120, 5867-70		123
1100	Lateral variation in upper mantle viscosity: role of water. <i>Earth and Planetary Science Letters</i> , 2004 , 222, 451-467	5.3	243
1099	The thermal effects of steady-state slab-driven mantle flow above a subducting plate: the Cascadia subduction zone and backarc. <i>Earth and Planetary Science Letters</i> , 2004 , 223, 35-48	5.3	119
1098	The onset of convection in fluids with strongly temperature-dependent viscosity cooled from above with implications for planetary lithospheres. <i>Earth and Planetary Science Letters</i> , 2004 , 224, 371-38	§€	36
1097	Phase relations of peridotites under H2O-saturated conditions and ability of subducting plates for transportation of H2O. <i>Earth and Planetary Science Letters</i> , 2004 , 227, 57-71	5.3	89
1096	The effects of a variation of the radial viscosity profile on mantle evolution. 2004, 384, 55-90		37
1095	Production and recycling of oceanic crust in the early Earth. 2004, 386, 41-65		102
1094	On the formation of continental silicic melts in thermochemical mantle convection models: implications for early Earth. 2004 , 394, 111-124		31
1093	Hydrous phase stability and partial melt chemistry in H2O-saturated KLB-1 peridotite up to the uppermost lower mantle conditions. 2004 , 143-144, 387-395		64
1092	Dehydration and earthquakes in the subducting slab: empirical link in intermediate and deep seismic zones. 2004 , 146, 297-311		91
1091	Stress measurements of deforming olivine at high pressure. 2004 , 143-144, 357-367		53
1090	Evolution of helium and argon isotopes in a convecting mantle. 2004 , 146, 417-439		109
1089	Possible effects of lateral viscosity variations induced by plate-tectonic mechanism on geoid inferred from numerical models of mantle convection. 2004 , 147, 67-85		5
1088	New type of olivine fabric from deformation experiments at modest water content and low stress. <i>Geology</i> , 2004 , 32, 1045	5	182
1087	Melting of fertile peridotite with variable amounts of H2O. 2004 , 69-80		7
1086	Trace Element Evidence for Hydrous Metasomatism at the Base of the North American Lithosphere and Possible Association with Laramide Low-Angle Subduction. 2005 , 113, 673-685		78
1085	Viscous Energy Dissipation and Strain Partitioning in Partially Molten Rocks. 2005 , 46, 2569-2592		60

(2005-2005)

1084	Seismic boundaries in the mantle beneath Iceland: a new constraint on temperature. <i>Geophysical Journal International</i> , 2005 , 160, 533-538	2.6	43
1083	Seismic structure of the Carnegie ridge and the nature of the Galpagos hotspot. <i>Geophysical Journal International</i> , 2005 , 161, 763-788	2.6	70
1082	Water-rich basalts at mid-ocean-ridge cold spots. <i>Nature</i> , 2005 , 434, 66-9	50.4	35
1081	Kin selection and cooperative courtship in wild turkeys. <i>Nature</i> , 2005 , 434, 69-72	50.4	141
1080	Water content in the transition zone from electrical conductivity of wadsleyite and ringwoodite. <i>Nature</i> , 2005 , 434, 746-9	50.4	317
1079	Particle size and energetics of gouge from earthquake rupture zones. <i>Nature</i> , 2005 , 434, 749-52	50.4	205
1078	A sharp lithosphere-asthenosphere boundary imaged beneath eastern North America. <i>Nature</i> , 2005 , 436, 542-5	50.4	154
1077	Geophysical evidence from the MELT area for compositional controls on oceanic plates. <i>Nature</i> , 2005 , 437, 249-52	50.4	2 00
1076	Effect of water on the strength and microstructure of Carrara marble axially compressed at high temperature. 2005 , 27, 265-281		59
1075	Electrical Structure in Marine Tectonic Settings. 2005 , 26, 701-731		36
1074	Source of the Quaternary Alkalic Basalts, Picrites and Basanites of the Potrillo Volcanic Field, New Mexico, USA: Lithosphere or Convecting Mantle?. 2005 , 46, 1603-1643		35
1073	High-strain zones: laboratory perspectives on strain softening during ductile deformation. 2005 , 245, 1-24		19
1072	Dynamic recrystallization and strain softening of olivine aggregates in the laboratory and the lithosphere. 2005 , 243, 143-158		40
1071	High-resolution 17O MAS NMR spectroscopy of forsterite (⊞-Mg2SiO4), wadsleyite (EMg2SiO4), and ringwoodite (EMg2SiO4). 2005 , 90, 1861-1870		16
1070	Testing a potential mantle geohygrometer; the effect of dissolved water on the intracrystalline partitioning of Al in orthopyroxene. <i>Earth and Planetary Science Letters</i> , 2005 , 238, 342-350	5.3	23
1069	Upper mantle tomographic Vp and Vs images of the Rocky Mountains in Wyoming, Colorado and New Mexico: Evidence for a thick heterogeneous chemical lithosphere. 2005 , 329-345		8
1068	On the effect of a low viscosity asthenosphere on the temporal change of the geoidA challenge for future gravity missions. 2005 , 39, 493-511		7

Major and trace element composition of the depleted MORB mantle (DMM). <i>Earth and Planetary Science Letters</i> , 2005 , 231, 53-72	5.3	1802
Deep structure and seismic anisotropy beneath the East Pacific Rise. <i>Earth and Planetary Science Letters</i> , 2005 , 232, 259-272	5.3	45
1064 Archean cratons and mantle dynamics. <i>Earth and Planetary Science Letters</i> , 2005 , 234, 1-14	5.3	116
Storage capacity of H2O in nominally anhydrous minerals in the upper mantle. <i>Earth and Planetary Science Letters</i> , 2005 , 236, 167-181	5.3	238
Seismic constraints on temperature of the Australian uppermost mantle. <i>Earth and Planetary Science Letters</i> , 2005 , 236, 227-237	5.3	54
Thermo-mechanical model of the Dead Sea Transform. <i>Earth and Planetary Science Letters</i> , 2005 , 238, 78-95	5.3	72
Numerical simulations of subduction zones: Effect of slab dehydration on the mantle wedge dynamics. 2005 , 149, 133-153		355
Thermal expansivity and elastic properties of the lithospheric mantle: results from mineral physics of composites. 2005 , 149, 279-306		64
Phase relations in hydrous MORB at 18\(\mathbb{Z}\)8GPa: implications for heterogeneity of the lower mantle. 2005 , 150, 239-263		115
1057 From Snowball to Phaneorozic Earth. 2005 , 47, 775-791		67
Heterogeneity in southern Central Indian Ridge MORB: Implications for ridgellot spot interaction. Geochemistry, Geophysics, Geosystems, 2005, 6, n/a-n/a	3.6	35
Adiabat_1ph: A new public front-end to the MELTS, pMELTS, and pHMELTS models. <i>Geochemistry, Geophysics, Geosystems</i> , 2005 , 6,	3.6	307
1054 Mineralogy and elasticity of the oceanic upper mantle: Origin of the low-velocity zone. 2005 , 110,		212
1053 Upper mantle structure beneath the eastern Pacific Ocean ridges. 2005 , 110,		27
Fault slip rates, effects of elastic heterogeneity on geodetic data, and the strength of the lower crust in the Salton Trough region, southern California. 2005 , 110,		59
Improved estimate of tidal dissipation within Mars from MOLA observations of the shadow of Phobos. 2005 , 110,		79
1050 Physical, chemical, and chronological characteristics of continental mantle. 2005 , 43,		345

(2006-2005)

1048	Lower Crustal Magma Genesis and Preservation: a Stochastic Framework for the Evaluation of Basalt T rust Interaction. 2005 , 46, 2167-2195		281
1047	Numerical and Laboratory Studies of Mantle Convection: Philosophy, Accomplishments, and Thermochemical Structure and Evolution. 2005 , 83-99		19
1046	Numerical Study of the Origin and Stability of Chemically Distinct Reservoirs Deep in Earth's Mantle. 2005 , 117-136		7
1045	Self-Gravity, Self-Consistency, and Self-Organization in Geodynamics and Geochemistry. 2005 , 165-186		7
1044	Fingerprinting the water site in mantle olivine. <i>Geology</i> , 2005 , 33, 869	5	146
1043	The Structure of Hydrous Species in Nominally Anhydrous Minerals: Information from Polarized IR Spectroscopy. 2006 , 62, 29-52		36
1042	Hydrogen incorporation in olivine from 2🛭 2 GPa. 2006 , 91, 285-294		150
1041	The Andes. 2006 ,		46
1040	Shear stresses on megathrusts: Implications for mountain building behind subduction zones. 2006 , 111,		123
1039	Overriding plate thinning in subduction zones: Localized convection induced by slab dehydration. <i>Geochemistry, Geophysics, Geosystems</i> , 2006 , 7, n/a-n/a	3.6	50
1038	Mantle dynamics beneath the East Pacific Rise at 17°S: Insights from the Mantle Electromagnetic and Tomography (MELT) experiment. 2006 , 111, n/a-n/a		138
1037	Differences between Archean and Proterozoic lithospheres: Assessment of the possible major role of thermal conductivity. <i>Geochemistry, Geophysics, Geosystems</i> , 2006 , 7, n/a-n/a	3.6	26
1036	Melting a high 3He/4He source in a heterogeneous mantle. <i>Geochemistry, Geophysics, Geosystems</i> , 2006 , 7, n/a-n/a	3.6	17
1035	Evidence suggesting fluid flow beneath Japan due to periodic seismic triggering from the 2004 Sumatra-Andaman earthquake. <i>Geophysical Research Letters</i> , 2006 , 33,	4.9	75
1034	Influence of continental roots and asthenosphere on plate-mantle coupling. <i>Geophysical Research Letters</i> , 2006 , 33,	4.9	148
1033	Mantle melting as a function of water content beneath back-arc basins. 2006, 111,		200
1032	A thinned lithospheric image of the Tanlu Fault Zone, eastern China: Constructed from wave equation based receiver function migration. 2006 , 111,		150
1031	The thermal structure of subduction zone back arcs. 2006 , 111,		240

1030	Influence of a variable thermal conductivity on the thermochemical evolution of Mars. 2006, 111, n/a-n/	'a	40
1029	Along-ridge petrological segmentation of the mantle in the Oman ophiolite. <i>Geochemistry, Geophysics, Geosystems</i> , 2006 , 7, n/a-n/a	3.6	57
1028	Stirring in 3-d spherical models of convection in the Earth's mantle. 2006 , 86, 3175-3204		5
1027	Archean Geodynamics and the Thermal Evolution of Earth. 2006 , 7-32		109
1026	Creation and Preservation of Cratonic Lithosphere: Seismic Constraints And Geodynamic Models. 2006 , 75-88		13
1025	Geochemical/Petrologic Constraints on the Origin of Cratonic Mantle. 2006 , 89-114		43
1024	Modes of Crustal Accretion in Back-Arc Basins: Inferences from the Lau Basin. 2006 , 5-30		22
1023	Mantle Structure and Flow Patterns Beneath Active Back-Arc Basins Inferred from Passive Seismic and Electromagnetic Methods. 2006 , 43-62		2
1022	Chemical Systematics and Hydrous Melting of the Mantle in Back-Arc Basins. 2006, 87-146		60
1021	Remote Sensing of Hydrogen in Earth's Mantle. 2006 , 62, 343-375		55
1020	Volatile and trace elements in basaltic glasses from Samoa: Implications for water distribution in the mantle. <i>Earth and Planetary Science Letters</i> , 2006 , 241, 932-951	5.3	137
1019	Understanding cratonic flood basalts. Earth and Planetary Science Letters, 2006, 245, 190-201	5.3	63
1018	Ancient melt extraction from the oceanic upper mantle revealed by ReDs isotopes in abyssal peridotites from the Mid-Atlantic ridge. <i>Earth and Planetary Science Letters</i> , 2006 , 244, 606-621	5.3	232
1017	Mantle temperature variations beneath back-arc spreading centers inferred from seismology, petrology, and bathymetry. <i>Earth and Planetary Science Letters</i> , 2006 , 248, 30-42	5.3	67
1016	The effect of large melt fraction on the deformation behavior of peridotite. <i>Earth and Planetary Science Letters</i> , 2006 , 246, 177-187	5.3	79
1015	Lower slab boundary in the Japan subduction zone. Earth and Planetary Science Letters, 2006, 247, 101-	19.3	16
1014	Grain size sensitive deformation mechanisms in naturally deformed peridotites. <i>Earth and Planetary Science Letters</i> , 2006 , 248, 438-450	5.3	259
1013	Partitioning of water during melting of the Earth's upper mantle at H2O-undersaturated conditions. <i>Earth and Planetary Science Letters</i> , 2006 , 248, 715-734	5.3	361

(2006-2006)

1012	Mantle instability beneath the Sierra Nevada Mountains in California and Death Valley extension. Earth and Planetary Science Letters, 2006 , 251, 104-119	5.3	86
1011	Geochemical investigation of serpentinized oceanic lithospheric mantle in the Feather River Ophiolite, California: Implications for the recycling rate of water by subduction. 2006 , 235, 161-185		72
1010	Matrix effects in hydrogen isotope analysis of silicate glasses by SIMS. 2006 , 235, 352-365		57
1009	Dynamics, crustal thicknesses, seismic anomalies, and electrical conductivities in dry and hydrous ridge-centered plumes. 2006 , 155, 16-41		11
1008	Water content and geotherm in the upper mantle above the stagnant slab: Interpretation of electrical conductivity and seismic P-wave velocity models. 2006 , 155, 1-15		92
1007	Effect of water and stress on the lattice-preferred orientation of olivine. 2006, 421, 1-22		279
1006	16. The Role of Water in High-Temperature Rock Deformation. 2006 , 377-396		16
1005	2. The Structure of Hydrous Species in Nominally Anhydrous Minerals: Information from Polarized IR Spectroscopy. 2006 , 29-52		13
1004	15. Remote Sensing of Hydrogen in Earth's Mantle. 2006 , 343-376		24
1003	4. Thermal and Magmatic Evolution of the Moon. 2006 , 365-518		60
1002	19. Water and Geodynamics. 2006 , 451-474		2
1001	17. The Effect of Water on Mantle Phase Transitions. 2006 , 397-420		4
1000	Electrical structure beneath the northern MELT line on the East Pacific Rise at 15°45?S. <i>Geophysical Research Letters</i> , 2006 , 33,	4.9	15
999	Applications of Vibrational Spectroscopy to Geology. 2006,		1
998	Effect of lithospheric root on decompression melting in plume-lithosphere interaction models. <i>Geophysical Journal International</i> , 2006 , 164, 259-270	2.6	16
997	Estimation of the average contents of H2O, Cl, F, and S in the depleted mantle on the basis of the compositions of melt inclusions and quenched glasses of mid-ocean ridge basalts. 2006 , 44, 209-231		26
996	Viscosity of the Martian mantle and its initial temperature: Constraints from crust formation history and the evolution of the magnetic field. 2006 , 54, 153-169		93
995	Water and Geodynamics. 2006 , 62, 451-473		15

994	WATER, MELTING, AND THE DEEP EARTH H2O CYCLE. 2006 , 34, 629-653	428
993	Composition and chemical structure of oceanic mantle plumes. 2006, 14, 452-476	13
992	Solubility and partitioning of water in synthetic forsterite and enstatite in the system MgOBiO2H2O-Al2O3. 2006 , 151, 651-664	46
991	D/H exchange in pure and Cr-doped enstatite: implications for hydrogen diffusivity. 2006 , 33, 601-611	27
990	Water content in natural eclogite and implication for water transport into the deep upper mantle. 2006 , 86, 245-259	111
989	Surface topography and internal strain variation in wide hot orogens from three-dimensional analogue and two-dimensional numerical vice models. 2006 , 253, 79-104	40
988	Deformation of olivine at mantle pressure using the D-DIA. 2006 , 18, 7-19	53
987	The westward drift of the lithosphere: A rotational drag?. 2006 , 118, 199-209	51
986	Surface erosion control on the evolution of the deep lithosphere. <i>Geology</i> , 2006 , 34, 225	64
985	The Effect of Water on Mantle Phase Transitions. 2006 , 62, 397-420	41
984	Sampling the Cape Verde Mantle Plume: Evolution of Melt Compositions on Santo Antö, Cape Verde Islands. 2006 , 47, 145-189	99
983	The Partitioning of Water Between Nominally Anhydrous Minerals and Silicate Melts. 2006, 62, 231-241	26
982	The Role of Water in High-Temperature Rock Deformation. 2006 , 62, 377-396	83
981	Curvature of oceanic arcs. <i>Geology</i> , 2006 , 34, 877	106
980	Rapid magma ascent recorded by water diffusion profiles in mantle olivine. <i>Geology</i> , 2006 , 34, 429 5	217
979	Thermal and Magmatic Evolution of the Moon. 2006 , 60, 365-518	273
978	From point defects to plate tectonic faults. 2006 , 86, 3373-3392	16
977	Theory and Observations IWave Propagation in Anisotropic Media. 2007 , 289-321	35

(2007-2007)

	Early Paleozoic Tectonic and Thermomechanical Evolution of Ultrahigh-Pressure (UHP) Metamorphic Rocks in the Northern Tibetan Plateau, Northwest China. 2007 , 49, 681-716	151
975	Water solubility in aluminous orthopyroxene and the origin of Earth's asthenosphere. 2007 , 315, 364-8	198
974	Properties of Rocks and Minerals ©constitutive Equations, Rheological Behavior, and Viscosity of Rocks. 2007 , 389-417	21
973	Seismic Anisotropy of the Deep Earth from a Mineral and Rock Physics Perspective. 2007 , 437-491	63
972	Thermal Evolution of the Mantle. 2007 , 197-216	11
971	Water, the Solid Earth, and the Atmosphere: The Genesis and Effects of a Wet Surface on a Mostly Dry Planet. 2007 , 121-143	
970	Petrology and Mineral Chemistry of Lower Crustal Intrusions: the Chilas Complex, Kohistan (NW Pakistan). 2007 , 48, 1895-1953	122
969	Physics of Mantle Convection. 2007 , 31-87	16
968	Mantle Geochemical Geodynamics. 2007 , 437-505	7
967	Partial Melting Experiments of Peridotite + CO2 at 3 GPa and Genesis of Alkalic Ocean Island Basalts. 2007 , 48, 2093-2124	404
966	Effects of a lithospheric weak zone on postglacial seismotectonics in eastern Canada and the	
	northeastern United States. 2007 ,	3
965		12
965	Global plume-fed asthenosphere flow[] Motivation and model development. 2007, 165-188	12
965 964	Global plume-fed asthenosphere flow Motivation and model development. 2007, 165-188 Geochemistry. Fuel for plate tectonics. 2007, 315, 338-9	12 6
965 964 963	Global plume-fed asthenosphere flow Motivation and model development. 2007, 165-188 Geochemistry. Fuel for plate tectonics. 2007, 315, 338-9 Geodynamic models for earthquake studies in intraplate North America. 2007, Bounds on the viscosity coefficient of continental lithosphere from removal of mantle lithosphere	12 6 21
965 964 963 962	Global plume-fed asthenosphere flowli Motivation and model development. 2007, 165-188 Geochemistry. Fuel for plate tectonics. 2007, 315, 338-9 Geodynamic models for earthquake studies in intraplate North America. 2007, Bounds on the viscosity coefficient of continental lithosphere from removal of mantle lithosphere beneath the Altiplano and Eastern Cordillera. 2007, 26, n/a-n/a Reply to the comments of S. Karato on Petrofabrics and seismic properties of garnet peridotites	12 6 21 35

958	Are Archean lithospheric keels inverted?. Earth and Planetary Science Letters, 2007, 254, 393-403	5.3	41
957	Possible density segregation of subducted oceanic lithosphere along a weak serpentinite layer and implications for compositional stratification of the Earth's mantle. <i>Earth and Planetary Science Letters</i> , 2007 , 255, 357-366	5.3	40
956	Slab surface temperature in subduction zones: Influence of the interplate decoupling depth and upper plate thinning processes. <i>Earth and Planetary Science Letters</i> , 2007 , 255, 324-338	5.3	59
955	Secular cooling and thermal structure of continental lithosphere. <i>Earth and Planetary Science Letters</i> , 2007 , 257, 83-96	5.3	33
954	Effective thermal expansivity of Maxwellian oceanic lithosphere. <i>Earth and Planetary Science Letters</i> , 2007 , 257, 343-349	5.3	29
953	Seismic attenuation near the East Pacific Rise and the origin of the low-velocity zone. <i>Earth and Planetary Science Letters</i> , 2007 , 258, 260-268	5.3	77
952	The partitioning of water between olivine, orthopyroxene and melt synthesised in the system albiteforsterite⊞2O. <i>Earth and Planetary Science Letters</i> , 2007 , 260, 227-241	5.3	53
951	A dynamical model for generating sharp seismic velocity contrasts underneath continents: Application to the Sorgenfreillornquist Zone. <i>Earth and Planetary Science Letters</i> , 2007 , 262, 77-91	5.3	37
950	Subduction zone evolution and low viscosity wedges and channels. <i>Earth and Planetary Science Letters</i> , 2007 , 264, 22-45	5.3	98
949	Rapid mantle flow beneath the Tonga volcanic arc. Earth and Planetary Science Letters, 2007, 264, 299-	30 7 3	47
948	The split fate of the early Earth, Mars, Venus, and Moon. 2007, 339, 917-927		30
947	Chemical composition of Earth's primitive mantle and its variance: 2. Implications for global geodynamics. 2007 , 112,		34
946	The Dynamics and Convective Evolution of the Upper Mantle. 2007, 305-323		3
945	Hot Spots and Melting Anomalies. 2007 , 371-435		16
944	Tectonic and Thermal Evolution of Venus and the Role of Volatiles: Implications for Understanding the Terrestrial Planets. 2007 , 45-71		15
943	Effect of variable carbonate concentration on the solidus of mantle peridotite. 2007 , 92, 370-379		104
942	Viscosity structure of the crust and upper mantle in western Nevada from isostatic rebound patterns of the late Pleistocene Lake Lahontan high shoreline. 2007 , 112,		50
941	Continental magmatism, volatile recycling, and a heterogeneous mantle caused by lithospheric gravitational instabilities. 2007 , 112,		119

(2007-2007)

940	Decompaction weakening and channeling instability in ductile porous media: Implications for asthenospheric melt segregation. 2007 , 112,		89
939	Early evolution of Mars with mantle compositional stratification or hydrothermal crustal cooling. 2007 , 112,		40
938	North American dynamics and western U.S. tectonics. 2007 , 45, n/a-n/a		104
937	Effective elastic thickness of South America and its implications for intracontinental deformation. <i>Geochemistry, Geophysics, Geosystems</i> , 2007 , 8, n/a-n/a	3.6	86
936	Evaluating hot spotfidge interaction in the Atlantic from regional-scale seismic observations. <i>Geochemistry, Geophysics, Geosystems</i> , 2007 , 8, n/a-n/a	3.6	23
935	Anomalous uplift of the Apennines and subsidence of the Adriatic: The result of active mantle flow?. <i>Geophysical Research Letters</i> , 2007 , 34,	4.9	17
934	Crystallization pressures of mid-ocean ridge basalts derived from major element variations of glasses from equilibrium and fractional crystallization experiments. 2007 , 112,		41
933	Rayleigh wave tomography beneath intraplate volcanic ridges in the South Pacific. 2007, 112,		56
932	Thermal cracking and the deep hydration of oceanic lithosphere: A key to the generation of plate tectonics?. 2007 , 112,		101
931	Stress, strain, and B-type olivine fabric in the fore-arc mantle: Sensitivity tests using high-resolution steady-state subduction zone models. 2007 , 112,		78
930	Diffusion creep of dry, melt-free olivine. 2007 , 112,		79
929	Global mantle flow and the development of seismic anisotropy: Differences between the oceanic and continental upper mantle. 2007 , 112,		120
928	P-to-S and S-to-P imaging of a sharp lithosphere-asthenosphere boundary beneath eastern North America. 2007 , 112,		132
927	Upper mantle structure beneath the Galpagos Archipelago from surface wave tomography. 2007 , 112,		49
926	Surface wave tomography of the upper mantle beneath the Reykjanes Ridge with implications for ridgeBot spot interaction. 2007 , 112,		33
925	Impact-induced convection as the main mechanism for formation of lunar mare basalts. 2007, 112,		29
924	Density structure and buoyancy of the oceanic lithosphere revisited. <i>Geophysical Research Letters</i> , 2007 , 34,	4.9	68
923	Instability of a chemically dense layer heated from below and overlain by a deep less viscous fluid. 2007 , 572, 433-469		31

922	Plate Rheology and Mechanics. 2007, 99-151		7
921	Heat Flow and Thermal Structure of the Lithosphere. 2007 , 217-251		21
920	Water follows carbon: CO2 incites deep silicate melting and dehydration beneath mid-ocean ridges. <i>Geology</i> , 2007 , 35, 135	5	85
919	Mantle Melting Beneath Mid-Ocean Ridges. 2007 , 20, 78-89		27
918	Volatiles in basaltic magmas of ocean islands and their mantle sources: II. Estimation of contents in mantle reservoirs. 2007 , 45, 313-326		6
917	Variation in styles of rifting in the Gulf of California. <i>Nature</i> , 2007 , 448, 466-9	50.4	211
916	Space geodesy validation of the global lithospheric flow. <i>Geophysical Journal International</i> , 2007 , 168, 491-506	2.6	62
915	Convective vigour and heat flow in chemically differentiated systems. <i>Geophysical Journal International</i> , 2007 , 169, 747-766	2.6	5
914	On subducting slab entrainment of buoyant asthenosphere. <i>Terra Nova</i> , 2007 , 19, 167-173	3	27
913	Controls of stable continental lithospheric thickness: the role of basal drag. 2007 , 96, 299-314		5
912	Average compositions of magmas and mantle sources of mid-ocean ridges and intraplate oceanic and continental settings estimated from the data on melt inclusions and quenched glasses of basalts. 2007 , 15, 335-368		16
911	High-pressure properties of diaspore, AlO(OH). 2007 , 34, 145-157		36
910	TC/EA-MS online determination of hydrogen isotope composition and water concentration in eclogitic garnet. 2007 , 34, 687-698		85
909	The Role of History-Dependent Rheology in Plate Boundary Lubrication for Generating One-Sided Subduction. 2007 , 164, 879-907		25
908	Water, Life, and Planetary Geodynamical Evolution. 2007, 129, 167-203		25
907	Water partitioning between mantle minerals from peridotite xenoliths. 2007 , 154, 15-34		151
906	Influence of hydrogen on FeMg interdiffusion in (Mg,Fe)O and implications for Earth lower mantle. 2007 , 154, 279-289		34
905	A modified iterative sandwich method for determination of near-solidus partial melt compositions. I. Theoretical considerations. 2007 , 154, 635-645		15

904	H2O storage capacity of MgSiO3 clinoenstatite at 8🗓 3 GPa, 1,100🗓,400°C. 2007 , 154, 663-674		31
903	Grain boundaries: a possible water reservoir in the Earth mantle?. 2008, 94, 1-8		15
902	Hydrogen partitioning between melt, clinopyroxene, and garnet at 3 GPa in a hydrous MORB with 6 wt.% H2O. 2008 , 156, 607-625		54
901	Hydrogen bonding and diffusion in mullite. 2008 , 28, 393-400		5
900	Laboratory Studies of the Rheological Properties of Minerals under Deep-Mantle Conditions. 2008 , 4, 191-196		30
899	Volatile content of lunar volcanic glasses and the presence of water in the Moon's interior. <i>Nature</i> , 2008 , 454, 192-5	50.4	420
898	Scaling relations of earthquakes and aseismic deformation in a damage rheology model. <i>Geophysical Journal International</i> , 2008 , 172, 651-662	2.6	57
897	Radial profiles of seismic attenuation in the upper mantle based on physical models. <i>Geophysical Journal International</i> , 2008 , 175, 116-134	2.6	22
896	Seismic evidence for a sharp lithospheric base persisting to the lowermost mantle beneath the Caribbean. <i>Geophysical Journal International</i> , 2008 , 174, 1019-1028	2.6	27
895	Topography associated with crustal flow in continental collisions, with application to Tibet. <i>Geophysical Journal International</i> , 2008 , 175, 375-385	2.6	19
894	Three-dimensional passive mantle flow beneath mid-ocean ridges: an analytical approach. <i>Geophysical Journal International</i> , 2008 , 175, 783-805	2.6	18
893	Plate tectonics, flood basalts and the evolution of Earth oceans. <i>Terra Nova</i> , 2008 , 20, 419-439	3	86
892	Regional conductance map of Andaman and Nicobar region. <i>Gondwana Research</i> , 2008 , 13, 386-395	5.1	5
891	Dynamics of cratons in an evolving mantle. 2008 , 102, 12-24		63
890	Formation of continental flood volcanism IThe perspective of setting of melting. 2008, 100, 49-65		24
889	Continental plate collision, PIED conditions and unstable vs. stable plate dynamics: Insights from thermo-mechanical modelling. 2008 , 103, 178-204		98
888	High-resolution numerical modeling of stress distribution in visco-elasto-plastic subducting slabs. 2008 , 103, 205-216		39
887	Plate tectonics on the early Earth: Limitations imposed by strength and buoyancy of subducted lithosphere. 2008 , 103, 217-235		197

886	Quantitative absorbance spectroscopy with unpolarized light: Part II. Experimental evaluation and development of a protocol for quantitative analysis of mineral IR spectra. 2008 , 93, 765-778		116
885	Ductile deformation of passive margins: A new mechanism for subduction initiation. 2008, 113,		27
884	Effective elastic thickness variations along the Andean margin and their relationship to subduction geometry. <i>Geochemistry, Geophysics, Geosystems</i> , 2008 , 9, n/a-n/a	3.6	62
883	Integrated geophysical-petrological modeling of the lithosphere and sublithospheric upper mantle: Methodology and applications. <i>Geochemistry, Geophysics, Geosystems</i> , 2008 , 9, n/a-n/a	3.6	162
882	Back-arc strain in subduction zones: Statistical observations versus numerical modeling. <i>Geochemistry, Geophysics, Geosystems</i> , 2008 , 9, n/a-n/a	3.6	42
881	Heat sources for mantle plumes. <i>Geochemistry, Geophysics, Geosystems</i> , 2008 , 9, n/a-n/a	3.6	2
880	A new analysis of experimental data on olivine rheology. 2008 , 113,		133
879	Attenuation in the upper mantle beneath Southern California: Physical state of the lithosphere and asthenosphere. 2008 , 113,		30
878	Grain size variations in the Earth's mantle and the evolution of primordial chemical heterogeneities. 2008 , 113,		52
877	Active megadetachment beneath the western United States. 2008, 113,		33
876	Water contents in mantle xenoliths from the Colorado Plateau and vicinity: Implications for the mantle rheology and hydration-induced thinning of continental lithosphere. 2008 , 113,		180
875	Internal distribution of Li and B in serpentinites from the Feather River Ophiolite, California, based on laser ablation inductively coupled plasma mass spectrometry. <i>Geochemistry, Geophysics, Geosystems</i> , 2008 , 9, n/a-n/a	3.6	28
874	Axial high topography and partial melt in the crust and mantle beneath the western Galpagos Spreading Center. <i>Geochemistry, Geophysics, Geosystems</i> , 2008 , 9, n/a-n/a	3.6	5
873	Geochemistry. Carbon in charge. 2008 , 322, 1338-40		5
872	Effects of water and iron content on the rheological contrast between garnet and olivine. 2008 , 166, 57-66		53
871	The effect of water on Si and O diffusion rates in olivine and implications for transport properties and processes in the upper mantle. 2008 , 166, 11-29		106
870	From passive continental margin to mountain belt: Insights from analytical and numerical models and application to Taiwan. 2008 , 171, 235-251		71
869	Three-dimensional numerical models of the evolution of pull-apart basins. 2008 , 171, 387-399		44

868	On the orientation of tensile dikes in a ridge-centered plume. 2008 , 447, 19-30		3
867	Effects of hydration on the elastic properties of olivine. <i>Geophysical Research Letters</i> , 2008 , 35,	4.9	55
866	Numerical models of stiffness and yield stress growth in crystal-melt suspensions. <i>Earth and Planetary Science Letters</i> , 2008 , 267, 32-44	5.3	28
865	A plume model of transient diachronous uplift at the Earth's surface. <i>Earth and Planetary Science Letters</i> , 2008 , 267, 146-160	5.3	58
864	Pressure and temperature dependence of H solubility in forsterite: An implication to water activity in the Earth interior. <i>Earth and Planetary Science Letters</i> , 2008 , 268, 354-363	5.3	77
863	Discordant contrasts of P- and S-wave speeds across the 660-km discontinuity beneath Tibet: A case for hydrous remnant of sub-continental lithosphere. <i>Earth and Planetary Science Letters</i> , 2008 , 268, 450-462	5.3	17
862	Thermally induced brittle deformation in oceanic lithosphere and the spacing of fracture zones. <i>Earth and Planetary Science Letters</i> , 2008 , 269, 259-270	5.3	11
861	Thinning of continental backarc lithosphere by flow-induced gravitational instability. <i>Earth and Planetary Science Letters</i> , 2008 , 269, 436-447	5.3	56
860	The role of water in connecting past and future episodes of subduction. <i>Earth and Planetary Science Letters</i> , 2008 , 273, 15-27	5.3	88
859	Numerical modelling of lithosphere literaction in a subduction zone. Earth and Planetary Science Letters, 2008, 272, 698-708	5.3	26
858	Water in minerals of the continental lithospheric mantle and overlying lower crust: A comparative study of peridotite and granulite xenoliths from the North China Craton. 2008 , 256, 33-45		109
857	Effects of compositional and rheological stratifications on small-scale convection under the oceans: Implications for the thickness of oceanic lithosphere and seafloor flattening. <i>Geophysical Research Letters</i> , 2008 , 35,	4.9	36
856	Near-surface diagnostics of dripping or delaminating lithosphere. 2008, 113,		118
855	Urey ratio and the structure and evolution of Earth's mantle. 2008, 46,		225
854	Effects of hydration on the structure and compressibility of wadsleyite, E(Mg2SiO4). 2008, 93, 598-607		36
853	Ultra-refractory Domains in the Oceanic Mantle Lithosphere Sampled as Mantle Xenoliths at Ocean Islands. 2008 , 49, 1223-1251		56
852	Rogue mantle helium and neon. 2008 , 319, 943-5		44
851	Basal Subduction Tectonic Erosion (STE), Butter Mlanges, and the Construction and Exhumation of HP-UHP Belts: The Alps Example and Some Comparisons. 2008 , 50, 685-754		1

850	Water in natural olivine⊞etermined by proton-proton scattering analysis. 2008, 93, 1613-1619		20
849	Strength and deformation of planetary lithospheres. 397-456		10
848	Geochemical Architecture of the Lower- to Middle-crustal Section of a Paleo-island Arc (Kohistan Complex, Jijal K amila Area, Northern Pakistan): Implications for the Evolution of an Oceanic Subduction Zone. 2009 , 50, 531-569		78
847	Hydrogen incorporation in Fe- and Na-doped diopsides. 2009 , 21, 691-704		11
846	The onset of the North Atlantic Igneous Province in a rifting perspective. 2009 , 146, 309-325		41
845	Thermal evolution of cratonic roots. 2009 , 109, 47-60		72
844	Origin of Archean subcontinental lithospheric mantle: Some petrological constraints. 2009 , 109, 61-71		89
843	An overview of electrical conductivity structures of the crust and upper mantle beneath the northwestern Pacific, the Japanese Islands, and continental East Asia. <i>Gondwana Research</i> , 2009 , 16, 545-562	5.1	35
842	Wet∏ow angle subduction: a possible mechanism below the Tanzania craton 2 Ga ago. 2009 , 96, 113-12	0	7
841	Implications of large elastic thicknesses for the composition and current thermal state of Mars. 2009 , 201, 540-548		30
840	North Arch volcanic fields near Hawaii are evidence favouring the restite-root hypothesis for the origin of hotspot swells. <i>Terra Nova</i> , 2009 , 21, 452-466	3	17
839	Dynamical modelling of lithospheric extension and small-scale convection: implications for magmatism during the formation of volcanic rifted margins. <i>Geophysical Journal International</i> , 2009 , 176, 327-350	2.6	37
838	Constraints on shallow low-viscosity zones in Northern Europe from future GOCE gravity data. <i>Geophysical Journal International</i> , 2009 , 178, 65-84	2.6	12
837	Mantle reflectivity structure beneath oceanic hotspots. <i>Geophysical Journal International</i> , 2009 , 178, 1456-1472	2.6	23
836	Scaling of stagnant-lid convection with Arrhenius rheology and the effects of mantle melting. <i>Geophysical Journal International</i> , 2009 , 179, 154-170	2.6	50
835	Volatile accretion history of the terrestrial planets and dynamic implications. <i>Nature</i> , 2009 , 461, 1227-3	350.4	324
834	Permeability of asthenospheric mantle and melt extraction rates at mid-ocean ridges. <i>Nature</i> , 2009 , 462, 209-12	50.4	75
833	Strain coupling between upper mantle and lower crust: natural example from the B\(\beta\)tvina granulite body, Bohemian Massif. 2009 , 27, 721-737		18

(2009-2009)

832	Emergence of a low-viscosity channel in subduction zones through the coupling of mantle flow and thermodynamics. <i>Earth and Planetary Science Letters</i> , 2009 , 278, 243-256	5.3	259
831	Implications of grain size evolution on the seismic structure of the oceanic upper mantle. <i>Earth and Planetary Science Letters</i> , 2009 , 282, 178-189	5.3	99
830	Well-wetted olivine grain boundaries in partially molten peridotite in the asthenosphere. <i>Earth and Planetary Science Letters</i> , 2009 , 283, 167-173	5.3	33
829	Global seismological shear velocity and attenuation: A comparison with experimental observations. <i>Earth and Planetary Science Letters</i> , 2009 , 284, 65-75	5.3	69
828	Seismic scatterers at the shallowest lower mantle beneath subducted slabs. <i>Earth and Planetary Science Letters</i> , 2009 , 286, 304-315	5.3	44
827	Seismological and experimental constraints on metastable phase transformations and rheology of the Mariana slab. <i>Earth and Planetary Science Letters</i> , 2009 , 287, 12-23	5.3	37
826	The volatile contents of the Galapagos plume; evidence for H2O and F open system behavior in melt inclusions. <i>Earth and Planetary Science Letters</i> , 2009 , 287, 442-452	5.3	67
825	Effect of plate bending on the Urey ratio and the thermal evolution of the mantle. <i>Earth and Planetary Science Letters</i> , 2009 , 287, 513-518	5.3	84
824	The effect of water on the electrical conductivity of olivine aggregates and its implications for the electrical structure of the upper mantle. <i>Earth and Planetary Science Letters</i> , 2009 , 288, 291-300	5.3	173
823	Inversion of extensional sedimentary basins: A numerical evaluation of the localisation of shortening. <i>Earth and Planetary Science Letters</i> , 2009 , 288, 492-504	5.3	55
822	Hydrogen partitioning between nominally anhydrous upper mantle minerals and melt between 3 and 5 GPa and applications to hydrous peridotite partial melting. 2009 , 262, 42-56		139
821	Trace element partitioning between garnet lherzolite and carbonatite at 6.6 and 8.6 GPa with applications to the geochemistry of the mantle and of mantle-derived melts. 2009 , 262, 57-77		184
820	Volatiles and volatile-bearing melts in the Earth's interior. 2009 , 262, 1-3		7
819	Fluid source-based modeling of melt initiation within the subduction zone mantle wedge: Implications for geochemical trends in arc lavas. 2009 , 266, 297-310		11
818	Noble gas isotopic compositions of mantle xenoliths from northwestern Pacific lithosphere. 2009 , 268, 313-323		18
817	The importance of melt extraction for tracing mantle heterogeneity. 2009 , 73, 218-238		164
816	Styles of lithospheric extension controlled by underplated mafic bodies. 2009, 468, 169-184		28
815	The three-dimensional thermo-mechanical signature of ridge subduction and slab window migration. 2009 , 464, 70-83		62

814	Tectonic features of the incipient arc-continent collision zone of Taiwan: Implications for seismicity. 2009 , 479, 28-42	67
813	Seismic structure and origin of active intraplate volcanoes in Northeast Asia. 2009 , 470, 257-266	32
812	Convergence of aqueous fluid at the corner of the mantle wedge: Implications for a generation mechanism of deep low-frequency earthquakes. 2009 , 469, 85-92	13
811	Siberian meimechites: origin and relation to flood basalts and kimberlites. 2009 , 50, 999-1033	104
810	Shear deformation of dry polycrystalline olivine under deep upper mantle conditions using a rotational Drickamer apparatus (RDA). 2009 , 174, 128-137	72
809	Experimental deformation of olivine single crystals at mantle pressures and temperatures. 2009 , 172, 74-83	79
808	New measurements of activation volume in olivine under anhydrous conditions. 2009 , 172, 67-73	57
807	Dehydration melting of nominally anhydrous mantle: The primacy of partitioning. 2009 , 176, 54-68	201
806	Potential role of strain hardening in the cessation of rifting at constant tectonic force. 2009 , 47, 47-62	8
805	Tectonics and thermal structure of western Satpura, India. 2009 , 34, 450-457	9
804	Lithospheric stress-states predicted from long-term tectonic models: Influence of rheology and possible application to Taiwan. 2009 , 36, 119-134	23
803	Shearing Melt Out of the Earth: An Experimentalist's Perspective on the Influence of Deformation on Melt Extraction. 2009 , 37, 561-593	146
802	Constraints on asthenospheric flow from the depths of oceanic spreading centers: The East Pacific Rise and the Australian-Antarctic Discordance. <i>Geochemistry, Geophysics, Geosystems,</i> 2009 , 10, n/a-n/a	15
801	Intraplate volcanism with complex age-distance patterns: A case for small-scale sublithospheric convection. <i>Geochemistry, Geophysics, Geosystems</i> , 2009 , 10, n/a-n/a	54
800	Destruction of lithosphere within the north China craton inferred from surface wave tomography. Geochemistry, Geophysics, Geosystems, 2009, 10, n/a-n/a	43
799	Geophysics. The thickness of tectonic plates. 2009 , 324, 474-6	67
798	Palaeoproterozoic supercontinents and global evolution: correlations from core to atmosphere. 2009 , 323, 1-26	76
797	Seismic evidence for sharp lithosphere-asthenosphere boundaries of oceanic plates. 2009 , 324, 499-502	391

(2010-2009)

796	Localization of shear along a lithospheric strength discontinuity: Application of a continuous deformation model to the boundary between Tibet and the Tarim Basin. 2009 , 28, n/a-n/a		36
795	Global electromagnetic induction constraints on transition-zone water content variations. <i>Nature</i> , 2009 , 460, 1003-6	50.4	183
794	Water-induced convection in the Earth's mantle transition zone. 2009 , 114,		51
793	First principles investigation of the structural and elastic properties of hydrous wadsleyite under pressure. 2009 , 114,		31
792	Viscosity of the asthenosphere from glacial isostatic adjustment and subduction dynamics at the northern Cascadia subduction zone, British Columbia, Canada. 2009 , 114,		49
791	Amphibole equilibria in mantle rocks: Determining values of mantle aH2O and implications for mantle H2O contents. 2009 , 94, 41-52		19
79 ⁰	Water in enstatite from Mid-Atlantic Ridge peridotite: Evidence for the water content of suboceanic mantle?. <i>Geology</i> , 2009 , 37, 543-546	5	50
789	Fluid-metasomatized mantle beneath the Ouachita belt of southern Laurentia: Fate of lithospheric mantle in a continental orogenic belt. 2009 , 1, 370-383		16
788	Source Parameters for Moderate Earthquakes in the Zagros Mountains with Implications for the Depth Extent of Seismicity. 2009 , 99, 2044-2049		15
787	THERMODYNAMIC LIMITS ON MAGNETODYNAMOS IN ROCKY EXOPLANETS. 2010 , 718, 596-609		66
786	Displacements of ridges and subduction zones in the models of mantle convection with lithospheric plates. 2010 , 46, 807-816		2
7 ⁸ 5	The Lithosphere-Asthenosphere Boundary. 2010 , 38, 551-575		312
7 ⁸ 4	Mechanisms for incorporation of hydrogen in and on terrestrial planetary surfaces. 2010 , 208, 425-437		42
7 ⁸ 3	The influence of mantle melting on the evolution of Mars. 2010 , 210, 43-57		65
782	Hydrogen diffusion in spinel grain boundaries and consequences for chemical homogenization in hydrous peridotite. 2010 , 160, 887-898		23
781	Dislocation creep accommodated by grain boundary sliding in dunite. 2010 , 21, 541-554		32
78o	A review of water contents of nominally anhydrous natural minerals in the mantles of Earth, Mars and the Moon. 2010 , 197, 239-258		152
779	Lithospheric thickness, thinning, subduction, and interaction with the asthenosphere beneath China from the joint inversion of seismic S-wave train fits and Rayleigh-wave dispersion curves. 2010 , 120, 116-130		24

778	A review of water contents and ductile deformation mechanisms of olivine: Implications for the lithosphere Bsthenosphere boundary of continents. 2010 , 120, 30-41		36
777	Rheology of the Earth's mantle: A historical review. <i>Gondwana Research</i> , 2010 , 18, 17-45	5.1	84
776	The interaction of fluid inclusions and migrating grain boundaries in a rock analogue: deformation and annealing of polycrystalline camphor@thanol mixtures. 2010 , 28, 1-18		17
775	Temporal evolution of the stress state in a supercontinent during mantle reorganization. <i>Geophysical Journal International</i> , 2010 , 180, 1-22	2.6	22
774	Long wavelength convection, PoiseuilleCouette flow in the low-viscosity asthenosphere and the strength of plate margins. <i>Geophysical Journal International</i> , 2010 , 180, 23-33	2.6	62
773	Water and its influence on the lithosphere-asthenosphere boundary. <i>Nature</i> , 2010 , 467, 448-51	50.4	238
772	Fragmentation of active continental plate margins owing to the buoyancy of the mantle wedge. <i>Nature Geoscience</i> , 2010 , 3, 257-261	18.3	49
771	Geophysical implications of Izu B onin mantle wedge hydration from chemical geodynamic modeling. 2010 , 19, 134-150		4
770	Stress-driven Melt Segregation in Partially Molten Feldspathic Rocks. 2010 , 51, 9-19		36
769	Letter. FTIR spectroscopy with a focal plane array detector: A novel tool to monitor the spatial OH-defect distribution in single crystals applied to synthetic enstatite. 2010 , 95, 888-891		10
768	First-principles study of the effect of water on the phase transitions in Mg2SiO4 forsterite. 2010 , 30, 318-324		4
767	Mechanisms of geochemical and geophysical variations along the western Galpagos Spreading Center. <i>Geochemistry, Geophysics, Geosystems</i> , 2010 , 11, n/a-n/a	3.6	41
766	Control of the symmetry of plume-ridge interaction by spreading ridge geometry. <i>Geochemistry, Geophysics, Geosystems</i> , 2010 , 11, n/a-n/a	3.6	42
765	Low water content of the Cenozoic lithospheric mantle beneath the eastern part of the North China Craton. 2010 , 115,		88
764	Earthquakes along the East African Rift System: A multiscale, system-wide perspective. 2010, 115,		56
763	New constraints on the properties of the Yellowstone mantle plume from P and S wave attenuation tomography. 2010 , 115,		8
762	Experimental constraints on the strength of the lithospheric mantle. 2010 , 115,		107
761	North American lithospheric discontinuity structure imaged by Ps and Sp receiver functions. 2010 , 115,		194

(2010-2010)

760	On the spatial variability of the Martian elastic lithosphere thickness: Evidence for mantle plumes?. 2010 , 115,		57
759	Upper mantle electrical resistivity structure beneath the central Mariana subduction system. <i>Geochemistry, Geophysics, Geosystems</i> , 2010 , 11,	3.6	61
758	Plate-driven mantle dynamics and global patterns of mid-ocean ridge bathymetry. <i>Geochemistry, Geophysics, Geosystems</i> , 2010 , 11, n/a-n/a	3.6	14
757	Samoan hot spot track on a flot spot highway[Implications for mantle plumes and a deep Samoan mantle source. <i>Geochemistry, Geophysics, Geosystems</i> , 2010 , 11, n/a-n/a	3.6	59
756	A mechanism for low-extent melts at the lithosphere-asthenosphere boundary. <i>Geochemistry, Geophysics, Geosystems</i> , 2010 , 11, n/a-n/a	3.6	45
755	Porosity-driven convection and asymmetry beneath mid-ocean ridges. <i>Geochemistry, Geophysics, Geosystems</i> , 2010 , 11, n/a-n/a	3.6	58
754	Organized melt, seismic anisotropy, and plate boundary lubrication. <i>Geochemistry, Geophysics, Geosystems</i> , 2010 , 11, n/a-n/a	3.6	108
753	Constraints on shallow mantle viscosity from morphology and deformation of fast-spreading ridges. <i>Geophysical Research Letters</i> , 2010 , 37, n/a-n/a	4.9	4
752	Geodynamic models of Archean continental collision and the formation of mantle lithosphere keels. <i>Geophysical Research Letters</i> , 2010 , 37, n/a-n/a	4.9	28
751	Scaling of plate tectonic convection with pseudoplastic rheology. 2010 , 115,		47
750	Long-wavelength stagnant lid convection with hemispheric variation in lithospheric thickness: Link between Martian crustal dichotomy and Tharsis?. 2010 , 115,		26
749	Possible crippling of the core dynamo of Mars by Borealis impact. 2010 , 115,		1
748	Evidence for low viscosity garnet-rich layers in the upper mantle. <i>Earth and Planetary Science Letters</i> , 2010 , 289, 54-67	5.3	6
747	Three-dimensional mantle lithosphere deformation at collisional plate boundaries: A subduction scissor across the South Island of New Zealand. <i>Earth and Planetary Science Letters</i> , 2010 , 289, 334-346	5.3	10
746	Small-scale sublithospheric convection reconciles geochemistry and geochronology of Buperplume Volcanism in the western and south Pacific. <i>Earth and Planetary Science Letters</i> , 2010 , 290, 224-232	5.3	42
745	Recent off-axis volcanism in the eastern Gulf of Aden: Implications for plumefidge interaction. <i>Earth and Planetary Science Letters</i> , 2010 , 293, 140-153	5.3	62
744	Preliminary three-dimensional model of mantle convection with deformable, mobile continental lithosphere. <i>Earth and Planetary Science Letters</i> , 2010 , 295, 205-218	5.3	59
743	Combining seismically derived temperature with heat flow and bathymetry to constrain the thermal structure of oceanic lithosphere. <i>Earth and Planetary Science Letters</i> , 2010 , 295, 390-400	5.3	21

742	Diffusion of hydrogen in olivine grain boundaries and implications for the survival of water-rich zones in the Earth's mantle. <i>Earth and Planetary Science Letters</i> , 2010 , 295, 305-313	5.3	68
741	The effect of tetrahedral Al3+ on the partitioning of water between clinopyroxene and silicate melt. <i>Earth and Planetary Science Letters</i> , 2010 , 297, 111-120	5.3	135
740	Geochemical and geophysical estimates of lithospheric thickness variation beneath Galpagos. <i>Earth and Planetary Science Letters</i> , 2010 , 300, 275-286	5.3	71
739	Steady-state laboratory flow laws alone fail to explain postseismic observations. <i>Earth and Planetary Science Letters</i> , 2010 , 300, 1-10	5.3	46
738	The lithospherellsthenosphere boundary and cratonic lithospheric layering beneath Australia from Sp wave imaging. <i>Earth and Planetary Science Letters</i> , 2010 , 300, 299-310	5.3	137
737	Shear-driven upwelling induced by lateral viscosity variations and asthenospheric shear: A mechanism for intraplate volcanism. 2010 , 178, 162-175		67
736	Partial melt in the oceanic low velocity zone. 2010 , 179, 60-71		201
735	The global range of subduction zone thermal models. 2010 , 183, 73-90		1044
734	Rheology of the deep upper mantle and its implications for the preservation of the continental roots: A review. 2010 , 481, 82-98		125
733	Dynamic models of continental rifting with melt generation. 2010 , 480, 33-47		40
733 732	Dynamic models of continental rifting with melt generation. 2010 , 480, 33-47 The effect of Al and water on the compressibility of diopside. 2010 , 95, 608-616		18
732	The effect of Al and water on the compressibility of diopside. 2010 , 95, 608-616 Insights from geodynamical modeling on possible fates of continental mantle lithosphere: collision, removal, and overturnThis article is one of a series of papers published in this Special Issue on the	3.6	18
73 ²	The effect of Al and water on the compressibility of diopside. 2010 , 95, 608-616 Insights from geodynamical modeling on possible fates of continental mantle lithosphere: collision, removal, and overturnThis article is one of a series of papers published in this Special Issue on the theme Lithoprobe [barameters, processes, and the evolution of a continent 2010 , 47, 541-563 Lateral, radial, and temporal variations in upper mantle viscosity and rheology under Scandinavia.	3.6 3.6	18
73 ² 73 ¹ 73 ⁰	The effect of Al and water on the compressibility of diopside. 2010 , 95, 608-616 Insights from geodynamical modeling on possible fates of continental mantle lithosphere: collision, removal, and overturnThis article is one of a series of papers published in this Special Issue on the theme Lithoprobe [barameters, processes, and the evolution of a continent 2010 , 47, 541-563 Lateral, radial, and temporal variations in upper mantle viscosity and rheology under Scandinavia. <i>Geochemistry, Geophysics, Geosystems</i> , 2011 , 12, n/a-n/a Thin oceanic crust and flood basalts: India-Seychelles breakup. <i>Geochemistry, Geophysics</i> ,		18 24 18
73 ² 73 ¹ 73 ⁰ 729	The effect of Al and water on the compressibility of diopside. 2010, 95, 608-616 Insights from geodynamical modeling on possible fates of continental mantle lithosphere: collision, removal, and overturnThis article is one of a series of papers published in this Special Issue on the theme Lithoprobe [parameters, processes, and the evolution of a continent 2010, 47, 541-563 Lateral, radial, and temporal variations in upper mantle viscosity and rheology under Scandinavia. Geochemistry, Geophysics, Geosystems, 2011, 12, n/a-n/a Thin oceanic crust and flood basalts: India-Seychelles breakup. Geochemistry, Geophysics, Geosystems, 2011, 12, n/a-n/a Imaging the seismic lithosphere-asthenosphere boundary of the oceanic plate. Geochemistry,	3.6	18 24 18 32
73 ² 73 ¹ 73 ⁰ 729 728	The effect of Al and water on the compressibility of diopside. 2010, 95, 608-616 Insights from geodynamical modeling on possible fates of continental mantle lithosphere: collision, removal, and overturnThis article is one of a series of papers published in this Special Issue on the theme Lithoprobe [parameters, processes, and the evolution of a continent 2010, 47, 541-563 Lateral, radial, and temporal variations in upper mantle viscosity and rheology under Scandinavia. Geochemistry, Geophysics, Geosystems, 2011, 12, n/a-n/a Thin oceanic crust and flood basalts: India-Seychelles breakup. Geochemistry, Geophysics, Geosystems, 2011, 12, n/a-n/a Imaging the seismic lithosphere-asthenosphere boundary of the oceanic plate. Geochemistry, Geophysics, Geosystems, 2011, 12, n/a-n/a On the heterogeneous electrical conductivity structure of the Earth§ mantle with implications for	3.6	18 24 18 32 83

724	Electrical lithosphere beneath the Kaapvaal craton, southern Africa. 2011, 116,		67
723	Trans-Pacific whole mantle structure. 2011 , 116,		7
722	Subduction factory: 4. Depth-dependent flux of H2O from subducting slabs worldwide. 2011 , 116,		504
721	Mantle rheology and the scaling of bending dissipation in plate tectonics. 2011 , 116,		13
720	Imaging the lithosphere-asthenosphere boundary beneath the Pacific using SS waveform modeling. 2011 , 116,		69
719	Viscous coupling at the lithosphere-asthenosphere boundary. <i>Geochemistry, Geophysics, Geosystems</i> , 2011 , 12, n/a-n/a	3.6	58
718	Seismic shear wave structure of the uppermost mantle beneath the Mohns Ridge. <i>Geochemistry, Geophysics, Geosystems</i> , 2011 , 12, n/a-n/a	3.6	10
717	Time dependence of intraplate volcanism caused by shear-driven upwelling of low-viscosity regions within the asthenosphere. 2011 , 116, n/a-n/a		10
716	The effects of deep water cycling on planetary thermal evolution. 2011 , 116,		44
715	Thermal evolution with a hydrating mantle and the initiation of plate tectonics in the early Earth. 2011 , 116,		82
714	P and S receiver function analysis of seafloor borehole broadband seismic data. 2011 , 116,		28
713	Mineral hydrogen isotopes and water contents in ultrahigh-pressure metabasite and metagranite: Constraints on fluid flow during continental subduction-zone metamorphism. 2011 , 281, 103-124		44
712	Mantle heterogeneity and off axis volcanism on young Pacific lithosphere. <i>Earth and Planetary Science Letters</i> , 2011 , 311, 306-315	5.3	35
711	Building and Destroying Continental Mantle. 2011 , 39, 59-90		300
710	Rheology and strength of the lithosphere. 2011 , 28, 1402-1443		241
709	Hydrating laterally extensive regions of continental lithosphere by flat subduction: A pilot study from the North American Cordillera. 2011 , 51, 17-24		12
708	Thermal localization as a potential mechanism to rift cratons. 2011 , 186, 125-137		25
707	Pressure effect on forsterite dislocation slip systems: Implications for upper-mantle LPO and low viscosity zone. 2011 , 188, 26-36		32

706	Effects of the Borealis impact on the mantle dynamics of Mars. 2011 , 188, 37-46		9
705	LithosphereEsthenosphere viscosity contrast and decoupling. 2011 , 189, 1-8		41
704	References. 678-766		
703	Grain boundary sliding in San Carlos olivine: Flow law parameters and crystallographic-preferred orientation. 2011 , 116,		169
702	Resolving the lithosphere-asthenosphere boundary with seismic Rayleigh waves. <i>Geophysical Journal International</i> , 2011 , 186, 1152-1164	6	28
701	Inferring nonlinear mantle rheology from the shape of the Hawaiian swell. <i>Nature</i> , 2011 , 473, 501-4 50	0.4	15
700	Heterogeneous mantle underneath the North Atlantic: Evidence from water in orthopyroxene, mineral composition and equilibrium conditions of spinel peridotite from different locations at the Mid-Atlantic Ridge. 2011 , 125, 308-320		33
699	H2O contents and their modification in the Cenozoic subcontinental lithospheric mantle beneath the Cathaysia block, SE China. 2011 , 126, 182-197		57
698	Supercontinents, mantle dynamics and plate tectonics: A perspective based on conceptual vs. numerical models. 2011 , 105, 1-24		93
697	The potential use of OH-defects in enstatite as geobarometer. 2011 , 162, 615-623		7
696	Crustal recycling, mantle dehydration, and the thermal evolution of Mars. 2011 , 212, 541-558		96
695			
093	Could giant impacts cripple core dynamos of small terrestrial planets?. 2011 , 212, 920-934		35
694	Could giant impacts cripple core dynamos of small terrestrial planets?. 2011 , 212, 920-934 Optimal dynamos in the cores of terrestrial exoplanets: Magnetic field generation and detectability. 2011 , 213, 12-23		35 58
	Optimal dynamos in the cores of terrestrial exoplanets: Magnetic field generation and		
694	Optimal dynamos in the cores of terrestrial exoplanets: Magnetic field generation and detectability. 2011 , 213, 12-23		58
694 693	Optimal dynamos in the cores of terrestrial exoplanets: Magnetic field generation and detectability. 2011 , 213, 12-23 Hydrous, Low-carbon Melting of Garnet Peridotite. 2011 , 52, 2079-2105 Earthquake-Prediction Research and the Earthquakes of 2000 in the South Iceland Seismic Zone.		58 32
694693692	Optimal dynamos in the cores of terrestrial exoplanets: Magnetic field generation and detectability. 2011, 213, 12-23 Hydrous, Low-carbon Melting of Garnet Peridotite. 2011, 52, 2079-2105 Earthquake-Prediction Research and the Earthquakes of 2000 in the South Iceland Seismic Zone. 2011, 101, 1590-1617 Monte Carlo Simulations of Metasomatic Enrichment in the Lithosphere and Implications for the		58 32 11

(2012-2012)

688	Dynamics of interplate domain in subduction zones: influence of rheological parameters and subducting plate age. 2012 , 3, 467-488	18
687	The Gutenberg discontinuity: melt at the lithosphere-asthenosphere boundary. 2012 , 335, 1480-3	169
686	WATER EFFECT ON HIGH-PRESSURE ELASTICITY OF OLIVINE, WADSLEYITE AND RINGWOODITE IN Mg2SiO4 BY FIRST-PRINCIPLES. 2012 , 26, 1250106	4
685	Three-dimensional thermal structure of subduction zones: effects of obliquity and curvature. 2012 , 3, 365-373	207
684	Three-dimensional thermal structure of subduction zones: effects of obliquity and curvature. 2012,	5
683	Dynamics of interplate domain in subduction zones: influence of rheological parameters and subducting plate age. 2012 ,	
682	Seismic constraints on the water flux delivered to the deep Earth by subduction. <i>Geology</i> , 2012 , 40, 235-338	28
681	THE COMPOSITIONAL DIVERSITY OF EXTRASOLAR TERRESTRIAL PLANETS. II. MIGRATION SIMULATIONS. 2012 , 760, 44	62
680	Mantle flow uplift of western Anatolia and the Aegean: Interpretations from geophysical analyses and geodynamic modeling. 2012 , 117, n/a-n/a	27
679	Depth-dependent viscosity and mantle stress amplification: implications for the role of the asthenosphere in maintaining plate tectonics. <i>Geophysical Journal International</i> , 2012 , 191, 30-41	53
678	Water in Earth mantle. 2012 , 65, 40-45	61
677	Low seismic velocities below mid-ocean ridges: Attenuation versus melt retention. 2012, 117, n/a-n/a	45
676	Small-scale convection at a continental back-arc to craton transition: Application to the southern Canadian Cordillera. 2012 , 117, n/a-n/a	25
675	A Chronostratigraphic Division of the Precambrian: Possibilities and Challenges. 2012 , 299-392	33
674	Origin of Columbia River flood basalt controlled by propagating rupture of the Farallon slab. <i>Nature</i> , 2012 , 482, 386-9	104
673	Rapid reequilibration of H2O and oxygen fugacity in olivine-hosted melt inclusions. <i>Geology</i> , 2012 , 40, 915-918	239
672	Crustal growth at active continental margins: Numerical modeling. 2012 , 192-193, 1-20	105
671	Mechanisms for the generation of plate tectonics by two-phase grain-damage and pinning. 2012 , 202-203, 27-55	152

670	An Experimental Study of Water in Nominally Anhydrous Minerals in the Upper Mantle near the Water-saturated Solidus. 2012 , 53, 2067-2093		75
669	Change of olivine a-axis alignment induced by water: Origin of seismic anisotropy in subduction zones. <i>Earth and Planetary Science Letters</i> , 2012 , 317-318, 111-119	5.3	32
668	How large is the subducted water flux? New constraints on mantle regassing rates. <i>Earth and Planetary Science Letters</i> , 2012 , 317-318, 396-406	5.3	78
667	A geophysical perspective on mantle water content and melting: Inverting electromagnetic sounding data using laboratory-based electrical conductivity profiles. <i>Earth and Planetary Science Letters</i> , 2012 , 317-318, 27-43	5.3	70
666	On the origin of the asthenosphere. Earth and Planetary Science Letters, 2012, 321-322, 95-103	5.3	200
665	The conditions for plate tectonics on super-Earths: Inferences from convection models with damage. <i>Earth and Planetary Science Letters</i> , 2012 , 331-332, 281-290	5.3	99
664	Olivine rheology, shear stress, and grain growth in the lithospheric mantle: Geological constraints from the Kaapvaal craton. <i>Earth and Planetary Science Letters</i> , 2012 , 333-334, 52-62	5.3	22
663	Superplasticity in hydrous melt-bearing dunite: Implications for shear localization in Earth upper mantle. <i>Earth and Planetary Science Letters</i> , 2012 , 335-336, 59-71	5.3	15
662	H2O storage capacity of olivine at 5BGPa and consequences for dehydration partial melting of the upper mantle. <i>Earth and Planetary Science Letters</i> , 2012 , 345-348, 104-116	5.3	63
661	Water storage capacity in olivine and pyroxene to 14 GPa: Implications for the water content of the Earth's upper mantle and nature of seismic discontinuities. <i>Earth and Planetary Science Letters</i> , 2012 , 349-350, 218-230	5.3	111
660	Linking continental drift, plate tectonics and the thermal state of the Earth's mantle. <i>Earth and Planetary Science Letters</i> , 2012 , 351-352, 134-146	5.3	77
659	Lithospheric structure in the Baikaldentral Mongolia region from integrated geophysical-petrological inversion of surface-wave data and topographic elevation. <i>Geochemistry, Geophysics, Geosystems</i> , 2012 , 13, n/a-n/a	3.6	45
658	The effect of H2O on partial melting of garnet peridotite at 3.5 GPa. <i>Geochemistry, Geophysics, Geosystems</i> , 2012 , 13, n/a-n/a	3.6	43
657	Geodynamic models of mature continental collision: Evolution of an orogen from lithospheric subduction to continental retreat/delamination. 2012 , 117,		58
656	Water in cratonic lithosphere: Calibrating laboratory-determined models of electrical conductivity of mantle minerals using geophysical and petrological observations. <i>Geochemistry, Geophysics, Geosystems,</i> 2012 , 13, n/a-n/a	3.6	58
655	Lithosphere versus asthenosphere mantle sources at the Big Pine Volcanic Field, California. <i>Geochemistry, Geophysics, Geosystems</i> , 2012 , 13, n/a-n/a	3.6	46
654	Multiple expressions of plume-ridge interaction in the Galpagos: Volcanic lineaments and ridge jumps. <i>Geochemistry, Geophysics, Geosystems</i> , 2012 , 13,	3.6	28
653	Birth of an ocean in the Red Sea: Initial pangs. <i>Geochemistry, Geophysics, Geosystems</i> , 2012 , 13, n/a-n/a	3.6	61

(2012-2012)

652	The effective elastic thickness of the continental lithosphere: Comparison between rheological and inverse approaches. <i>Geochemistry, Geophysics, Geosystems</i> , 2012 , 13,	3.6	48
651	The Pacific lithosphere-asthenosphere boundary: Seismic imaging and anisotropic constraints from SS waveforms. <i>Geochemistry, Geophysics, Geosystems</i> , 2012 , 13,	3.6	37
650	Subduction of oceanic asthenosphere: Evidence from sub-slab seismic anisotropy. <i>Geophysical Research Letters</i> , 2012 , 39, n/a-n/a	4.9	72
649	Terrestrial planet evolution in the stagnant-lid regime: Size effects and the formation of self-destabilizing crust. 2012 , 221, 1043-1060		48
648	Effects of heterogeneous hydration in the incoming plate, slab rehydration, and mantle wedge hydration on slab-derived H2O flux in subduction zones. <i>Earth and Planetary Science Letters</i> , 2012 , 353-354, 60-71	5.3	69
647	Evidence from mantle xenoliths for lithosphere removal beneath the central Rio Grande Rift. <i>Earth and Planetary Science Letters</i> , 2012 , 355-356, 82-93	5.3	30
646	Small-scale convection in the subduction zone mantle wedge. <i>Earth and Planetary Science Letters</i> , 2012 , 357-358, 111-118	5.3	20
645	Effects of stress-driven melt segregation on the viscosity of rocks. <i>Earth and Planetary Science Letters</i> , 2012 , 359-360, 184-193	5.3	23
644	Shear heating induced lithospheric-scale localization: Does it result in subduction?. <i>Earth and Planetary Science Letters</i> , 2012 , 359-360, 1-13	5.3	99
643	Glacial isostatic adjustment constrains dehydration stiffening beneath Iceland. <i>Earth and Planetary Science Letters</i> , 2012 , 359-360, 152-161	5.3	8
642	Metasomatic control of water contents in the Kaapvaal cratonic mantle. 2012 , 97, 213-246		71
641	Recognizing juvenile and relict lithospheric mantle beneath the North China Craton: Combined analysis of H2O, major and trace elements and SrNd isotope compositions of clinopyroxenes. 2012 , 149, 136-145		36
640	Earth electromagnetic environment. 50-95		21
639	Unradiogenic lead in Earth⊠upper mantle. <i>Nature Geoscience</i> , 2012 , 5, 570-573	18.3	48
638	Evolutionary aspects of lithosphere discontinuity structure in the western U.S <i>Geochemistry, Geophysics, Geosystems</i> , 2012 , 13, n/a-n/a	3.6	105
637	Martian crustal dichotomy and Tharsis formation by partial melting coupled to early plume migration. 2012 , 117,		34
636	OH in natural orthopyroxene: an in situ FTIR investigation at varying temperatures. 2012 , 39, 413-418		8
635	Possible layering of mantle convection at the top of the Iceland Hotspot: a crosscheck between 3-D numerical models and gravimetric, seismic and petrological data. <i>Geophysical Journal International</i> , 2012 , 188, 35-60	2.6	2

634	An analytic model of convection in a system with layered viscosity and plates. <i>Geophysical Journal International</i> , 2012 , 188, 61-78	2.6	48
633	Rheology of the continental lithosphere: Progress and new perspectives. <i>Gondwana Research</i> , 2012 , 21, 4-18	5.1	42
632	Constraints on mantle plumes on Venus: Implications for volatile history. 2012 , 217, 510-523		39
631	A thin-sheet model for global electromagnetic induction. <i>Geophysical Journal International</i> , 2012 , 189, 343-356	2.6	13
630	Dependency of slab geometry on absolute velocities and conditions for cyclicity: insights from numerical modelling. <i>Geophysical Journal International</i> , 2012 , 189, 747-760	2.6	24
629	Plate tectonics and planetary habitability: current status and future challenges. 2012 , 1260, 87-94		14
628	H2O storage capacity of olivine and low-Ca pyroxene from 10 to 13 GPa: consequences for dehydration melting above the transition zone. 2012 , 163, 297-316		58
627	Constraints on melting processes and plume-ridge interaction from comprehensive study of the FAMOUS and North Famous segments, Mid-Atlantic Ridge. <i>Earth and Planetary Science Letters</i> , 2013 , 365, 209-220	5.3	43
626	Seismic imaging of melt in a displaced Hawaiian plume. <i>Nature Geoscience</i> , 2013 , 6, 657-660	18.3	60
625	Structures of the oceanic lithosphere-asthenosphere boundary: Mineral-physics modeling and seismological signatures. <i>Geochemistry, Geophysics, Geosystems</i> , 2013 , 14, 880-901	3.6	51
624	Geochemistry of subduction zone serpentinites: A review. 2013 , 178, 96-127		370
623	A review of heterogeneous materials and their implications for relationships between kinematics and dynamics in continents. 2013 , 32, n/a-n/a		4
622	Self-consistent thermal model of the subcontinental mantle. 2013 , 448, 262-264		1
621	Low-temperature evolution of OH bands in synthetic forsterite, implication for the nature of H defects at high pressure. 2013 , 40, 499-510		27
620	The distribution of water in the continental lithospheric mantle and its implications for the stability of continents. 2013 , 58, 3879-3889		12
619	Water solubility in orthopyroxene: Dependence on temperature and Al content. 2013 , 58, 3895-3902		1
618	Organization of the tectonic plates in the last 200Myr. <i>Earth and Planetary Science Letters</i> , 2013 , 373, 93-101	5.3	29
617	Seismological Constraints on Earth's Deep Water Cycle. 2013 , 13-27		5

616	Influence of Hydrogen-Related Defects on the Electrical Conductivity and Plastic Deformation of Mantle Minerals: A Critical Review. 2013 , 113-129		21
615	Raman Spectroscopic Studies of Hydrous and Nominally Anhydrous Deep Mantle Phases. 2013 , 69-93		3
614	Towards Mapping the Three-Dimensional Distribution of Water in the Upper Mantle from Velocity and Attenuation Tomography. 2013 , 225-236		10
613	Seismic Evidence for Subduction-Transported Water in the Lower Mantle. 2013 , 251-261		20
612	Contemporary Fault Mechanics in Southern Alaska. 2013 , 321-336		7
611	Gephysical Constraints upon the Thermal Regime of the Ocean Crust. 2013 , 19-62		3
610	The Rheology and Morphology of Oceanic Lithosphere and Mid-Ocean Ridges. 2013 , 63-93		11
609	Hydration adjacent to a deeply subducting slab: The roles of nominally anhydrous minerals and migrating fluids. <i>Journal of Geophysical Research: Solid Earth</i> , 2013 , 118, 5753-5770	3.6	15
608	Olivine from spinel peridotite xenoliths: Hydroxyl incorporation and mineral composition. 2013 , 98, 187	70-188	028
607	Why do mafic arc magmas contain ~4wt% water on average?. <i>Earth and Planetary Science Letters</i> , 2013 , 364, 168-179	5.3	312
606	Experimental partitioning of halogens and other trace elements between olivine, pyroxenes, amphibole and aqueous fluid at 2 GPa and 900-1,300 °C. 2013 , 166, 639-653		35
605	Experimental chlorine partitioning between forsterite, enstatite and aqueous fluid at upper mantle conditions. 2013 , 121, 684-700		21
604	Lull f and Smld garnet geochronology: Chronometric closure and implications for dating petrological processes. <i>Earth and Planetary Science Letters</i> , 2013 , 381, 222-233	5.3	117
603	The structure of thermal convection and geotherms beneath a continent and ocean. 2013 , 49, 668-674		
602	The mean composition of ocean ridge basalts. <i>Geochemistry, Geophysics, Geosystems</i> , 2013 , n/a-n/a	3.6	9
601	Development of A-type olivine fabric in water-rich deep upper mantle. <i>Earth and Planetary Science Letters</i> , 2013 , 362, 20-30	5.3	25
600	Volatile loss from melt inclusions in pyroclasts of differing sizes. 2013 , 165, 129-153		139
599	Long-Term Evolution of the Martian Crust-Mantle System. 2013 , 174, 49-111		107

598	Dynamics of slab rollback and induced back-arc basin formation. <i>Earth and Planetary Science Letters</i> , 2013 , 361, 287-297	5.3	75
597	Strong lateral strength contrasts in the mantle lithosphere of continents: A case study from the hot SW Canadian Cordillera. 2013 , 602, 87-105		7
596	High water content in Mesozoic primitive basalts of the North China Craton and implications on the destruction of cratonic mantle lithosphere. <i>Earth and Planetary Science Letters</i> , 2013 , 361, 85-97	5.3	138
595	Constraints of the topography, gravity and volcanism on Venusian mantle dynamics and generation of plate tectonics. <i>Earth and Planetary Science Letters</i> , 2013 , 362, 207-214	5.3	25
594	Thermal and compositional evolution of the martian mantle: Effects of water. 2013 , 220, 50-72		19
593	Double layering of a thermochemical plume in the upper mantle beneath Hawaii. <i>Earth and Planetary Science Letters</i> , 2013 , 376, 155-164	5.3	60
592	Crustal construction and magma chamber properties along the Eastern Lau Spreading Center. <i>Earth and Planetary Science Letters</i> , 2013 , 371-372, 112-124	5.3	22
591	The origin and geophysical implications of a weak C-type olivine fabric in the Xugou ultrahigh pressure garnet peridotite. <i>Earth and Planetary Science Letters</i> , 2013 , 376, 63-73	5.3	16
590	Melt-rich channel observed at the lithosphere-asthenosphere boundary. <i>Nature</i> , 2013 , 495, 356-9	50.4	175
589	Initiation and Evolution of Plate Tectonics on Earth: Theories and Observations. 2013, 41, 117-151		298
589 588	Initiation and Evolution of Plate Tectonics on Earth: Theories and Observations. 2013 , 41, 117-151 The mean composition of ocean ridge basalts. <i>Geochemistry, Geophysics, Geosystems</i> , 2013 , 14, 489-518	3.6	298 798
		3.6	Í
588	The mean composition of ocean ridge basalts. <i>Geochemistry, Geophysics, Geosystems</i> , 2013 , 14, 489-518	3.6	798
588 587	The mean composition of ocean ridge basalts. <i>Geochemistry, Geophysics, Geosystems</i> , 2013 , 14, 489-518 Rheological Properties of Minerals and Rocks. 2013 , 94-144	3.6	798
588 587 586	The mean composition of ocean ridge basalts. <i>Geochemistry, Geophysics, Geosystems</i> , 2013 , 14, 489-518 Rheological Properties of Minerals and Rocks. 2013 , 94-144 Mantle Mixing: Processes and Modeling. 2013 , 351-371 Low strength of Earth® uppermost mantle inferred from tri-axial deformation experiments on dry	3.6	798
588 587 586	The mean composition of ocean ridge basalts. <i>Geochemistry, Geophysics, Geosystems</i> , 2013 , 14, 489-518 Rheological Properties of Minerals and Rocks. 2013 , 94-144 Mantle Mixing: Processes and Modeling. 2013 , 351-371 Low strength of EarthB uppermost mantle inferred from tri-axial deformation experiments on dry olivine crystals. 2013 , 220, 37-49	3.6 3.6	79 ⁸ 3
588 587 586 585	The mean composition of ocean ridge basalts. <i>Geochemistry, Geophysics, Geosystems</i> , 2013, 14, 489-518 Rheological Properties of Minerals and Rocks. 2013, 94-144 Mantle Mixing: Processes and Modeling. 2013, 351-371 Low strength of Earth uppermost mantle inferred from tri-axial deformation experiments on dry olivine crystals. 2013, 220, 37-49 Electrical Conductivity of Mantle Minerals: Role of Water in Conductivity Anomalies. 2013, 41, 605-628 Influence of viscosity pressure dependence on deep lithospheric tectonics during continental		79 ⁸ 3

(2013-2013)

580	Geochemical variations at ridge-centered hotspots caused by variable melting of a veined mantle plume. <i>Earth and Planetary Science Letters</i> , 2013 , 371-372, 191-202	5.3	4
579	Small effect of water on upper-mantle rheology based on silicon self-diffusion coefficients. <i>Nature</i> , 2013 , 498, 213-5	50.4	123
57 ⁸	Water contents of the Cenozoic lithospheric mantle beneath the western part of the North China Craton: Peridotite xenolith constraints. <i>Gondwana Research</i> , 2013 , 23, 108-118	5.1	54
577	Effects of permeability fields on fluid, heat, and oxygen isotope transport in extensional detachment systems. <i>Geochemistry, Geophysics, Geosystems</i> , 2013 , 14, 1493-1522	3.6	22
576	Investigating seismic anisotropy beneath the Reykjanes Ridge using models of mantle flow, crystallographic evolution, and surface wave propagation. <i>Geochemistry, Geophysics, Geosystems</i> , 2013 , 14, 3250-3267	3.6	6
575	The solid Earth's influence on sea level. 2013 , 125, 1027-1052		117
574	Strain Localization in Pyroxenite by Reaction-Enhanced Softening in the Shallow Subcontinental Lithospheric Mantle. 2013 , 54, 1997-2031		27
573	Deep water gives up another secret. 2013 , 110, 6616-7		2
572	Small-scale convection in a plume-fed low-viscosity layer beneath a moving plate. <i>Geophysical Journal International</i> , 2013 , 194, 591-610	2.6	22
571	P-wave tomography for 3-D radial and azimuthal anisotropy of Tohoku and Kyushu subduction zones. <i>Geophysical Journal International</i> , 2013 , 193, 1166-1181	2.6	112
570	Predicting surface dynamic topographies of stagnant lid planetary bodies. <i>Geophysical Journal International</i> , 2013 , 195, 1494-1508	2.6	6
569	Dynamics of outer-rise faulting in oceanic-continental subduction systems. <i>Geochemistry, Geophysics, Geosystems</i> , 2013 , 14, 2310-2327	3.6	53
568	Convergence depths of tectonic regions from an ensemble of global tomographic models. <i>Journal of Geophysical Research: Solid Earth</i> , 2013 , 118, 4196-4225	3.6	13
567	Influence of Water on Major Phase Transitions in the Earth's Mantle. 2013 , 95-111		21
566	Lithospheric deformation induced by loading of the Hawaiian Islands and its implications for mantle rheology. <i>Journal of Geophysical Research: Solid Earth</i> , 2013 , 118, 6025-6048	3.6	55
565	Thermal evolution of the North Atlantic lithosphere: New constraints from magnetic anomaly inversion with a fractal magnetization model. <i>Geochemistry, Geophysics, Geosystems</i> , 2013 , 14, 5078-510	3.6	46
564	Correction to Leodynamic models of Archean continental collision and the formation of mantle lithosphere keels (Geophysical Research Letters, 2013, 40, 3394-3394)	4.9	
563	Effects of present-day deglaciation in Iceland on mantle melt production rates. <i>Journal of Geophysical Research: Solid Earth</i> , 2013 , 118, 3366-3379	3.6	30

562	Lithospheric cooling trends and deviations in oceanic PP-P and SS-S differential traveltimes. <i>Journal of Geophysical Research: Solid Earth</i> , 2013 , 118, 996-1007	3.6	11
561	Termination of a 6 year ridge-spreading event observed using a seafloor seismic network on the Endeavour Segment, Juan de Fuca Ridge. <i>Geochemistry, Geophysics, Geosystems</i> , 2013 , 14, 1375-1398	3.6	18
560	The instability of continental passive margins and its effect on continental topography and heat flow. <i>Journal of Geophysical Research: Solid Earth</i> , 2013 , 118, 1817-1836	3.6	12
559	Correction to Geodynamic models of mature continental collision: Evolution of an orogen from lithospheric subduction to continental retreat/delamination <i>Journal of Geophysical Research: Solid Earth</i> , 2013 , 118, 5733-5735	3.6	
558	Linking mantle upwelling with the lithosphere descent [corrected] and the Japan Sea evolution: a hypothesis. <i>Scientific Reports</i> , 2013 , 3, 1137	4.9	16
557	Single-crystal equation of state of phase D to lower mantle pressures and the effect of hydration on the buoyancy of deep subducted slabs. <i>Journal of Geophysical Research: Solid Earth</i> , 2013 , 118, 6124-	-6 ³ 183	14
556	The role of harzburgite layers in the morphology of subducting plates and the behavior of oceanic crustal layers. <i>Geophysical Research Letters</i> , 2013 , 40, 5387-5392	4.9	9
555	Timescale and morphology of Martian mantle overturn immediately following magma ocean solidification. 2014 , 119, 454-467		22
554	Controls on segmentation and morphology along the back-arc Eastern Lau Spreading Center and Valu Fa Ridge. <i>Journal of Geophysical Research: Solid Earth</i> , 2014 , 119, 1678-1700	3.6	13
553	. 2014,		5
553 552	. 2014, Weak ductile shear zone beneath a major strike-slip fault: Inferences from earthquake cycle model constrained by geodetic observations of the western North Anatolian Fault Zone. <i>Journal of Geophysical Research: Solid Earth</i> , 2014, 119, 3678-3699	3.6	5 45
	Weak ductile shear zone beneath a major strike-slip fault: Inferences from earthquake cycle model constrained by geodetic observations of the western North Anatolian Fault Zone. <i>Journal of</i>	3.6	
552	Weak ductile shear zone beneath a major strike-slip fault: Inferences from earthquake cycle model constrained by geodetic observations of the western North Anatolian Fault Zone. <i>Journal of Geophysical Research: Solid Earth</i> , 2014 , 119, 3678-3699 Geochemical and Planetary Dynamical Views on the Origin of Earth's Atmosphere and Oceans. 2014	3.6	45
55 ² 55 ¹	Weak ductile shear zone beneath a major strike-slip fault: Inferences from earthquake cycle model constrained by geodetic observations of the western North Anatolian Fault Zone. <i>Journal of Geophysical Research: Solid Earth</i> , 2014 , 119, 3678-3699 Geochemical and Planetary Dynamical Views on the Origin of Earth's Atmosphere and Oceans. 2014 , 1-35 Hot upwelling conduit beneath the Atlas Mountains, Morocco. <i>Geophysical Research Letters</i> , 2014 ,		45 16
55 ² 55 ¹	Weak ductile shear zone beneath a major strike-slip fault: Inferences from earthquake cycle model constrained by geodetic observations of the western North Anatolian Fault Zone. <i>Journal of Geophysical Research: Solid Earth</i> , 2014 , 119, 3678-3699 Geochemical and Planetary Dynamical Views on the Origin of Earth's Atmosphere and Oceans. 2014 , 1-35 Hot upwelling conduit beneath the Atlas Mountains, Morocco. <i>Geophysical Research Letters</i> , 2014 , 41, 8037-8044		45 16 11
55 ² 55 ¹ 55 ⁰	Weak ductile shear zone beneath a major strike-slip fault: Inferences from earthquake cycle model constrained by geodetic observations of the western North Anatolian Fault Zone. <i>Journal of Geophysical Research: Solid Earth</i> , 2014 , 119, 3678-3699 Geochemical and Planetary Dynamical Views on the Origin of Earth's Atmosphere and Oceans. 2014 , 1-35 Hot upwelling conduit beneath the Atlas Mountains, Morocco. <i>Geophysical Research Letters</i> , 2014 , 41, 8037-8044 Physics and Chemistry of Deep Continental Crust Recycling. 2014 , 423-456	4.9	45 16 11
552 551 550 549 548	Weak ductile shear zone beneath a major strike-slip fault: Inferences from earthquake cycle model constrained by geodetic observations of the western North Anatolian Fault Zone. <i>Journal of Geophysical Research: Solid Earth</i> , 2014 , 119, 3678-3699 Geochemical and Planetary Dynamical Views on the Origin of Earth's Atmosphere and Oceans. 2014 , 1-35 Hot upwelling conduit beneath the Atlas Mountains, Morocco. <i>Geophysical Research Letters</i> , 2014 , 41, 8037-8044 Physics and Chemistry of Deep Continental Crust Recycling. 2014 , 423-456 50 & 100 Years Ago. <i>Nature</i> , 2014 , 509, 41-41 Volatile cycling of H2O, CO2, F, and Cl in the HIMU mantle: A new window provided by melt inclusions from oceanic hot spot lavas at Mangaia, Cook Islands. <i>Geochemistry, Geophysics</i> ,	4.9	45 16 11 41

544	Partial melting control of water contents in the Cenozoic lithospheric mantle of the Cathaysia block of South China. 2014 , 380, 7-19	44
543	Estimating the electrical conductivity of the melt phase of a partially molten asthenosphere from seafloor magnetotelluric sounding data. 2014 , 227, 41-47	19
542	Interpretation of Magnetotelluric Results Using Laboratory Measurements. 2014 , 35, 41-84	60
541	On the Causes of Electrical Conductivity Anomalies in Tectonically Stable Lithosphere. 2014 , 35, 219-257	116
540	Order of magnitude increase in subducted H2O due to hydrated normal faults within the Wadati-Benioff zone. <i>Geology</i> , 2014 , 42, 207-210	45
539	Hydration of mantle olivine under variable water and oxygen fugacity conditions. 2014 , 167, 1	40
538	Craton stability and longevity: The roles of composition-dependent rheology and buoyancy. <i>Earth and Planetary Science Letters</i> , 2014 , 391, 224-233	54
537	Lethal interactions between parasites and prey increase niche diversity in a tropical community. 2014 , 343, 1240-4	51
536	Changes in seismic anisotropy shed light on the nature of the Gutenberg discontinuity. 2014 , 343, 1237-40	86
535	High water contents in the Siberian cratonic mantle linked to metasomatism: An FTIR study of Udachnaya peridotite xenoliths. 2014 , 137, 159-187	105
535534		
	Udachnaya peridotite xenoliths. 2014 , 137, 159-187 Electrical conductivity during incipient melting in the oceanic low-velocity zone. <i>Nature</i> , 2014 , 509, 81-5 50.	
534	Udachnaya peridotite xenoliths. 2014 , 137, 159-187 Electrical conductivity during incipient melting in the oceanic low-velocity zone. <i>Nature</i> , 2014 , 509, 81-5 50 Geophysics: Making the Earth move. <i>Nature</i> , 2014 , 509, 40-1	1 137
534 533	Udachnaya peridotite xenoliths. 2014 , 137, 159-187 Electrical conductivity during incipient melting in the oceanic low-velocity zone. <i>Nature</i> , 2014 , 509, 81-5 50 Geophysics: Making the Earth move. <i>Nature</i> , 2014 , 509, 40-1	1 137
534533532	Udachnaya peridotite xenoliths. 2014 , 137, 159-187 Electrical conductivity during incipient melting in the oceanic low-velocity zone. <i>Nature</i> , 2014 , 509, 81-5 50 Geophysics: Making the Earth move. <i>Nature</i> , 2014 , 509, 40-1 Astronomy: A new spin on exoplanets. <i>Nature</i> , 2014 , 509, 41-2 Interaction of a mantle plume and a segmented mid-ocean ridge: Results from numerical modeling.	1 137 1 2 1 1
534533532531	Udachnaya peridotite xenoliths. 2014, 137, 159-187 Electrical conductivity during incipient melting in the oceanic low-velocity zone. Nature, 2014, 509, 81-5 50 Geophysics: Making the Earth move. Nature, 2014, 509, 40-1 Astronomy: A new spin on exoplanets. Nature, 2014, 509, 41-2 Interaction of a mantle plume and a segmented mid-ocean ridge: Results from numerical modeling. Earth and Planetary Science Letters, 2014, 392, 113-120 Crystallographic preferred orientation of wadsleyite and ringwoodite: Effects of phase transformation and water on seismic anisotropy in the mantle transition zone. Earth and Planetary 5.3	1 137 1 2 1 1
534533532531530	Electrical conductivity during incipient melting in the oceanic low-velocity zone. <i>Nature</i> , 2014 , 509, 81-5 50 Geophysics: Making the Earth move. <i>Nature</i> , 2014 , 509, 40-1 Astronomy: A new spin on exoplanets. <i>Nature</i> , 2014 , 509, 41-2 Interaction of a mantle plume and a segmented mid-ocean ridge: Results from numerical modeling. <i>Earth and Planetary Science Letters</i> , 2014 , 392, 113-120 Crystallographic preferred orientation of wadsleyite and ringwoodite: Effects of phase transformation and water on seismic anisotropy in the mantle transition zone. <i>Earth and Planetary Science Letters</i> , 2014 , 397, 133-144 Behaviour of subducted water and its role in magma genesis in the NE Japan arc: A combined	1 137 1 2 1 1 5

526	The hydrous properties of subcontinental lithospheric mantle: Constraints from water content and hydrogen isotope composition of phenocrysts from Cenozoic continental basalt in North China. 2014 , 143, 285-302		24
525	A new GPS velocity field for the Pacific Plate IPart 1: constraints on plate motion, intraplate deformation, and the viscosity of Pacific basin asthenosphere. <i>Geophysical Journal International</i> , 2014 , 199, 1878-1899	2.6	12
524	Stability of the boundary layer between the lithosphere and convecting mantle and the steady-state lithospheric geotherm. 2014 , 50, 543-561		1
523	Seismic anisotropy and shear wave splitting associated with mantle plume-plate interaction. <i>Journal of Geophysical Research: Solid Earth</i> , 2014 , 119, 4923-4937	3.6	15
522	Craton formation: Internal structure inherited from closing of the early oceans. 2014 , 6, 35-42		34
521	A wet, heterogeneous lunar interior: Lower mantle and core dynamo evolution. 2014 , 119, 1061-1077		41
520	Experimental Study of the Influence of Water on Melting and Phase Assemblages in the Upper Mantle. 2014 , 55, 2067-2096		96
519	Mantle flow and multistage melting beneath the Galpagos hotspot revealed by seismic imaging. Nature Geoscience, 2014 , 7, 151-156	18.3	51
518	Effects of Al content on water partitioning between orthopyroxene and olivine: Implications for lithosphere Bsthenosphere boundary. <i>Earth and Planetary Science Letters</i> , 2014 , 400, 284-291	5.3	16
517	Plume-Ridge Interaction in the Galpagos. 2014 , 285-334		9
516	Calculating melting temperatures and pressures of peridotite protoliths: Implications for the origin of cratonic mantle. <i>Earth and Planetary Science Letters</i> , 2014 , 403, 273-286	5.3	49
515	Sp receiver function imaging of a passive margin: Transect across Texas's Gulf Coastal Plain. <i>Earth and Planetary Science Letters</i> , 2014 , 402, 138-147	5.3	10
514	Linking rift propagation barriers to excess magmatism at volcanic rifted margins. <i>Geology</i> , 2014 , 42, 10	7 1 -107	' 4 45
513	Oceanic- and continental-type metamorphic terranes: Occurrence and exhumation mechanisms. 2014 , 139, 33-46		31
512	FTIR spectroscopy of Ti-chondrodite, Ti-clinohumite, and olivine in deeply subducted serpentinites and implications for the deep water cycle. 2014 , 167, 1		21
511	Advances and challenges in geotectonic modelling. 2014 , 185, 147-168		3
510	Water content of the Tanzanian lithosphere from magnetotelluric data: Implications for cratonic growth and stability. <i>Earth and Planetary Science Letters</i> , 2014 , 388, 175-186	5.3	45
509	The magmatic activity mechanism of the fossil spreading center in the Southwest sub-basin, South China Sea. 2014 , 57, 1653-1663		3

508	The Alps 2: Controls on crustal subduction and (ultra)high-pressure rock exhumation in Alpine-type orogens. <i>Journal of Geophysical Research: Solid Earth</i> , 2014 , 119, 5987-6022	3.6	32
507	TIDAL HEATING IN MULTILAYERED TERRESTRIAL EXOPLANETS. 2014 , 789, 30		63
506	Efficient early global relaxation of asteroid Vesta. 2014 , 240, 133-145		19
505	Electrical structure of the central Cascadia subduction zone: The EMSLAB Lincoln Line revisited. <i>Earth and Planetary Science Letters</i> , 2014 , 402, 265-274	5.3	38
504	Partial melting in one-plate planets: Implications for thermo-chemical and atmospheric evolution. 2014 , 98, 50-65		26
503	Rheological and geodynamic controls on the mechanisms of subduction and HP/UHP exhumation of crustal rocks during continental collision: Insights from numerical models. 2014 , 631, 212-250		36
502	The lithospherellsthenosphere boundary and the tectonic and magmatic history of the northwestern United States. <i>Earth and Planetary Science Letters</i> , 2014 , 402, 69-81	5.3	68
501	Water in the slab: A trilogy. 2014 , 614, 1-30		123
500	Receiver function imaging of lithospheric structure and the onset of melting beneath the Galpagos Archipelago. <i>Earth and Planetary Science Letters</i> , 2014 , 388, 156-165	5.3	31
499	Coupled mantle dripping and lateral dragging controlling the lithosphere structure of the NW-Moroccan margin and the Atlas Mountains: A numerical experiment. 2014 , 189, 16-27		5
498	Viscoplasticity of polycrystalline olivine experimentally deformed at high pressure and 900 °C. 2014 , 623, 123-135		42
497	Reduction of OH contamination in quantification of water contents using NanoSIMS imaging. 2014 , 380, 20-26		14
496	Seismological study of Lau back arc crust: Mantle water, magmatic differentiation, and a compositionally zoned basin. <i>Earth and Planetary Science Letters</i> , 2014 , 390, 304-317	5.3	27
495	Water contents and electrical conductivity of peridotite xenoliths from the North China Craton: Implications for water distribution in the upper mantle. 2014 , 189, 105-126		22
494	Polycrystalline olivine rheology in dislocation creep: Revisiting experimental data to 8.1GPa. 2014 , 228, 211-219		13
493	Did large volcanic channel systems develop on Earth during the Hadean and Archean?. 2014 , 246, 226-	239	9
492	Metasomatic hydration of the Oeyama forearc peridotites: Tectonic implications. 2014 , 184-187, 346-3	360	10
491	Upper mantle surprises derived from the recent Virginia earthquake waveform data. <i>Earth and Planetary Science Letters</i> , 2014 , 402, 167-175	5.3	12

490	Some remarks on the models of plate tectonics on terrestrial planets: From the view-point of mineral physics. 2014 , 631, 4-13		7
489	Constraints on Vestall interior structure using gravity and shape models from the Dawn mission. 2014 , 240, 146-160		46
488	The distribution of H2O between silicate melt and nominally anhydrous peridotite and the onset of hydrous melting in the deep upper mantle. <i>Earth and Planetary Science Letters</i> , 2014 , 400, 1-13	5.3	67
487	Mechanisms of continental subduction and exhumation of HP and UHP rocks. <i>Gondwana Research</i> , 2014 , 25, 464-493	5.1	56
486	A systematic 2-D investigation into the mantle wedge's transient flow regime and thermal structure: Complexities arising from a hydrated rheology and thermal buoyancy. <i>Geochemistry, Geophysics, Geosystems</i> , 2014 , 15, 28-51	3.6	25
485	Rayleigh wave phase velocities in the Atlantic upper mantle. <i>Geochemistry, Geophysics, Geosystems</i> , 2014 , 15, 4305-4324	3.6	16
484	Patterns in Galpagos Magmatism Arising from the Upper Mantle Dynamics of Plume-Ridge Interaction. 2014 , 245-261		7
483	Helium Isotope Variations and Mantle Plume-Spreading Ridge Interactions Along the Galpagos Spreading Center. 2014 , 393-414		5
482	Toward a unified hydrous olivine electrical conductivity law. <i>Geochemistry, Geophysics, Geosystems</i> , 2014 , 15, 4984-5000	3.6	85
481	Roadmap to continental rupture: Is obliquity the route to success?. <i>Geology</i> , 2014 , 42, 271-272	5	1
480	Low-Velocity Layer Atop the Mantle Transition Zone in the Lower Yangtze Craton from P Waveform Triplication. 2014 , 57, 532-542		3
479	Dynamics of lithospheric thinning and mantle melting by edge-driven convection: Application to Moroccan Atlas mountains. <i>Geochemistry, Geophysics, Geosystems</i> , 2014 , 15, 3175-3189	3.6	62
478	Temperature, lithosphere-asthenosphere boundary, and heat flux beneath the Antarctic Plate inferred from seismic velocities. <i>Journal of Geophysical Research: Solid Earth</i> , 2015 , 120, 8720-8742	3.6	91
477	Grain-size dynamics beneath mid-ocean ridges: Implications for permeability and melt extraction. <i>Geochemistry, Geophysics, Geosystems</i> , 2015 , 16, 925-946	3.6	17
476	Advantages of a conservative velocity interpolation (CVI) scheme for particle-in-cell methods with application in geodynamic modeling. <i>Geochemistry, Geophysics, Geosystems</i> , 2015 , 16, 2015-2023	3.6	45
475	Melting systematics in mid-ocean ridge basalts: Application of a plagioclase-spinel melting model to global variations in major element chemistry and crustal thickness. <i>Journal of Geophysical Research: Solid Earth</i> , 2015 , 120, 4863-4886	3.6	33
474	How partial melting affects small-scale convection in a plume-fed sublithospheric layer beneath fast-moving plates. <i>Geochemistry, Geophysics, Geosystems</i> , 2015 , 16, 3924-3945	3.6	5
473	Conjugate rifted margins width and asymmetry: The interplay between lithospheric strength and	3.6	57

472	Chemical Composition of Mantle Wedge Fluids. 2015 , 124, 473-501		2
471	An upper mantle seismic discontinuity beneath the Galpagos Archipelago and its implications for studies of the lithosphere-asthenosphere boundary. <i>Geochemistry, Geophysics, Geosystems</i> , 2015 , 3. 16, 1070-1088	.6	11
470	Plume-cratonic lithosphere interaction recorded by water and other trace elements in peridotite xenoliths from the Labait volcano, Tanzania. <i>Geochemistry, Geophysics, Geosystems</i> , 2015 , 16, 1687-1710 ³ ·	.6	27
469	Mantle plume capture, anchoring, and outflow during Galpagos plume-ridge interaction. <i>Geochemistry, Geophysics, Geosystems</i> , 2015 , 16, 1634-1655	.6	17
468	An efficient and general approach for implementing thermodynamic phase equilibria information in geophysical and geodynamic studies. <i>Geochemistry, Geophysics, Geosystems</i> , 2015 , 16, 3767-3777	.6	6
467	Water effects on the anharmonic properties of forsterite. 2015 , 100, 2185-2190		6
466	Intraplate volcanism at the edges of the Colorado Plateau sustained by a combination of triggered edge-driven convection and shear-driven upwelling. <i>Geochemistry, Geophysics, Geosystems</i> , 2015 , 16, 366-379	.6	26
465	Imaging continental breakup using teleseismic body waves: The Woodlark Rift, Papua New Guinea. <i>Geochemistry, Geophysics, Geosystems</i> , 2015 , 16, 2529-2548	.6	23
464	Basalt volatile fluctuations during continental rifting: An example from the Rio Grande Rift, USA. <i>Geochemistry, Geophysics, Geosystems</i> , 2015 , 16, 1254-1273	.6	12
463	Water in Hawaiian peridotite minerals: A case for a dry metasomatized oceanic mantle lithosphere. <i>Geochemistry, Geophysics, Geosystems</i> , 2015 , 16, 1211-1232	.6	46
462	Transport properties of silicate melts. 2015 , 53, 715-744		55
461	Quantification of water in hydrous ringwoodite. 2015 , 2,		20
460	THE PERSISTENCE OF OCEANS ON EARTH-LIKE PLANETS: INSIGHTS FROM THE DEEP-WATER CYCLE. 2015 , 801, 40		58
459	Crust and Lithospheric Structure - Seismological Constraints on the Lithosphere-Asthenosphere Boundary. 2015 , 587-612		12
458	Heat Flow and Thermal Structure of the Lithosphere. 2015 , 217-253		14
457	The Dynamics of Continental Breakup and Extension. 2015 , 325-379		8
456	Crust and Lithospheric Structure - Seismic Structure of Mid-Ocean Ridges. 2015 , 419-451		3
455	Negligible effect of hydrogen content on plate strength in East Africa. <i>Nature Geoscience</i> , 2015 , 8, 543-5	6 .3	29

454	Petrogenesis of mafic collision zone magmatism: The Armenian sector of the TurkishIranian Plateau. 2015 , 403, 24-41	58
453	Water disequilibrium in olivines from Hawaiian peridotites: Recent metasomatism, H diffusion and magma ascent rates. 2015 , 154, 98-117	56
452	A melt-focusing zone in the lithospheric mantle preserved in the Santa Elena Ophiolite, Costa Rica. 2015 , 230, 189-205	15
451	A seismic reflection image for the base of a tectonic plate. <i>Nature</i> , 2015 , 518, 85-8	·4 77
450	Earth science: The slippery base of a tectonic plate. <i>Nature</i> , 2015 , 518, 39-40	.4 1
449	Deformation of forsterite polycrystals at mantle pressure: Comparison with Fe-bearing olivine and the effect of iron on its plasticity. 2015 , 240, 95-104	13
448	Water in Hawaiian garnet pyroxenites: Implications for water heterogeneity in the mantle. 2015 , 397, 61-75	55
447	Late Cenozoic intraplate volcanism in Changbai volcanic field, on the border of China and North Korea: insights into deep subduction of the Pacific slab and intraplate volcanism. 2015 , 172, 648-663	34
446	Polarized Plate Tectonics. 2015 , 1-167	58
445	Asymmetric Dynamical Behavior of Thermochemical Plumes and Implications for Hawaiian Lava Composition. 2015 , 35-57	5
444	Strain localization at the margins of strong lithospheric domains: Insights from analog models. 2015 , 34, 396-412	20
443	The origin of shear wave splitting beneath Iceland. <i>Geophysical Journal International</i> , 2015 , 201, 1297-13 12	5
442	Dynamics and Thermal History of the Terrestrial Planets, the Moon, and Io. 2015, 255-305	22
441	Analysis of the spatial viscosity variation in the crust beneath the western North Anatolian Fault. 2015 , 88, 80-89	3
440	Speciation and solubility of reduced CDHN volatiles in mafic melt: Implications for volcanism, atmospheric evolution, and deep volatile cycles in the terrestrial planets. 2015 , 171, 283-302	55
439	Plate Rheology and Mechanics. 2015 , 95-152	6
438	H2O in olivine and garnet inclusions still trapped in diamonds from the Siberian craton: Implications for the water content of cratonic lithosphere peridotites. 2015 , 230, 180-183	31
437	The Generation of Plate Tectonics from Mantle Dynamics. 2015 , 271-318	32

436 The Dynamics and Convective Evolution of the Upper Mantle. **2015**, 319-337

435	Dynamics of Subducting Slabs: Numerical Modeling and Constraints from Seismology, Geoid,	7
155	Topography, Geochemistry, and Petrology. 2015 , 339-391	,
434	Constitutive Equations, Rheological Behavior, and Viscosity of Rocks. 2015, 441-472	35
433	Seismic Anisotropy of the Deep Earth from a Mineral and Rock Physics Perspective. 2015 , 487-538	28
432	Physics of Mantle Convection. 2015 , 23-71	12
431	Hotspots, Large Igneous Provinces, and Melting Anomalies. 2015 , 393-459	9
430	Mantle Geochemical Geodynamics. 2015 , 521-585	10
429	The effects of internal heating and large scale climate variations on tectonic bi-stability in terrestrial planets. <i>Earth and Planetary Science Letters</i> , 2015 , 420, 85-94	57
428	OH-defects in multiple-doped orthoenstatite at 4-8 GPa: filling the gap between pure and natural systems. 2015 , 169, 38	15
427	The electrical structure of the central Pacific upper mantle constrained by the NoMelt experiment. <i>Geochemistry, Geophysics, Geosystems,</i> 2015 , 16, 1115-1132	52
426	The thinning of subcontinental lithosphere: The roles of plume impact and metasomatic weakening. <i>Geochemistry, Geophysics, Geosystems</i> , 2015 , 16, 1156-1171	50
425	Garnet in cratonic and non-cratonic mantle and lower crustal xenoliths from southern Africa: Composition, water incorporation and geodynamic constraints. 2015 , 270, 285-299	12
424	Upper mantle temperature and the onset of extension and break-up in Afar, Africa. <i>Earth and Planetary Science Letters</i> , 2015 , 418, 78-90	35
423	Water in orthopyroxene from abyssal spinel peridotites of the East Pacific Rise (ODP Leg 147: Hess Deep). 2015 , 232, 23-34	15
422	Intraplate orogenesis within accreted and scarred lithosphere: Example of the Eurekan Orogeny, Ellesmere Island. 2015 , 664, 202-213	13
421	High surface topography related to upper mantle flow beneath Eastern Anatolia. <i>Geophysical Journal International</i> , 2015 , 203, 1263-1273	10
420	Decrease of hydrogen incorporation in forsterite from CO2-H2O-rich kimberlitic liquid. 2015 , 100, 1912-1920	7
419	Couette and Poiseuille flows in a low viscosity asthenosphere: Effects of internal heating rate, Rayleigh number, and plate representation. 2015 , 246, 31-40	2

418	Temporal variation of H 2 O content in the lithospheric mantle beneath the eastern North China Craton: Implications for the destruction of cratons. <i>Gondwana Research</i> , 2015 , 28, 276-287	5.1	31
417	Thermal regime of the North China Craton: Implications for craton destruction. 2015 , 140, 14-26		89
416	Inherited structure and coupled crust-mantle lithosphere evolution: Numerical models of Central Australia. <i>Geophysical Research Letters</i> , 2016 , 43, 4962-4970	4.9	6
415	Mechanical anisotropy control on strain localization in upper mantle shear zones. 2016 , 35, 1177-1204		4
414	High-resolution seismic constraints on flow dynamics in the oceanic asthenosphere. <i>Nature</i> , 2016 , 535, 538-41	50.4	67
413	Thermal structure and melting conditions in the mantle beneath the Basin and Range province from seismology and petrology. <i>Geochemistry, Geophysics, Geosystems</i> , 2016 , 17, 1312-1338	3.6	62
412	Postcollisional lithospheric evolution of the Southeast Carpathians: Comparison of geodynamical models and observations. 2016 , 35, 1205-1224		27
411	References. 507-594		
410	Finite-frequency wave propagation through outer rise fault zones and seismic measurements of upper mantle hydration. <i>Geophysical Research Letters</i> , 2016 , 43, 7982-7990	4.9	12
409	Lasting mantle scars lead to perennial plate tectonics. 2016 , 7, 11834		42
408	Making it and breaking it in the Midwest: Continental assembly and rifting from modeling of EarthScope magnetotelluric data. 2016 , 278, 337-361		22
407	Reconciling laboratory and observational models of mantle rheology in geodynamic modelling. 2016 , 100, 33-50		22
406	Homologous temperature of olivine: Implications for creep of the upper mantle and fabric transitions in olivine. 2016 , 59, 1138-1156		7
405	Data-Driven Numerical Modelling in Geodynamics: Methods and Applications. 2016 ,		1
404	Methodological progress in trace amounts of structural water in nominally anhydrous minerals. 2016 , 59, 901-909		6
403	High-P/T experimental studies and water in the silicate mantle. 2016 , 59, 683-695		1
402	How craton margins are preserved: Insights from geodynamic models. 2016 , 100, 144-158		29
401	Nuclear Reaction Analysis. 2016 , 315-336		3

400	The water content and hydrogen isotope composition of continental lithospheric mantle and mantle-derived mafic igneous rocks in eastern China. 2016 , 59, 910-926		6	
399	Constraining lithosphere deformation modes during continental breakup for the IberiaNewfoundland conjugate rifted margins. 2016 , 680, 28-49		14	
398	Olivine anisotropy suggests Gutenberg discontinuity is not the base of the lithosphere. 2016 , 113, 105	03-6	26	
397	Gravity anomalies, flexure and mantle rheology seaward of circum-Pacific trenches. <i>Geophysical Journal International</i> , 2016 , 207, 288-316	2.6	40	
396	Origin of high-velocity anomalies beneath the Siberian craton: A fingerprint of multistage magma underplating since the Neoarchean. 2016 , 57, 713-722		2	
395	3-D multiobservable probabilistic inversion for the compositional and thermal structure of the lithosphere and upper mantle: III. Thermochemical tomography in the Western-Central U.S <i>Journal of Geophysical Research: Solid Earth</i> , 2016 , 121, 7337-7370	3.6	47	
394	Olivine inclusions in Siberian diamonds and mantle xenoliths: Contrasting water and trace-element contents. 2016 , 265, 31-41		22	
393	Evolution of the rheological and microstructural properties of olivine aggregates during dislocation creep under hydrous conditions. <i>Journal of Geophysical Research: Solid Earth</i> , 2016 , 121, 92-113	3.6	20	
392	Ridge asymmetry and deep aqueous alteration at the trench observed from Rayleigh wave tomography of the Juan de Fuca plate. <i>Journal of Geophysical Research: Solid Earth</i> , 2016 , 121, 7298-73	2³ ^{.6}	29	
391	Upper-mantle water stratification inferred from observations of the 2012 Indian Ocean earthquake. <i>Nature</i> , 2016 , 538, 373-377	50.4	51	
390	Tomography reveals buoyant asthenosphere accumulating beneath the Juan de Fuca plate. 2016 , 353, 1406-1408		45	
389	Evidence and models for lower crustal flow beneath the Galpagos platform. <i>Geochemistry, Geophysics, Geosystems</i> , 2016 , 17, 113-142	3.6	6	
388	Nature of the seismic lithosphere-asthenosphere boundary within normal oceanic mantle from high-resolution receiver functions. <i>Geochemistry, Geophysics, Geosystems</i> , 2016 , 17, 1265-1282	3.6	27	
387	Imaging the Lithosphere and Upper Mantle. 2016 , 191-218		18	
386	A flow law for ilmenite in dislocation creep: Implications for lunar cumulate mantle overturn. <i>Geophysical Research Letters</i> , 2016 , 43, 532-540	4.9	23	
385	Dynamics of plumelriple junction interaction: Results from a series of three-dimensional numerical models and implications for the formation of oceanic plateaus. <i>Journal of Geophysical Research: Solid Earth</i> , 2016 , 121, 1316-1342	3.6	11	
384	Upper mantle structure of the Tonga-Lau-Fiji region from Rayleigh wave tomography. <i>Geochemistry, Geophysics, Geosystems</i> , 2016 , 17, 4705-4724	3.6	8	
383	Identifying mantle lithosphere inheritance in controlling intraplate orogenesis. <i>Journal of Geophysical Research: Solid Earth</i> , 2016 , 121, 6966-6987	3.6	14	

382	Water in the Martian interior⊞he geodynamical perspective. 2016 , 51, 1959-1992	17	,
381	Titanium-hydroxyl defect-controlled rheology of the Earth's upper mantle. <i>Earth and Planetary Science Letters</i> , 2016 , 452, 227-237	42	2
380	Lithospheric strength variations in Mainland China: Tectonic implications. 2016 , 35, 2313-2333	26	<u>,</u>
379	The Role of Volatiles in Reactive Melt Transport in the Asthenosphere. 2016 , 57, 1073-1108	85	5
378	A review of volatiles in the Martian interior. 2016 , 51, 1935-1958	33	
377	Seismic imaging of a mid-lithospheric discontinuity beneath Ontong Java Plateau. <i>Earth and Planetary Science Letters</i> , 2016 , 450, 62-70	32	
376	Implications for metal and volatile cycles from the pH of subduction zone fluids. <i>Nature</i> , 2016 , 539, 420-424	4 6 <u>9</u>)
375	Questions on the existence, persistence, and mechanical effects of a very small melt fraction in the asthenosphere. <i>Geochemistry, Geophysics, Geosystems</i> , 2016 , 17, 470-484	43	5
374	A new approach to computing steady-state geotherms: The marginal stability condition. 2016 , 693, 32-46		
373	Constraining mantle convection models with palaeomagnetic reversals record and numerical dynamos. <i>Geophysical Journal International</i> , 2016 , 207, 1165-1184	4	
372	A consistent model for fluid distribution, viscosity distribution, and flow-thermal structure in subduction zone. <i>Journal of Geophysical Research: Solid Earth</i> , 2016 , 121, 3238-3260	30)
371	Variations in timing of lithospheric failure on terrestrial planets due to chaotic nature of mantle convection. <i>Geochemistry, Geophysics, Geosystems</i> , 2016 , 17, 1569-1585	4	
370	Highly Siderophile Element and Os Isotope Systematics of Volcanic Rocks at Divergent and Convergent Plate Boundaries and in Intraplate Settings.		
369	Major element composition of an Early Enriched Reservoir: constraints from 142Nd/144Nd isotope systematics in the early Earth and high-pressure melting experiments of a primitive peridotite. 2016 , 3,	1	
368	Whole planet coupling between climate, mantle, and core: Implications for rocky planet evolution. <i>Geochemistry, Geophysics, Geosystems</i> , 2016 , 17, 1885-1914	53	•
367	Lithospheric structure of Central Europe: Puzzle pieces from Pannonian Basin to Trans-European Suture Zone resolved by geophysical-petrological modeling. 2016 , 35, 722-753	10)
366	On water in nominally anhydrous minerals from mantle peridotites and magmatic rocks. 2016 , 59, 1157-117	2 7	
365	Numerical models of mantle lithosphere weakening, erosion and delamination induced by melt extraction and emplacement. 2016 , 105, 1741-1760	10)

364	Density and visco-elasticity of Natrosol 250 HH solutions: Determining their suitability for experimental tectonics. 2016 , 86, 153-165		12	
363	Present-day dynamic and residual topography in Central Anatolia. <i>Geophysical Journal International</i> , 2016 , 206, 1515-1525	2.6	20	
362	Origin of plagiogranites in oceanic complexes: A case study of the Nicoya and Santa Elena terranes, Costa Rica. 2016 , 262, 75-87		18	
361	Dynamic cause of marginal lithospheric thinning and implications for craton destruction: a comparison of the North China, Superior, and Yilgarn cratons. 2016 , 53, 1121-1141		12	
360	Two-component mantle melting-mixing model for the generation of mid-ocean ridge basalts: Implications for the volatile content of the Pacific upper mantle. 2016 , 176, 44-80		85	
359	The mantle wedge's transient 3-D flow regime and thermal structure. <i>Geochemistry, Geophysics, Geosystems</i> , 2016 , 17, 78-100	3.6	22	
358	On Earth Mantle Constitution and Structure from Joint Analysis of Geophysical and Laboratory-Based Data: An Example. 2016 , 37, 149-189		19	
357	Melting-induced crustal production helps plate tectonics on Earth-like planets. <i>Earth and Planetary Science Letters</i> , 2016 , 439, 18-28	5.3	36	
356	Water and fabric in an ophiolitic peridotite from a supra-subduction zone. 2016 , 171, 1		7	
355	Proton conduction and hydrogen diffusion in olivine: an attempt to reconcile laboratory and field observations and implications for the role of grain boundary diffusion in enhancing conductivity. 2016 , 43, 237-265		17	
354	Highly Siderophile Element and Os Isotope Systematics of Volcanic Rocks at Divergent and Convergent Plate Boundaries and in Intraplate Settings. 2016 , 81, 651-724		38	
353	Distribution and transport of hydrogen in the lithospheric mantle: A review. 2016 , 240-243, 402-425		127	
352	Decarbonation of subducting slabs: Insight from petrologicalEhermomechanical modeling. <i>Gondwana Research</i> , 2016 , 36, 314-332	5.1	20	
351	Thickness of the oceanic crust, the lithosphere, and the mantle transition zone in the vicinity of the Tristan da Cunha hot spot estimated from ocean-bottom and ocean-island seismometer receiver functions. 2017 , 716, 33-51		20	
350	Imaging Pacific lithosphere seismic discontinuitiesIhsights from SS precursor modeling. <i>Journal of Geophysical Research: Solid Earth</i> , 2017 , 122, 2131	3.6	17	
349	Volatiles beneath mid-ocean ridges: Deep melting, channelised transport, focusing, and metasomatism. <i>Earth and Planetary Science Letters</i> , 2017 , 464, 55-68	5.3	70	
348	Experimental constraints on the damp peridotite solidus and oceanic mantle potential temperature. 2017 , 355, 942-945		49	
347	Origins of water content variations in the suboceanic upper mantle: Insight from Southwest Indian Ridge abyssal peridotites. <i>Geochemistry, Geophysics, Geosystems</i> , 2017 , 18, 1298-1329	3.6	7	

346	The dynamical control of subduction parameters on surface topography. <i>Geochemistry, Geophysics, Geosystems</i> , 2017 , 18, 1661-1687	3.6	19
345	The fate of water within Earth and super-Earths and implications for plate tectonics. 2017, 375,		18
344	Water transport by subduction: Clues from garnet of Erzgebirge UHP eclogite. 2017 , 102, 975-986		12
343	Using mineral equilibria to estimate H2O activities in peridotites from the Western Gneiss Region of Norway. 2017 , 102, 1021-1036		5
342	Formation age and metasomatism of the sub-continental lithospheric mantle beneath southeast China: Sr-Nd-Hf-Os isotopes of Mingxi mantle xenoliths. 2017 , 145, 591-604		12
341	Crustal deformation induced by mantle dynamics: insights from models of gravitational lithosphere removal. <i>Geophysical Journal International</i> , 2017 , 210, 1070-1091	2.6	4
340	High seismic attenuation at a mid-ocean ridge reveals the distribution of deep melt. <i>Science Advances</i> , 2017 , 3, e1602829	14.3	41
339	High water content in primitive mid-ocean ridge basalt from Southwest Indian Ridge (51.56"E): Implications for recycled hydrous component in the mantle. 2017 , 28, 411-421		5
338	Hydration-reduced lattice thermal conductivity of olivine in Earth's upper mantle. 2017 , 114, 4078-4081		32
337	Chemical interactions in the subduction factory: New insights from an in situ trace element and hydrogen study of the Ichinomegata and Oki-Dogo mantle xenoliths (Japan). 2017 , 208, 234-267		17
336	Forearc structure in the Lesser Antilles inferred from depth to the Curie temperature and thermo-mechanical simulations. 2017 , 706-707, 71-90		5
335	The initiation and tectonic regimes of the Cenozoic extension in the Bohai Bay Basin, North China revealed by numerical modelling. 2017 , 140, 92-107		5
334	New SIMS reference materials for measuring water in upper mantle minerals. 2017 , 102, 537-547		19
333	Geodynamical Models for Continental Delamination and Ocean Lithosphere Peel Away in an Orogenic Setting. 2017 , 121-139		5
332	The structural evolution of the deep continental lithosphere. 2017 , 695, 100-121		22
331	Subduction Initiation With Vertical Lithospheric Heterogeneities and New Fault Formation. <i>Geophysical Research Letters</i> , 2017 , 44, 11,349-11,356	4.9	15
330	On Joint Modelling of Electrical Conductivity and Other Geophysical and Petrological Observables to Infer the Structure of the Lithosphere and Underlying Upper Mantle. 2017 , 38, 963-1004		14
329	H2O solubility in basalt at upper mantle conditions. 2017 , 172, 1		15

328	Diffusion Creep of Enstatite at High Pressures Under Hydrous Conditions. <i>Journal of Geophysical Research: Solid Earth</i> , 2017 , 122, 7718-7728	3.6	6
327	Submarine Basaltic Glasses from the Galapagos Archipelago: Determining the Volatile Budget of the Mantle Plume. 2017 , 58, 1419-1450		14
326	The interior structure of Ceres as revealed by surface topography. <i>Earth and Planetary Science Letters</i> , 2017 , 476, 153-164	5.3	99
325	Crustal-Scale Seismic Structure From Trench to Forearc in the Cascadia Subduction Zone. <i>Journal of Geophysical Research: Solid Earth</i> , 2017 , 122, 7311-7328	3.6	4
324	Subsolidus hydrogen partitioning between nominally anhydrous minerals in garnet-bearing peridotite. 2017 , 102, 1822-1831		28
323	Effects of Partial Melting on Seismic Velocity and Attenuation: A New Insight from Experiments. 2017 , 45, 447-470		60
322	Dependence of the Brittle Ductile Transition on Strain-Rate-Dependent Critical Homologous Temperature. <i>Geophysical Journal International</i> , 2017 ,	2.6	
321	Fabric heterogeneity in the Mojave lower crust and lithospheric mantle in Southern California. Journal of Geophysical Research: Solid Earth, 2017 , 122, 5000-5025	3.6	15
320	Decarbonation in an intracratonic setting: Insight from petrological-thermomechanical modeling. Journal of Geophysical Research: Solid Earth, 2017 , 122, 5992-6013	3.6	4
319	Fluid migration in the mantle wedge: Influence of mineral grain size and mantle compaction. Journal of Geophysical Research: Solid Earth, 2017 , 122, 6247-6268	3.6	27
318	Water, lithium and trace element compositions of olivine from Lanzo South replacive mantle dunites (Western Alps): New constraints into melt migration processes at cold thermal regimes. 2017 , 214, 51-72		18
317	Mantle dynamics beneath the discrete and diffuse plate boundaries of the Juan de Fuca plate: Results from Cascadia Initiative body wave tomography. <i>Geochemistry, Geophysics, Geosystems</i> , 2017 , 18, 2906-2929	3.6	19
316	The importance of grain size to mantle dynamics and seismological observations. <i>Geochemistry, Geophysics, Geosystems</i> , 2017 , 18, 3034-3061	3.6	41
315	Water in the Earth⊠Interior: Distribution and Origin. 2017 , 212, 743-810		92
314	Long-term preservation of early formed mantle heterogeneity by mobile lid convection: Importance of grainsize evolution. <i>Earth and Planetary Science Letters</i> , 2017 , 475, 94-105	5.3	12
313	A seismic shift in continental tectonic plates. 2017 , 357, 549-550		
312	Lower Crustal Strength Controls on Melting and Serpentinization at Magma-Poor Margins: Potential Implications for the South Atlantic. <i>Geochemistry, Geophysics, Geosystems</i> , 2017 , 18, 4538-4557	, 3.6	28
311	Evidence for frozen melts in the mid-lithosphere detected from active-source seismic data. <i>Scientific Reports</i> , 2017 , 7, 15770	4.9	7

310	Drip tectonics and the enigmatic uplift of the Central Anatolian Plateau. 2017, 8, 1538		59
309	Causes and Consequences of Diachronous V-Shaped Ridges in the North Atlantic Ocean. <i>Journal of Geophysical Research: Solid Earth</i> , 2017 , 122, 8675-8708	3.6	8
308	Thermal Equation of State of Natural Ti-Bearing Clinohumite. <i>Journal of Geophysical Research: Solid Earth</i> , 2017 , 122, 8943-8951	3.6	7
307	Flow behavior and microstructures of hydrous olivine aggregates at upper mantle pressures and temperatures. 2017 , 172, 1		5
306	The role of pargasitic amphibole in the formation of major geophysical discontinuities in the shallow upper mantle. 2017 , 52, 183-204		11
305	Origins of cratonic mantle discontinuities: A view from petrology, geochemistry and thermodynamic models. 2017 , 268-271, 364-382		52
304	Propagating buoyant mantle upwelling on the Reykjanes Ridge. <i>Earth and Planetary Science Letters</i> , 2017 , 457, 10-22	5.3	9
303	Rift@rift transition in a magma-rich system: the Gop Rift@axmi Basin case study, West India. 2017 , 445, 95-117		12
302	Marine magnetotellurics imaged no distinct plume beneath the Tristan da Cunha hotspot in the southern Atlantic Ocean. 2017 , 716, 52-63		15
301	Distribution, cycling and impact of water in the Earth's interior. 2017 , 4, 879-891		15
300	Determination of intrinsic attenuation in the oceanic lithosphere-asthenosphere system. 2017 , 358, 1	593-159	96 18
299	How seismic waves lose energy. 2017 , 358, 1536-1537		1
298	Crystal preferred orientations of olivine, orthopyroxene, serpentine, chlorite, and amphibole, and implications for seismic anisotropy in subduction zones: a review. 2017 , 21, 985-1011		41
298 297		3.6	41 31
-	implications for seismic anisotropy in subduction zones: a review. 2017 , 21, 985-1011 Hydrolytic weakening in olivine single crystals. <i>Journal of Geophysical Research: Solid Earth</i> , 2017 ,	3.6 3.6	
297	implications for seismic anisotropy in subduction zones: a review. 2017 , 21, 985-1011 Hydrolytic weakening in olivine single crystals. <i>Journal of Geophysical Research: Solid Earth</i> , 2017 , 122, 3465-3479 Constraints on the anisotropic contributions to velocity discontinuities at ~60 km depth beneath		31
² 97	implications for seismic anisotropy in subduction zones: a review. 2017, 21, 985-1011 Hydrolytic weakening in olivine single crystals. <i>Journal of Geophysical Research: Solid Earth</i> , 2017, 122, 3465-3479 Constraints on the anisotropic contributions to velocity discontinuities at ~60 km depth beneath the Pacific. <i>Geochemistry, Geophysics, Geosystems</i> , 2017, 18, 2855-2871 Effect of water on rock deformation and rheological structures of continental and oceanic plates.		31

292	Scattered wave imaging of the oceanic plate in Cascadia. Science Advances, 2018, 4, eaao1908	14.3	32
291	Halogens in the Earth Mantle: What We Know and What We Don El 2018, 847-869		12
290	Water and the Interior Structure of Terrestrial Planets and Icy Bodies. 2018 , 214, 1		23
289	Evaluating the Influence of Plate Boundary Friction and Mantle Viscosity on Plate Velocities. <i>Geochemistry, Geophysics, Geosystems</i> , 2018 , 19, 642-666	3.6	11
288	Diffuse Extension of the Southern Mariana Margin. <i>Journal of Geophysical Research: Solid Earth</i> , 2018 , 123, 892-916	3.6	14
287	Water-rich sublithospheric melt channel in the equatorial Atlantic Ocean. <i>Nature Geoscience</i> , 2018 , 11, 65-69	18.3	26
286	The Generation of Barriers to Melt Ascent in the Martian Lithosphere. 2018 , 123, 47-66		5
285	Redox-influenced seismic properties of upper-mantle olivine. <i>Nature</i> , 2018 , 555, 355-358	50.4	83
284	Low hydrogen contents in the cores of terrestrial planets. <i>Science Advances</i> , 2018 , 4, e1701876	14.3	31
283	Stress evolution and associated microstructure during transient creep of olivine at 1000\darksquare 2018, 278, 34-46		25
282	Making Archean cratonic roots by lateral compression: A two-stage thickening and stabilization model. 2018 , 746, 562-571		26
281	Slab-triggered wet upwellings produce large volumes of melt: Insights into the destruction of the North China Craton. 2018 , 746, 266-279		20
280	Deep mantle roots and continental emergence: implications for whole-Earth elemental cycling, long-term climate, and the Cambrian explosion. 2018 , 60, 431-448		45
279	Can metasomatic weakening result in the rifting of cratons?. 2018 , 746, 3-21		15
278	The deep structure and reactivation of the Kyrgyz Tien Shan: Modelling the past to better constrain the present. 2018 , 746, 530-548		12
277	Water in garnet pyroxenite from the Sulu orogen: Implications for crust-mantle interaction in continental subduction zone. 2018 , 478, 18-38		8
276	On the Grain Size Sensitivity of Olivine Rheology. <i>Journal of Geophysical Research: Solid Earth</i> , 2018 , 123, 674-688	3.6	13
275	Control on off-rift magmatism: A case study of the Baikal Rift Zone. <i>Earth and Planetary Science Letters</i> , 2018 , 482, 501-509	5.3	8

274	A Geophysical Perspective on the Bulk Composition of Mars. 2018 , 123, 575-611		75
273	Tectonic controls on Ni and Cu contents of primary mantle-derived magmas for the formation of magmatic sulfide deposits. 2018 , 103, 1545-1567		20
272	. 2018,		4
271	The Evolution of the Oceanic Lithosphere. 2018 , 35-53		1
270	Geological understanding of plate tectonics: Basic concepts, illustrations, examples and new perspectives. 2018 , 10, 23-46		82
269	Water and Oxygen Fugacity in the Lithospheric Mantle Wedge beneath the Northern Canadian Cordillera (Alligator Lake). <i>Geochemistry, Geophysics, Geosystems</i> , 2018 , 19, 3844-3869	3.6	9
268	Fluid Controls on the Heterogeneous Seismic Characteristics of the Cascadia Margin. <i>Geophysical Research Letters</i> , 2018 , 45, 11,021	4.9	31
267	Crustal evolution and mantle dynamics through Earth history. 2018 , 376,		50
266	Electrical Discontinuities in the Continental Lithosphere Imaged with Magnetotellurics. 2018 , 89-109		8
265	On the Origin of the Upper Mantle Seismic Discontinuities. 2018 , 5-34		9
265 264	On the Origin of the Upper Mantle Seismic Discontinuities. 2018, 5-34 Imaging Lithospheric Discontinuities Beneath the Northern East African Rift Using -to- Receiver Functions. <i>Geochemistry, Geophysics, Geosystems</i> , 2018, 19, 4048-4062	3.6	9
	Imaging Lithospheric Discontinuities Beneath the Northern East African Rift Using -to- Receiver	3.6	
264	Imaging Lithospheric Discontinuities Beneath the Northern East African Rift Using -to- Receiver Functions. <i>Geochemistry, Geophysics, Geosystems</i> , 2018 , 19, 4048-4062 Measurement of Activation Volume for Creep of Dry Olivine at Upper-Mantle Conditions. <i>Journal of</i>		16
264	Imaging Lithospheric Discontinuities Beneath the Northern East African Rift Using -to- Receiver Functions. <i>Geochemistry, Geophysics, Geosystems</i> , 2018 , 19, 4048-4062 Measurement of Activation Volume for Creep of Dry Olivine at Upper-Mantle Conditions. <i>Journal of Geophysical Research: Solid Earth</i> , 2018 , 123, 8459-8473 Lateral H2O variation in the Zealandia lithospheric mantle controls orogen width. <i>Earth and</i>	3.6	16 9
264 263 262	Imaging Lithospheric Discontinuities Beneath the Northern East African Rift Using -to-Receiver Functions. <i>Geochemistry, Geophysics, Geosystems</i> , 2018 , 19, 4048-4062 Measurement of Activation Volume for Creep of Dry Olivine at Upper-Mantle Conditions. <i>Journal of Geophysical Research: Solid Earth</i> , 2018 , 123, 8459-8473 Lateral H2O variation in the Zealandia lithospheric mantle controls orogen width. <i>Earth and Planetary Science Letters</i> , 2018 , 502, 200-209 Spatiotemporal Variation of Mantle Viscosity and the Presence of Cratonic Mantle Inferred From 8 Years of Postseismic Deformation Following the 2010 Maule, Chile, Earthquake. <i>Geochemistry</i> ,	3.6 5·3	16 9 12
264263262261	Imaging Lithospheric Discontinuities Beneath the Northern East African Rift Using -to- Receiver Functions. <i>Geochemistry, Geophysics, Geosystems</i> , 2018 , 19, 4048-4062 Measurement of Activation Volume for Creep of Dry Olivine at Upper-Mantle Conditions. <i>Journal of Geophysical Research: Solid Earth</i> , 2018 , 123, 8459-8473 Lateral H2O variation in the Zealandia lithospheric mantle controls orogen width. <i>Earth and Planetary Science Letters</i> , 2018 , 502, 200-209 Spatiotemporal Variation of Mantle Viscosity and the Presence of Cratonic Mantle Inferred From 8 Years of Postseismic Deformation Following the 2010 Maule, Chile, Earthquake. <i>Geochemistry, Geophysics, Geosystems</i> , 2018 , 19, 3272-3285 Early planetary atmospheres and surfaces: Origin of the Earth® water, crust and atmosphere. 2018 ,	3.6 5·3	16 9 12
264263262261260	Imaging Lithospheric Discontinuities Beneath the Northern East African Rift Using -to-Receiver Functions. <i>Geochemistry, Geophysics, Geosystems</i> , 2018, 19, 4048-4062 Measurement of Activation Volume for Creep of Dry Olivine at Upper-Mantle Conditions. <i>Journal of Geophysical Research: Solid Earth</i> , 2018, 123, 8459-8473 Lateral H2O variation in the Zealandia lithospheric mantle controls orogen width. <i>Earth and Planetary Science Letters</i> , 2018, 502, 200-209 Spatiotemporal Variation of Mantle Viscosity and the Presence of Cratonic Mantle Inferred From 8 Years of Postseismic Deformation Following the 2010 Maule, Chile, Earthquake. <i>Geochemistry, Geophysics, Geosystems</i> , 2018, 19, 3272-3285 Early planetary atmospheres and surfaces: Origin of the Earth® water, crust and atmosphere. 2018, 14, 156-163 Seismic Imaging of Thickened Lithosphere Resulting From Plume Pulsing Beneath Iceland.	3.6 5·3 3.6	16 9 12 10

256	On the (mis)behavior of water in the mantle: Controls on nominally anhydrous mineral water content in mantle peridotites. <i>Earth and Planetary Science Letters</i> , 2018 , 499, 219-229	5.3	10
255	Craton Destruction 1: Cratonic Keel Delamination Along a Weak Midlithospheric Discontinuity Layer. <i>Journal of Geophysical Research: Solid Earth</i> , 2018 , 123, 10,040-10,068	3.6	15
254	High-pressure single-crystal elasticity of wadsleyite and the seismic signature of water in the shallow transition zone. <i>Earth and Planetary Science Letters</i> , 2018 , 498, 77-87	5.3	36
253	Aqueous Fluid Connectivity in Subducting Oceanic Crust at the Mantle Transition Zone Conditions. <i>Journal of Geophysical Research: Solid Earth</i> , 2018 , 123, 6562	3.6	3
252	Encyclopedia of Geochemistry. 2018 , 477-483		2
251	Primary Melt Compositions in the Earth's Mantle. 2018 , 3-42		6
250	The Influence of Pressure on the Properties and Origins of Hydrous Silicate Liquids in Earth's Interior. 2018 , 83-113		3
249	Dynamics of fault motion and the origin of contrasting tectonic style between Earth and Venus. <i>Scientific Reports</i> , 2018 , 8, 11884	4.9	18
248	Dynamics of rheological heterogeneities in mantle plumes. <i>Earth and Planetary Science Letters</i> , 2018 , 499, 74-82	5.3	10
247	Spreading Dynamics of an Intermediate Ridge: Insights from U-series Disequilibria, Endeavour Segment, Juan de Fuca Ridge. 2018 , 59, 1847-1868		2
246	Upper mantle xenoliths as sources of geophysical information: the Perlini Mts. area as a case study. 2018 , 53, 415-438		6
245	Destruction of the North China Craton triggered by the Triassic Yangtze continental subduction/collision: A review. 2018 , 164, 72-82		14
244	Composition and evolution of the lithospheric mantle beneath the interior of the South China Block: insights from trace elements and water contents of peridotite xenoliths. 2018 , 173, 1		9
243	Shear attenuation beneath the Juan de Fuca plate: Implications for mantle flow and dehydration. <i>Earth and Planetary Science Letters</i> , 2018 , 496, 189-197	5.3	9
242	Water Migration in the Subduction Mantle Wedge: A Two-Phase Flow Approach. <i>Journal of Geophysical Research: Solid Earth</i> , 2019 , 124, 9208-9225	3.6	10
241	Constraining Mantle Heterogeneity beneath the South China Sea: A New Perspective on Magma Water Content. 2019 , 9, 410		3
240	Coupled inter-site reaction and diffusion: Rapid dehydrogenation of silicon vacancies in natural olivine. 2019 , 262, 220-242		15
239	An experimental investigation on fluid transfer mechanisms in ultramafic rocks. 2019 , 127, 103871		

238	Evolution of the Josephine Peridotite Shear Zones: 1. Compositional Variation and Shear Initiation. <i>Geochemistry, Geophysics, Geosystems</i> , 2019 , 20, 5765-5785	3.6	4
237	Toward a boot strap hypothesis of plate tectonics: Feedbacks between plates, the asthenosphere, and the wavelength of mantle convection. 2019 , 296, 106299		12
236	Pacific Lithosphere Evolution Inferred from Aitutaki Mantle Xenoliths. 2019 , 60, 1753-1772		8
235	Crystal structure change in grossularBiffree katoite solid solution: Oxygen position splitting in katoite. 2019 , 114, 189-200		4
234	High-Temperature Evolution of Point Defect Equilibria in Hydrous Forsterite Synthesized at 1100 °C and up to 4 GPa. 2019 , 9, 574		0
233	Hydrous LABZ beneath a subduction zone was reconstructed for the first time. 2019 , 104, 1219-1220		
232	Origin and abundances of H2O in the terrestrial planets, Moon, and asteroids. <i>Earth and Planetary Science Letters</i> , 2019 , 526, 115771	5.3	31
231	Reconstruction of the lithosphere-asthenosphere boundary zone beneath Ichinomegata maar, Northeast Japan, by geobarometry of spinel peridotite xenoliths. 2019 , 104, 1285-1306		4
230	Thin lithosphere beneath the central Appalachian Mountains: A combined seismic and magnetotelluric study. <i>Earth and Planetary Science Letters</i> , 2019 , 519, 308-316	5.3	11
229	Evaluating the roles of melt-rock interaction and partial degassing on the CO2/Ba ratios of MORB: Implications for the CO2 budget in the Earth depleted upper mantle. 2019 , 260, 29-48		7
228	Joint modeling of lithosphere and mantle dynamics: Sensitivity to viscosities within the lithosphere, asthenosphere, transition zone, and D" layers. 2019 , 293, 106263		9
227	Identifying volatile mantle trend with the waterfluorinederium systematics of basaltic glass. 2019 , 522, 283-294		12
226	Impact of Mafic Underplating and Mantle Depletion on Subsequent Rifting: A Numerical Modeling Study. 2019 , 38, 2185-2207		4
225	Mechanism of subsidence of the Northeast Japan forearc during the late period of a gigantic earthquake cycle. <i>Scientific Reports</i> , 2019 , 9, 5726	4.9	4
224	Relationships Between Olivine CPO and Deformation Parameters in Naturally Deformed Rocks and Implications for Mantle Seismic Anisotropy. <i>Geochemistry, Geophysics, Geosystems</i> , 2019 , 20, 3469-3494	3.6	20
223	Activation of [100](001) slip system by water incorporation in olivine and the cause of seismic anisotropy decrease with depth in the asthenosphere. 2019 , 104, 47-52		4
222	Geochemical Variability Along the Northern East Pacific Rise: Coincident Source Composition and Ridge Segmentation. <i>Geochemistry, Geophysics, Geosystems</i> , 2019 , 20, 1889-1911	3.6	11
221	Chemical Disequilibria, Lithospheric Thickness, and the Source of Ocean Island Basalts. 2019 , 60, 755-79	0	4

(2020-2019)

220	Thermal nature and resolution of the lithospherellsthenosphere boundary under the Pacific from surface waves. <i>Geophysical Journal International</i> , 2019 , 216, 1441-1465	2.6	6
219	Anisotropic high-temperature creep in hydrous olivine single crystals and its geodynamic implications. 2019 , 290, 1-9		12
218	Low water content in the mantle source of the Hainan plume as a factor inhibiting the formation of a large igneous province. <i>Earth and Planetary Science Letters</i> , 2019 , 515, 221-230	5.3	14
217	Evidence for dehydration-modulated small-scale convection in the oceanic upper mantle from seafloor bathymetry and Rayleigh wave phase velocity. <i>Earth and Planetary Science Letters</i> , 2019 , 510, 12-25	5.3	5
216	New constraints on mantle carbon from Mid-Atlantic Ridge popping rocks. <i>Earth and Planetary Science Letters</i> , 2019 , 511, 67-75	5.3	14
215	Quantifying the Correlation Between Mobile Continents and Elevated Temperatures in the Subcontinental Mantle. <i>Geochemistry, Geophysics, Geosystems</i> , 2019 , 20, 1358-1386	3.6	3
214	Crustal and lithospheric mantle conductivity structure in the Dharwar craton, India. 2019, 176, 253-263		7
213	The ability of significant tidal stress to initiate plate tectonics. 2019 , 325, 55-66		6
212	Onset and Evolution of Plate Tectonics: Geodynamical Constraints. 2019,		
211	Synthesizing EarthScope data to constrain the thermal evolution of the continental U.S. lithosphere. 2019 , 15, 1722-1737		3
210	Two Stages of Thermal Evolution of the Continental Lithosphere. 2019 , 55, 679-686		2
209	Illuminating subduction zone rheological properties in the wake of a giant earthquake. <i>Science Advances</i> , 2019 , 5, eaax6720	14.3	23
208	Tectonic Controls on Carbon and Serpentinite Storage in Subducted Upper Oceanic Lithosphere for the Past 320 Ma. 2019 , 7,		5
207	Dynamics in the Uppermost Lower Mantle: Insights into the Deep Mantle Water Cycle Based on the Numerical Modeling of Subducted Slabs and Global-Scale Mantle Dynamics. 2019 , 47, 41-66		3
206	The dynamic life of an oceanic plate. 2019 , 760, 107-135		20
205	Water in the upper mantle and deep crust of eastern China: concentration, distribution and implications. 2019 , 6, 125-144		52
204	Reykjanes Ridge evolution: Effects of plate kinematics, small-scale upper mantle convection and a regional mantle gradient. 2020 , 206, 102956		6

202	Bridging the water solubility and ion diffusivity in the mantle silicates by a thermodynamic model. 2020 , 114, 1-13		2
201	Petrological geodynamics of mantle melting III. AlphaMELTS + multiphase flow: The effect of water. 2020 , 11, 1381-1402		
200	Application of a Premelting Model to the Lithosphere-Asthenosphere Boundary. <i>Geochemistry, Geophysics, Geosystems</i> , 2020 , 21, e2020GC009338	3.6	2
199	Rates of Olivine Grain Growth During Dynamic Recrystallization and Postdeformation Annealing. <i>Journal of Geophysical Research: Solid Earth</i> , 2020 , 125, e2020JB020415	3.6	8
198	Thermobarometry of CO2-rich, silica-undersaturated melts constrains cratonic lithosphere thinning through time in areas of kimberlitic magmatism. <i>Earth and Planetary Science Letters</i> , 2020 , 550, 116549	5.3	10
197	Thermal History of the Earth: On the Importance of Surface Processes and the Size of Tectonic Plates. <i>Geochemistry, Geophysics, Geosystems</i> , 2020 , 21, e2020GC009123	3.6	O
196	Effects of Water on the Rheology of Dominant Minerals and Rocks in the Continental Lower Crust: A Review. 2020 , 31, 1170-1182		3
195	Metasomatic control of hydrogen contents in the layered cratonic mantle lithosphere sampled by Lac de Gras xenoliths in the central Slave craton, Canada. 2020 , 286, 29-53		6
194	Effect of sulfur speciation on chemical and physical properties of very reduced mercurian melts. 2020 , 286, 1-18		4
193	Uppermost crustal structure across the eastern Lau spreading center from P-to-S converted waves. 2020 , 41, 1		2
192	The Antarctic Crust and Upper Mantle: A Flexible 3D Model and Software Framework for Interdisciplinary Research. 2020 , 8,		3
191	Thermochemical lithosphere differentiation and the origin of cratonic mantle. <i>Nature</i> , 2020 , 588, 89-94	50.4	13
190	Synergy of Experimental Rock Mechanics, Seismology, and Geodynamics Reveals Still Elusive Upper Mantle Rheology. <i>Journal of Geophysical Research: Solid Earth</i> , 2020 , 125, e2020JB019896	3.6	3
189	Grain-Boundary Diffusion Creep of Olivine: 2. Solidus Effects and Consequences for the Viscosity of the Oceanic Upper Mantle. <i>Journal of Geophysical Research: Solid Earth</i> , 2020 , 125, e2020JB019416	3.6	5
188	Convective Instability in Intraplate Oceanic Mantle Caused by Amphibolite-Derived Garnet-Pyroxenites A Xenolith Perspective (Hyblean Plateau, Sicily). 2020 , 10, 378		
187	Metasomatism-controlled hydrogen distribution in the Spitsbergen upper mantle. 2020 , 105, 1326-134	1	2
186	Editorial for the Special Issue P roperties of Melt and Minerals at High Pressures and High Temperature 2020 , 10, 723		1
185	Lithospheric structures of and tectonic implications for the centralBast Tibetan plateau inferred from joint tomography of receiver functions and surface waves. <i>Geophysical Journal International</i> , 2020 , 223, 1688-1707	2.6	3

(2020-2020)

184	The Nature of the Lithosphere-Asthenosphere Boundary. <i>Journal of Geophysical Research: Solid Earth</i> , 2020 , 125, e2018JB016463	3.6	23
183	Deep Water Cycling and the Multi-Stage Cooling of the Earth. <i>Geochemistry, Geophysics, Geosystems</i> , 2020 , 21, e2020GC009106	3.6	2
182	A Lithosphere-Asthenosphere Boundary and Partial Melt Estimated Using Marine Magnetotelluric Data at the Central Middle Atlantic Ridge. <i>Geochemistry, Geophysics, Geosystems</i> , 2020 , 21, e2020GC00	9377	12
181	Quantitative vesicle analyses and total CO2 reconstruction in mid-ocean ridge basalts. 2020 , 407, 1071	09	3
180	A comparison of oceanic and continental mantle lithosphere. 2020 , 309, 106600		11
179	Impact of power-law rheology on the viscoelastic relaxation pattern and afterslip distribution following the 2010 Mw 8.8 Maule earthquake. <i>Earth and Planetary Science Letters</i> , 2020 , 542, 116292	5.3	12
178	Decoupled water and iron enrichments in the cratonic mantle: A study on peridotite xenoliths from Tok, SE Siberian Craton. 2020 , 105, 803-819		1
177	Continental lithospheric temperatures: A review. 2020 , 306, 106509		15
176	Crustal Structure of the Niuafo'ou Microplate and Fonualei Rift and Spreading Center in the Northeastern Lau Basin, Southwestern Pacific. <i>Journal of Geophysical Research: Solid Earth</i> , 2020 , 125, e2019JB019184	3.6	4
175	Inversion of Longer-Period OBS Waveforms for P Structures in the Oceanic Lithosphere and Asthenosphere. <i>Journal of Geophysical Research: Solid Earth</i> , 2020 , 125, e2019JB018810	3.6	4
174	Depth-Dependent Azimuthal Anisotropy Beneath the Juan de Fuca Plate System. <i>Journal of Geophysical Research: Solid Earth</i> , 2020 , 125, e2020JB019477	3.6	7
173	Hadean Earth. 2020 ,		5
172	Seismicity of the Incoming Plate and Forearc Near the Mariana Trench Recorded by Ocean Bottom Seismographs. <i>Geochemistry, Geophysics, Geosystems</i> , 2020 , 21, e2020GC008953	3.6	4
171	Thermal and decompression history of the Lanzo Massif, northern Italy: Implications for the thermal structure near the lithospherellsthenosphere boundary. 2020 , 372-373, 105661		1
170	Probing space to understand Earth. 2020 , 1, 170-181		9
169	Metasomatism and Hydration of the Oceanic Lithosphere: a Case Study of Peridotite Xenoliths from Samoa. 2020 , 61,		10
168	Shear attenuation and anelastic mechanisms in the central Pacific upper mantle. <i>Earth and Planetary Science Letters</i> , 2020 , 536, 116148	5.3	12
167	Experimental constraints on the solidification of a hydrous lunar magma ocean. 2020 , 55, 207-230		10

166	High HO Content in Pyroxenes of Residual Mantle Peridotites at a Mid Atlantic Ridge Segment. Scientific Reports, 2020 , 10, 579	4.9	5
165	Long Wavelength Progressive Plateau Uplift in Eastern Anatolia Since 20 Ma: Implications for the Role of Slab Peel-Back and Break-Off. <i>Geochemistry, Geophysics, Geosystems</i> , 2020 , 21, e2019GC008726	3.6	14
164	Plate tectonics and surface environment: Role of the oceanic upper mantle. 2020 , 205, 103185		10
163	The Brittle-Plastic Transition, Earthquakes, Temperatures, and Strain Rates. <i>Journal of Geophysical Research: Solid Earth</i> , 2020 , 125, e2019JB019335	3.6	11
162	Unravelling partial melt distribution in the oceanic low velocity zone. <i>Earth and Planetary Science Letters</i> , 2020 , 540, 116242	5.3	11
161	Three-dimensional thermo-rheological structure of the lithosphere in the North China Craton determined by integrating multiple observations: Implications for the formation of rifts. 2020 , 63, 969-9	984	4
160	A Disequilibrium Reactive Transport Model for Mantle Magmatism. 2021 , 61,		4
159	Rift migration and transition during multiphase rifting: Insights from the proximal domain, northern South China Sea rifted margin. 2021 , 123, 104729		O
158	Effect of water on the rheology of the lithospheric mantle in young extensional basin systems as shown by xenoliths from the Carpathian-Pannonian region. 2021 , 196, 103364		4
157	Low hydrogen concentrations in Dharwar cratonic lithosphere inferred from peridotites, Wajrakarur kimberlites field: Implications for mantle viscosity and carbonated silicate melt metasomatism. 2021 , 352, 105982		2
156	Permian plume-strengthened Tarim lithosphere controls the Cenozoic deformation pattern of the Himalayan-Tibetan orogen. <i>Geology</i> , 2021 , 49, 96-100	5	7
155	Strength models of the terrestrial planets and implications for their lithospheric structure and evolution. 2021 , 8,		6
154	Encyclopedia of Solid Earth Geophysics. 2021 , 1059-1079		
153	SIMS simultaneous measurement of oxygenflydrogen isotopes and water content for hydrous geological samples. 2021 , 36, 706-715		O
152	Thermal Monitoring of the Lithosphere by the Interaction of Deep Low-Frequency and Ordinary High-Frequency Earthquakes in Northeastern Japan. 2021 , 14, 1546		2
151	Dehydrogenation of deep-seated hydrous olivine in B lack-colored Id unites of arc origin. 2021 , 384-385, 105967		3
150	Balanced Cross-Sections and Numerical Modeling of the Lithospheric-Scale Evolution of the Hindu Kush and Pamir. <i>Journal of Geophysical Research: Solid Earth</i> , 2021 , 126, e2020JB020678	3.6	2
149	The role of edge-driven convection in the generation of volcanism Part 1: A 2D systematic study. 2021 , 12, 613-632		5

148	Electrical conductivity of the lithosphere-asthenosphere system. 2021 , 313, 106661		4
147	Lithosphere structure and its implications for the metallogenesis of the Nanling Range, South China: Constraints from 3-D magnetotelluric imaging. 2021 , 131, 104064		3
146	Water in the Supra-Subduction-Zone Mantle of the Mariana-Izu-Bonin Forearc: Constraints From Peridotitic Orthopyroxene. <i>Geochemistry, Geophysics, Geosystems</i> , 2021 , 22, e2020GC009586	3.6	1
145	Constraints on the Depth, Thickness, and Strength of the G Discontinuity in the Central Pacific From S Receiver Functions. <i>Journal of Geophysical Research: Solid Earth</i> , 2021 , 126, e2019JB019256	3.6	3
144	The Lithospheric Architecture of Australia From Seismic Receiver Functions. <i>Journal of Geophysical Research: Solid Earth</i> , 2021 , 126, e2020JB020999	3.6	3
143	The potential for aqueous fluid-rock and silicate melt-rock interactions to re-equilibrate hydrogen in peridotite nominally anhydrous minerals. 2021 , 106, 701-714		3
142	Geophysical and Geochemical Constraints on Neogene-Recent Volcanism in the North American Cordillera. <i>Geochemistry, Geophysics, Geosystems</i> , 2021 , 22, e2021GC009637	3.6	2
141	Pre-collisional extension of microcontinental terranes by a subduction pulley. <i>Nature Geoscience</i> , 2021 , 14, 443-450	18.3	5
140	Reduced Viscosity of Mg2GeO4 with Minor MgGeO3 between 1000 and 1150 °C Suggests Solid-State Lubrication at the Lithosphere Asthenosphere Boundary. 2021 , 11, 600		1
139	Postmelting hydrogen enrichment in the oceanic lithosphere. <i>Science Advances</i> , 2021 , 7,	14.3	2
139	Postmelting hydrogen enrichment in the oceanic lithosphere. <i>Science Advances</i> , 2021 , 7, Lithosphere thickness controls the extent of mantle melting, depth of melt extraction and basalt compositions in all tectonic settings on Earth [A review and new perspectives. 2021 , 217, 103614	14.3	2
	Lithosphere thickness controls the extent of mantle melting, depth of melt extraction and basalt	14.3	
138	Lithosphere thickness controls the extent of mantle melting, depth of melt extraction and basalt compositions in all tectonic settings on Earth [A review and new perspectives. 2021 , 217, 103614	3.6	14
138	Lithosphere thickness controls the extent of mantle melting, depth of melt extraction and basalt compositions in all tectonic settings on Earth [A review and new perspectives. 2021, 217, 103614] H diffusion in orthopyroxene and the retention of mantle water signatures. 2021, 305, 263-281 Volatile Element Evidence of Local MORB Mantle Heterogeneity Beneath the Southwest Indian		14
138 137 136	Lithosphere thickness controls the extent of mantle melting, depth of melt extraction and basalt compositions in all tectonic settings on Earth IA review and new perspectives. 2021, 217, 103614 H diffusion in orthopyroxene and the retention of mantle water signatures. 2021, 305, 263-281 Volatile Element Evidence of Local MORB Mantle Heterogeneity Beneath the Southwest Indian Ridge, 48°B1°E. <i>Geochemistry, Geophysics, Geosystems</i> , 2021, 22, e2021GC009647 Lithosphere as a constant-velocity plate: Chasing a dynamical LAB in a homogeneous mantle		14
138 137 136	Lithosphere thickness controls the extent of mantle melting, depth of melt extraction and basalt compositions in all tectonic settings on Earth IA review and new perspectives. 2021, 217, 103614 H diffusion in orthopyroxene and the retention of mantle water signatures. 2021, 305, 263-281 Volatile Element Evidence of Local MORB Mantle Heterogeneity Beneath the Southwest Indian Ridge, 48°B1°E. <i>Geochemistry, Geophysics, Geosystems</i> , 2021, 22, e2021GC009647 Lithosphere as a constant-velocity plate: Chasing a dynamical LAB in a homogeneous mantle material. 2021, 316, 106710 The Role of Subduction Interface and Upper Plate Strength on Back-Arc Extension: Application to		14
138 137 136 135	Lithosphere thickness controls the extent of mantle melting, depth of melt extraction and basalt compositions in all tectonic settings on Earth IA review and new perspectives. 2021, 217, 103614 H diffusion in orthopyroxene and the retention of mantle water signatures. 2021, 305, 263-281 Volatile Element Evidence of Local MORB Mantle Heterogeneity Beneath the Southwest Indian Ridge, 48°B1°E. <i>Geochemistry, Geophysics, Geosystems</i> , 2021, 22, e2021GC009647 Lithosphere as a constant-velocity plate: Chasing a dynamical LAB in a homogeneous mantle material. 2021, 316, 106710 The Role of Subduction Interface and Upper Plate Strength on Back-Arc Extension: Application to Mediterranean Back-Arc Basins. 2021, 40, e2021TC006795 Eastern China continental lithosphere thinning is a consequence of paleo-Pacific plate subduction:		14 1 1

130	Diffuse spreading, a newly recognized mode of crustal accretion in the southern Mariana Trough backarc basin.		0
129	Hadean geodynamics and the nature of early continental crust. 2021 , 359, 106178		18
128	Water contents of nominally anhydrous orthopyroxenes from oceanic peridotites determined by SIMS and FTIR. 2021 , 115, 611		0
127	Upper Mantle Hydration Indicated by Decreased Shear Velocity Near the Southern Mariana Trench From Rayleigh Wave Tomography. <i>Geophysical Research Letters</i> , 2021 , 48, e2021GL093309	4.9	O
126	Origin, Accretion, and Reworking of Continents. 2021 , 59, e2019RG000689		5
125	Oceanic transform fault seismicity and slip mode influenced by seawater infiltration. <i>Nature Geoscience</i> , 2021 , 14, 606-611	18.3	6
124	KineDyn: Thermomechanical forward method for validation of seismic interpretations and investigation of dynamics of rifts and rifted margins. 2021 , 317, 106748		3
123	Mantle metasomatic influence on water contents in continental lithosphere: New constraints from garnet pyroxenite xenoliths (France & Cameroon volcanic provinces). 2021 , 575, 120257		1
122	The abundances of F, Cl, and H2O in eucrites: Implications for the origin of volatile depletion in the asteroid 4 Vesta. 2021 , 314, 270-270		0
121	Scaling laws for stagnant-lid convection with a buoyant crust. <i>Geophysical Journal International</i> , 2021 , 228, 631-663	2.6	1
120	Thermoelasticity of Water in Silicate Melts: Implications for Melt Buoyancy in Earth's Mantle. Journal of Geophysical Research: Solid Earth, 2021 , 126, e2021JB022359	3.6	
119	The effect of fluorine on reaction rim growth dynamics in the ternary CaO-MgO-SiO2 system. 2021 ,		
118	Machine Learning for Identification of Primary Water Concentrations in Mantle Pyroxene. <i>Geophysical Research Letters</i> , 2021 , 48, e2021GL095191	4.9	3
117	Antarctic Upper Mantle Rheology. M56-2020-19		5
116	The rupture mechanisms of intraslab earthquakes: A multiscale review and re-evaluation. 2021 , 221, 103782		1
115	From dry to damp and stiff mantle lithosphere by reactive melt percolation atop the Hawaiian plume. <i>Earth and Planetary Science Letters</i> , 2021 , 574, 117159	5.3	
114	Encyclopedia of Solid Earth Geophysics. 2021 , 893-906		1
113	Encyclopedia of Solid Earth Geophysics. 2021 , 906-915		1

112	Slab-driven Mantle Weakening and Rapid Mantle Flow. 135-155	3
111	Microscopic Models for the Effects of Hydrogen on Physical and Chemical Properties of Earth Materials. 2007 , 321-356	3
110	Subduction Zone: The Water Channel to the Mantle. 2007 , 113-138	8
109	Dynamics of Superplumes in the Lower Mantle. 2007 , 239-268	9
108	Long-Term Evolution of the Martian Crust-Mantle System. 2012 , 49-111	1
107	Partial Melting in the Central Andean Crust: a Review of Geophysical, Petrophysical, and Petrologic Evidence. 2006 , 459-474	41
106	Numerical Study of Weakening Processes in the Central Andean Back-Arc. 2006 , 495-512	13
105	Mechanism of the Andean Orogeny: Insight from Numerical Modeling. 2006 , 513-535	39
104	Fluid Dynamics of Mantle Plumes. 2007 , 1-48	7
103	4.2.3.5 Planetary geology: Craters and chronology, Volcanism, Tectonics. 2009 , 345-433	3
102	The Influence of Partial Melt on Mantle Convection. 2012 , 551-565	1
101	Encyclopedia of Solid Earth Geophysics. 2011 , 832-851	5
100	Water in the Earth⊠Interior: Distribution and Origin. 2017 , 83-150	1
99	An upper bound on the electrical conductivity of hydrated oceanic mantle at the onset of dehydration melting. <i>Earth and Planetary Science Letters</i> , 2018 , 482, 357-366	12
98	Variable extent of dehydration of clinopyroxene megacrysts from Gezi volcano of Inner Mongolia. 2020 , 401, 106934	2
97	Late-Pleistocene, Holocene and present-day ice load evolution in the Antarctic Peninsula: Models and predicted vertical crustal motion. 2002 , 133-155	5
96	The Role of Lithosphere Thickness in the Formation of Ocean Islands and Seamounts: Contrasts between the Louisville and Emperor Hawaiian Hotspot Trails. 2021 , 61,	3
95	Strength of the continental lithosphere: Time to abandon the jelly sandwich?. 2002 , 12, 4	715

94	Geophysical characterization of mantle melting anomalies: A crustal view. 2007, 507-524		2
93	IR spectroscopic characterisation of hydrous species in minerals. 227-279		23
92	Deep mantle melting, global water circulation and its implications for the stability of the ocean mass. 2020 , 7,		9
91	Solid-state redistribution of mineral particles in the upwelling mantle flow as a mechanism of chromite concentration in the ophiolite ultramafic rocks (on the example of Kraka ophiolite, the Southern Urals). 2019 , 21, 31-46		10
90	Rock Deformation and Formation of LPO of Minerals in the Upper Mantle: Implications for Seismic Anisotropy. 2012 , 21, 249-261		2
89	Terrane geodynamics: Evolution on the subduction conveyor from pre-collision to post-collision and implications on Tethyan orogeny. <i>Gondwana Research</i> , 2021 ,	5.1	1
88	Insights Into the Nature of Plume-Ridge Interaction and Outflux of H2O From the Galpagos Spreading Center. <i>Geochemistry, Geophysics, Geosystems</i> , 2021 , 22, e2020GC009560	3.6	О
87	Water, Life, and Planetary Geodynamical Evolution. 2007 , 167-203		
86	Mantle Dynamics 🖟 Case Study. 2009 , 139-181		
85	Anisotropy and Flow in Pacific Subduction Zone Back-arcs. 1998 , 463-475		
84	Encyclopedia of Lunar Science. 2015 , 1-6		
84	Encyclopedia of Lunar Science. 2015, 1-6 Amplitude and Duration of Thermal and Tectonic Activation of Basins An Assessment in the GALO System. 2016, 3-30		
	Amplitude and Duration of Thermal and Tectonic Activation of BasinsAn Assessment in the GALO		
83	Amplitude and Duration of Thermal and Tectonic Activation of Basins An Assessment in the GALO System. 2016 , 3-30		
83	Amplitude and Duration of Thermal and Tectonic Activation of Basins An Assessment in the GALO System. 2016, 3-30 Application of the QRV Method to Modelling of Plate Subduction. 2016, 83-99		
8 ₃ 8 ₂	Amplitude and Duration of Thermal and Tectonic Activation of Basins An Assessment in the GALO System. 2016, 3-30 Application of the QRV Method to Modelling of Plate Subduction. 2016, 83-99 Encyclopedia of Geochemistry. 2018, 1-18		
83 82 81 80	Amplitude and Duration of Thermal and Tectonic Activation of Basins An Assessment in the GALO System. 2016, 3-30 Application of the QRV Method to Modelling of Plate Subduction. 2016, 83-99 Encyclopedia of Geochemistry. 2018, 1-18 Encyclopedia of Geochemistry. 2018, 498-513		0

76 Encyclopedia of Solid Earth Geophysics. **2020**, 1-14

	Oxidation of the Interiors of Carbide Exoplanets. 2020 , 1, 39		2
75	Oxidation of the interiors of Carbide Exoptanets. 2020, 1, 39		2
74	Encyclopedia of Solid Earth Geophysics. 2020 , 1-10		
73	Constraints on Olivine Deformation From SKS Shear-Wave Splitting Beneath the Southern Cascadia Subduction Zone Back-Arc. <i>Geochemistry, Geophysics, Geosystems</i> , 2021 , 22, e2021GC010091	3.6	1
72	Crustal thickness (H) and Vp/Vs ratio (🖺) images beneath the central Tien Shan revealed by the H-🗓-c method. 2022 , 822, 229157		2
71	MCMC inversion of the transient and steady-state creep flow law parameters of dunite under dry and wet conditions. 2021 , 73,		O
70	Constraints on the behaviour and content of volatiles in Galpagos magmas from melt inclusions and nominally anhydrous minerals. 2021 ,		О
69	Numerical modeling of North Sulawesi subduction zone: Implications for the eastWest differential evolution. 2021 , 822, 229172		1
68	Geodynamics of East Anatolia-Caucasus Domain: Inferences From 3D Thermo-Mechanical Models, Residual Topography, and Admittance Function Analyses. 2021 , 40,		
67	Global trends in novel stable isotopes in basalts: Theory and observations. 2022, 318, 388-414		2
66	Rapid-quenching of high-pressure depolymerized hydrous silicate (peridotitic) glasses. 2022 , 578, 1213	47	O
65	Seismic evidence of two cryptic sutures in Northwestern Australia: Implications for the style of subduction during the Paleoproterozoic assembly of Columbia. <i>Earth and Planetary Science Letters</i> , 2022 , 579, 117342	5.3	1
64	Mantle melting, lithospheric strength and transform fault stability: Insights from the North Atlantic. <i>Earth and Planetary Science Letters</i> , 2022 , 579, 117351	5.3	O
63	Incipient ocean spreading beneath the Arabian shield. 2022 , 226, 103955		O
62	Nature of the lithosphere-asthenosphere boundary beneath the Eastern Dharwar Craton of the Indian Shield. 2022 , 227, 105071		1
61	Terminal tectono-magmatic phase of the New England Orogen driven by lithospheric delamination. <i>Gondwana Research</i> , 2022 , 106, 105-125	5.1	
60	Effect of second SiD vibrational overtones/combinations on quantifying water in silicate and silica minerals using infrared spectroscopy, and an experimental method for its removal. 2022 , 49, 1		0
59	Enhancement of ductile deformation in polycrystalline anorthite due to the addition of water. 2022 , 156, 104547		O

58	A New Model of Archean Craton Formation and Plate Tectonics Based on Discoveries in the Yilgarn Province of Western Australia.		
57	Long-Term Lithospheric Strength and Upper-Plate Seismicity in the Southern Central Andes, 29°B9°S. <i>Geochemistry, Geophysics, Geosystems</i> , 2022 , 23,	3.6	1
56	Magmatism at Passive Margins: Effects of Depth-Dependent Wide Rifting and Lithospheric Counterflow. <i>Journal of Geophysical Research: Solid Earth</i> , 2022 , 127,	3.6	О
55	Calculated phase equilibria for high-pressure serpentinites and compositionally-related rocks close to the MgO-Al2O3-SiO2-H2O (MASH) system		
54	Geophysics of Vesta and Ceres. 2022 , 173-196		
53	New Insights Into Lithospheric Structure and Melting Beneath the Colorado Plateau. <i>Geochemistry, Geophysics, Geosystems</i> , 2022 , 23,	3.6	Ο
52	Effects of Hotspot-Induced Long-Wavelength Mantle Melting Variations on Magmatic Segmentation at the Reykjanes Ridge: Insights From 3D Geodynamic Modeling. <i>Journal of Geophysical Research: Solid Earth</i> , 2022 , 127,	3.6	1
51	Inefficient Water Degassing Inhibits Ocean Formation on Rocky Planets: An Insight from Self-Consistent Mantle Degassing Models <i>Astrobiology</i> , 2022 ,	3.7	Ο
50	A wet heterogeneous mantle creates a habitable world in the Hadean <i>Nature</i> , 2022 , 603, 86-90	50.4	2
49	High Water Contents in Zircons Suggest Water-Fluxed Crustal Melting During Cratonic Destruction. <i>Geophysical Research Letters</i> , 2022 , 49,	4.9	
48	Craton formation in early Earth mantle convection regimes. <i>Journal of Geophysical Research: Solid Earth</i> ,	3.6	2
47	Rapid surface uplift and crustal flow in the Central Andes (southern Peru) controlled by lithospheric drip dynamics <i>Scientific Reports</i> , 2022 , 12, 5500	4.9	1
46	A plume origin for hydrous melt at the lithosphere-asthenosphere boundary <i>Nature</i> , 2022 , 604, 491-49	94 0.4	1
45	datasheet1.pdf. 2020 ,		
44	Mantle Degassing Lifetimes through Galactic Time and the Maximum Age Stagnant-lid Rocky Exoplanets Can Support Temperate Climates. <i>Astrophysical Journal Letters</i> , 2022 , 930, L6	7.9	1
43	Deep and surface driving forces to shape the Earth: Insights from the evolution of the northern South China Sea margin. <i>Gondwana Research</i> , 2022 ,	5.1	O
42	Cenozoic delamination of the southwestern Yangtze craton owing to densification during subduction and collision. <i>Geology</i> ,	5	O
41	Water storage in cratonic mantle. <i>Terra Nova</i> ,	3	O

40	An experimental study to explore hydrogen diffusion in clinopyroxene at low temperatures (195 - 400 °C) and consequences for re-equilibration at near surface conditions.		
39	Simultaneous Inference of Plate Boundary Stresses and Mantle Rheology Using Adjoints: Large-Scale Two-Dimensional Models. <i>Geophysical Journal International</i> ,	2.6	
38	What Drives Plate Motion?.		
37	Grain-size-evolution controls on lithospheric weakening during continental rifting. <i>Nature Geoscience</i> ,	18.3	O
36	Generation and evolution of the oceanic lithosphere in the North Atlantic. <i>Rivista Del Nuovo Cimento</i> ,	3.5	
35	Discovery of distinct lithosphere-asthenosphere boundary and the Gutenberg discontinuity in the Atlantic Ocean. <i>Science Advances</i> , 2022 , 8,	14.3	О
34	Constraining Upper Mantle Viscosity Using Temperature and Water Content Inferred from Seismic and Magnetotelluric Data. <i>Journal of Geophysical Research: Solid Earth</i> ,	3.6	1
33	What is a Rifted Margin? From the Early Models to Modern Views and Future Challenges. 2022 , 71-176		
32	Contribution of Viscoelastic Stress to the Synchronization of Earthquake Cycles on Oceanic Transform Faults. 2022 , 127,		1
31	Strain localization at brittle-ductile transition depths during Miocene magmatism and exhumation in the southern Basin and Range. 2022 , 104709		
30	Dynamic Evolution of Back-Arc Basins Affected by Double Subduction. 2022, 127,		
29	Global water distribution in the mantle transition zone from a seismic isotropic velocity model and mineral physics modeling. 10,		
28	Development of major element proxies for magmatic H2O content in oceanic basalts. 2022, 121068		
27	Relative continent/mid-ocean ridge elevation: A reference case for isostasy in geodynamics. 2022 , 1041	53	2
26	The fate of delaminated cratonic lithosphere. 2022 , 594, 117740		1
25	Lithospheric structure of the Dharwar Craton (India) from joint analysis of gravity, topography, and teleseismic travel-time residuals. 2022 , 239, 105397		О
24	The structure and dynamics of the uppermost mantle of southwestern Canada from a joint analysis of geophysical observations.		O
23	Will Earth's next supercontinent assemble through the closure of the Pacific Ocean?.		О

22	The effect of low-viscosity sediments on the dynamics and accretionary style of subduction margins. 2022 , 13, 1455-1473	O
21	Adsorption behavior of molecular hydrogen in forsterite. 2022 , 106967	O
20	Mass transport. 2023 , 821-876	0
19	Reply to Comment by Steinberger on Will Earth's next supercontinent assemble through the closure of the Pacific Ocean?	O
18	A Subsurface Magma Ocean on Io: Exploring the Steady State of Partially Molten Planetary Bodies. 2022 , 3, 256	0
17	Building archean cratonic roots. 10,	O
16	Craton Destruction Induced by Drastic Drops in Lithospheric Mantle Viscosity. 2022 , 9,	0
15	A unified numerical model for two-phase porous, mush and suspension flow dynamics in magmatic systems.	o
14	Hydrogen Diffusion in Clinopyroxene at Low Temperatures (195°C400°C) and Consequences for Subsurface Processes. 2022 , 23,	O
13	Hydrogen Partitioning between Olivine and Orthopyroxene: Implications for the Lithosphere-Asthenosphere Structure.	o
12	Absence of water content contrast between lithosphere and asthenosphere in subduction zone. 2023 , 603, 117981	0
11	Potential clinopyroxene and orthopyroxene reference materials for SIMS water content analysis.	O
10	Geological confirmation for water-effected incipient melt origin of seismic low velocity zone (LVZ) beneath ocean basins. 2023 ,	O
9	Small effect of partial melt on electrical anomalies in the asthenosphere. 2023 , 9,	o
8	Rapid solidification of Earth magma ocean limits early lunar recession. 2023, 400, 115564	O
7	Asthenospheric low-velocity zone consistent with globally prevalent partial melting. 2023, 16, 175-181	O
6	The Physics and Origin of Plate Tectonics From Grains to Global Scales. 2023 , 5-33	0
5	Evidence of ghost plagioclase signature induced by kinetic fractionation of europium in the Earth mantle. 2023 , 14,	О

CITATION REPORT

4	Ductile Deformation of the Lithospheric Mantle. 2023 , 51,	Ο
3	Formation and geophysical character of transitional crust at the passive continental margin around Walvis Ridge, Namibia. 2023 , 14, 237-259	O
2	Selective Interstitial Hydration Explains Anomalous Structural Distortions and Ionic Conductivity in 6H-Ba4Ta2O9[1/2H2O. 2023 , 35, 2740-2751	0
1	Strike slip motion and the triggering of subduction initiation. 11,	O